UNIVERSITY OF AGDER

An Approach to Day Ahead Forecasting of Solar Irradiance with an Application to Energy Gain in Solar Thermal Collectors

Dimuthu Dharshana Kodippili Arachchige

Supervisor
Professor Hans George Beyer

This master's thesis is carried out as a part of the education at the University of Agder and is therefore approved as a part of this education. However, this does not imply that the University answers for the methods that are used or the conclusions that are drawn.

University of Agder, 2014
Faculty of Engineering and Science
Department of Engineering Sciences

Abstract

Today, for the management of energy supply systems forecast information on load and the production of meteorology dependent (wind, solar, hydro) generation is ever rising. Solar irradiance forecasting is given a unique priority as it spans over major applications such as management of grids with a high share of photovoltaic generation and thermal power supply systems relying on solar heat generation. This thesis will address the day ahead prediction of the local irradiances intended to be applied for the management of solar assistant systems for heat and hot water supply. The forecast method presented here is based on the statistical analysis of historical data in Kristiansand, Southern Norway. For this, satellite derived irradiance data covering seven years provided by Geomodel Solar, Slovacia [11] can be used. In this approach, it is assumed that the irradiance sum of today shows a dependence on the irradiance sum of yesterday (Markov Assumption [26]). This day to day dependency is assessed by obtaining conditional probability distributions of irradiance sum on next day for a given status of weather, given here by the irradiance sum on previous day. Based on such probabilistic approach two schemes are introduced to obtain values for the forecasting. The first scheme is based on most probable expected irradiance sum of tomorrow and the second approach is based on the average expected irradiance sum, both extracted from the probability distributions. Having obtained forecasted values for the irradiance, the validity of prediction methods are investigated by comparing with the actual measured data giving the statistical parameters, relative monthly Bias and relative monthly Root Mean Square Error (RMSE). The approach using the average expected irradiance sum, gives more accurate results showing low RMSE. Concerning the application, the irradiance data, both measured and forecasted are used to analyze the daily energy gain of a solar thermal collector and its forecastability. These data are analyzed similar to the irradiance sets. The monthly RMSE of the prediction of daily energy gain is investigated over a year. This shows that there are significant changes of forecast quality over the year with quite satisfactory behavior in summer months with higher irradiances and thus higher gains, but however lower quality in the winter months with lower irradiance levels.

Key words: **Irradiance, Forecast, Energy, Day-ahead, Collector, RMSE**

Preface

The framework for this master thesis was given by the project; “Optimal Harvesting of Intermittent Renewable Energy” in 2012 initiated by Sekretariatet for fellesprosjekt at University of Agder (UiA) and Telemark University College (HiT). First of all I would like to express my sincere gratitude to the project coordinator, Professor Bernt Lie in HiT, having offered me the summer job in 2013, as the initial work of this research.

I owe my profound gratitude to Professor Hans George Beyer; who has always been at the frontier, extending relentless guidance by way of providing much needed supervision throughout the project.

I am also heartily thankful to my masters’ coordinator, Mr. Stein Bergsmark for his precious advices on thesis writing, presentation and particularly, remarks on the progress.

Finally, I would like to thank everybody who supported me throughout this work by way of extending kind hands, whenever necessary.

Dimuthu Dharshana Kodippili Arachchige
Grimstad, June 2014.

Content

List of Figures

List of Tables

Abbreviations

MSG	Meteosat Second Generation	
T	Temperature	$[K]$
σ	Stefan's- Boltzmann Constant	$[Wm^{-2}K^{-4}]$
A_{Sun}	Surface Area of the Sun	$[m^2]$
M_{Sun}	Total Radiation Emitted by the Sun	$[Wm^{-2}]$
ϕ_{Sun}	Total Radiation Flux Emitted by the Sun	$[W]$
r_{ES}	The Mean Distance between Sun and Earth	$[m]$
E_{Sc}	Solar Constant	$[Wm^{-2}]$
ϕ_{Earth}	Flux Received by the Cross Sectional Area of the Earth	$[Wm^{-2}]$
ε_0	Sun-Earth Eccentricity Correction Factor	$[dimensionless]$
L_l	Local Longitude	[°]
L_s	Standard Longitude	[°]
TST	True Solar Time	$[h]$
LST	Local Time	$[h]$
GHI	Global Horizontal Irradiance	$[Wm^{-2}]$
GTI	Global Tilted Irradiance	$[Wm^{-2}]$
GEI	Global Extraterrestrial Irradiance	$[Wm^{-2}]$
G_b	Direct Beam Horizontal Irradiance	$[Wm^{-2}]$
G_d	Global Diffuse Horizontal Irradiance	$[Wm^{-2}]$
G_t	Global Irradiance on a Tilted Plane	$[Wm^{-2}]$
G_{bt}	Direct Beam Irradiance on a Tilted Plane	$[Wm^{-2}]$
G_{rt}	Ground Reflected Irradiance on a Tilted Plane	$[Wm^{-2}]$
G_{dt}	Sky Diffuse Irradiance on a Tilted Plane	$[Wm^{-2}]$
G_{extr}	Global Extraterrestrial Irradiance	$[Wm^{-2}]$

ρ	Albedo of the Surface	[*dimensionless*]
δ	Solar Declination	[°]
θ	Zenith Angle	[°]
ω	Hour Angle	[°]
ψ	Azimuthal Angle	[°]
α	Solar Altitude	[°]
φ	Longitude Angle	[°]
β	Slope Angle	[°]
η_0	Zero Lost Coefficient of a Solar Thermal Collector	[*dimensionless*]
a_1,	1st Heat Lost Coefficients of the Collector	$[Wm^{-2}K^{-1}]$
a_2	2nd Heat Lost Coefficients of the Collector	$[Wm^{-2}K^{-2}]$
$T_{ambient}$	Ambient Temperature	[*K*]
$T_{collector}$	Collector Temperature	[*K*]
A	Collector Aperture Area	$[m^2]$
$\dot{Q}$	Thermal Power Output of the Collector	[*W*]

1. Introduction

Chapter 1 reveals the motivation and ground floor behind the overall research. It gives a quick insight to the roots of initializing this work as a master thesis. The project is set to develop an approach to forecast daily energy gain of thermal collectors which could be used in solar assisted house heating. Essential theoretical background and motivation of the thesis is discussed in section 1.1 including an introduction to the main project which is recognized as the key motivation factor behind this work. Section 1.2 presents the previous work carried out by researches which are closely related with obtaining intended outcomes. Section 1.3 defines the research work in terms of initial approach, and objectives of the thesis. Section 1.4 reveals the limitations and key assumptions of the project. Subsequently, Section 1.5 discusses the approach of obtaining the solution. Also, the contribution and importance of the work is discussed in Section 1.6. Lastly, Section 1.7 outlines the rest of the remaining chapters of the report.

1.1 Background and Motivation

Today, use of renewable energy is ever increasing. As both wind and solar irradiance are highly variable and uncontrollable, this gives new challenges for the design and control of energy supply systems and calls for tools to as least partly predict these energy flows. Concerning wind power, power prediction systems have already shown their strong economic impact and improve the integration of wind energy into the management of grids with high penetration levels [1], [2]. For solar power forecasts come up to the same importance in grids with high PV penetration. For that application, the forecast of the regionally integrated irradiance affecting the PV systems distributed in the respective region is of importance, and scheme for the prediction of the spatially averaged irradiance had been developed yielding good quality [2]. The prediction of single point irradiance still fights with higher uncertainties. But, as for the control of local systems for solar thermal applications, this single point forecast is the relevant parameter. The thesis will address the day ahead prediction of single point irradiances and apply it for domestic and commercial power management systems to achieve of economic benefits.

The Frame for this project is given by the project; “Optimal Harvesting of Intermittent Renewable Energy” in 2012 initiated by Sekretariatet for fellesprosjekt at University of Agder (UiA) and Telemark University College (HiT) [3]. The Project is further discussed in section 1.3. As an essential task toward fulfilling the requirements of the main project, it is expected to develop a forecasting method for solar irradiation based on site specified data in Kristiansand region, Southern Norway. Initial stage of the research work began as a summer job in 2013. The work carried out during the summer period is continued as the thesis work to obtain desired outcomes of the overall project. For this goal, the following chapters will give an insight to the characteristics of solar radiation and the basic approaches to forecast its temporal variation. Concerning the application, relevant characteristics of solar thermal collector systems, their structure and control will be given.

The transmission media of solar power is defined as solar radiation. Solar radiation mainly emanates as electromagnetic radiation from the surface of the sun (photosphere) [4]. Solar irradiance incident on a given plane on the earth's surface is mainly determined by several factors such as sun earth astronomy, solar geometry and other extinction processes in the atmosphere. Position of the sun with respect to the receivable surface is explained in terms of latitude, declination, solar time, azimuth and tilt angle of the receiving surface. Hour by hour and day by day sun position changes, so does irradiance intensity. Also available radiation flux at the surface is affected by extinction processes in the atmosphere such as absorption and scattering by air molecules, water vapor, aerosols, clouds, etc. [4].

Solar thermal collectors play a significant role as an effective intermittent transmission media of solar radiation in to energy. Solar energy can be absorbed as heat thorough solar collectors and later they can be used for domestic or commercial use. In a solar collector, a fluid is heated up by catching solar power. Solar collectors can be in different configuration which may be occupied depending on the required capacity. They are employed in typical solar thermal energy management systems. Such systems may consist, solar collectors along with storage tank and the respective heat distribution system. Chapter 2 will give an introduction to solar heating systems and a detailed description about solar thermal collector modelling.

In a hot water collector, amount of heat absorbed by the water is determined by typical collector model parameters and other meteorological quantities. Energy gain depends on the key meteorological parameter; solar irradiance. Chapter 2 will further discuss basics on solar irradiance with respect to the energy gain of a typical collector. Early prediction of the energy gain of solar collectors is an essential step towards improving the energy management of solar heating systems. Thesis emphasizes on building a forecast methodology for the energy gain of a typical collector based on irradiance prediction model.

1.2 Literature Review

In recent years, popularity of solar assisted thermal heating is ever rising as one of the best alternative energy sources. Solar thermal collectors stand as the key element in such schemes. When such systems are employed in energy management systems, energy gain of the collector is considerably concerned to obtain a high output. Also energy gain depends on solar irradiance. Recent research shows a high interest of obtaining forecasting schemes for irradiance which could easily be applied to predict energy gain of solar thermal collectors. Hence, some of the main previous work on irradiance forecasting is discussed.

Different approaches for irradiance forecasting are currently proposed. One of the most recognized scheme is, irradiance forecasting based on statistical time series models. They depend on making relationships between past observations, i.e. historical data and, future values for prediction. This thesis work also focuses on prediction of solar irradiance based on a statistical analysis of historic data, which will be discussed in Chapter 3.

As a popular time series model, Artificial Neural Network (ANN)-wavelet methods are frequently employed to obtain local predictions. In papers [5], [6], Continuous Wavelet Transform (DWT) method is used and the quality of the forecast; Root Mean Square Error (RMSE) is depicted as 5.1 % [5], 8.3% [6] respectively. Also paper [7] employs the Discrete Wavelet Transform (DWT) method with a RMSE of 8.4%. These models are applicable for sites where the solar radiation was measured during one year [5], two years [6], or longer time intervals [5], [7]. The DWT method is able to forecast the motion of clouds using satellite imaging over the earth surface for any site or area.

Numerical Weather Predication (NWP) models are also used to obtain information on cloud cover and incoming solar radiation [8] by solving the equations on physics and dynamics of the atmosphere. These equations do not stand for a unique solution due to its nonlinearity. By the model, Global Forecasting System (GFS) [9], author has performed numerical modeling in a (0.5 x 0.5)° earth surface grid with sampling interval of three hours. In order to improve the performance of local forecasts, the data of the global model are assimilated by regional NWP

models. By using the hydrostatic ETA model, author in paper [10] has obtained a RMSE of 43.9 % and 43.6 % for the daily total of incoming solar radiation, for two different sites in Brazil. Performance of the NWP models can be improved by the techniques of Model Output Statistics (MOS). The Multiple Linear Regression (MLR) as shown in [8] and [10] or an Artificial Neural Network (ANN) [10] or Kalman filter [9] can be used as statistic models or model variables to enhance the quality of NWP forecast.

1.3 Problem Definition

Sekretariatet for fellesprosjekt at University of Agder (UiA) and Telemark University College (HiT) has allocated NOK 300 000 to the project "Optimal Harvesting of Intermittent Renewable Energy" [3]. The participants of this work are Professor Bernt Lie from HiT and Professor Hans-Georg Beyer at UiA, as well as number of students for the summer jobs and master theses [3]. The main objective of this work is to build up an energy management system which could optimally harvest the solar power in domestic level. Here using forecasted irradiance profiles in combination with a simulation tool for the performance of a solar assisted house heating, the best setting of the control scheme for each possible solar input will be estimated. This scheme will be validated by comparing the resulting system performance with the performance under application of a fixed optimal control without forecast uncertainty information.

1.3.1 Initial Approach

Over the years, different approaches of solar irradiance prediction systems have been developing depending on the application and the corresponding time scale. Section 1.2, Literature Review depicted a summary of different approaches to forecast solar irradiance. In this work, it is desired to develop a short term method, i.e. one-day-ahead forecasting of irradiance information using probabilistic approach. Finally the same approach is used to predict the energy gain of a site specified solar thermal collector. The description in Problem Definition presented a detailed description about the original project which fertilized this research work as a master thesis.

1.3.2 Thesis Definition and Objectives

To fulfil the above mentioned requirements of the main project, thesis work is bound for developing an approach to set up a day ahead prediction solar irradiation. The test location is Kristiansand region in Southern Norway. Finally the proposed method is used to predict energy gain of a domestic solar thermal collector.

Main Goals:

1. Proposing a method to forecast global irradiance on horizontal and tilted surfaces by means of a probabilistic approach derived from the analysis of historical sets measured irradiance data. For this, the approach of predicting the irradiance directly or using the two step approach of predicting the clearness index describing the stochastic cloud situation and modifying the systematic astronomical variation of the solar irradiance.

2. Developing an approach to predict daily energy gain of solar thermal collectors for solar assisted house heating.

3. Obtaining time series forecasted information for solar irradiance behaviour and energy gain.

4. Investigation of the quality of forecasts with statistical parameters.

5. **If time allows:** Investigating the possibility of extending developed forecast approach in Kristiansand region, to the Porsgrunn region.

1.4 Limitations

- Proposed method is based on statistical analysis of local data. Therefore the forecast is only valid for Kristiansand region, Southern Norway.

- It is assumed that statistics are stable for future analysis, i.e. we assume, there will not be significant changes in the conditional probability distributions obtained through the analysis of historical data over seven years.

- In the solar thermal collector, energy gain is forecasted by keeping operational temperature at a constant value. Further to explain, it is assumed that water enters to solar thermal collector at a temperature of 30 °C and water leaves at a temperature of 60 °C. Thus, collector temperature is considered as mean value, 45 °C.

- Proposed approach does not introduce a method to predict ambient temperature. To obtain a strict energy gain forecast, ambient temperature has also to be forecasted.

1.5 Solution Approach Method

This section sums up the overall method of achieving irradiance forecasting. The method is in-detail implemented in Chapter 3, 4, 5 and 6.

1.5.1 Measurement of Irradiance Data

In this project, the basic solar irradiance data are given by satellite derived information supplied by Geomodel Solar [12], Slovacia, SolarGIS database. Since, calculation of solar radiation is based on satellite and atmospheric data, reliability of the measurement is above 99 % [12]. These data are derived for the location with latitude of 58.15° and a longitude of 8.00° Kristiansand city, Southern Norway. Data are from a period of seven years from 01/01/2007 to 07/04/2013. Spatial resolution for solar irradiance data and meteorological parameters is recognized as values representing in an area of 1000*m* x 1000*m*. Meteosat Second Generation (MSG) database provides data for every 15 minutes. With respect to above specifications, Global Horizontal Irradiance (GHI), Diffuse Horizontal Irradiance (DIF), Global Tilted Irradiance (GTI) and Air Temperature at 2*m* above the sea level were obtained from the satellite images and spatial interpolation of station temperature data. Table 1.1 shows a sample of measured data set from Geomodel SolarGIS database.

Table 1.1. A Sample of Measured Data Set from Geomodel Solar

Date;Time;GHI;DIF;TEMP;GTI
19.04.2007;13:11;407;286;8.5;463
19.04.2007;13:26;669;248;8.2;826
19.04.2007;13:41;629;168;7.9;792
19.04.2007;13:56;527;195;7.6;645
19.04.2007;14:11;557;145;7.3;693
19.04.2007;14:26;545;101;7.0;679
19.04.2007;14:41;511;95;6.7;631
19.04.2007;14:56;464;128;6.4;561
19.04.2007;15:11;402;131;6.1;474
19.04.2007;15:26;357;135;5.9;413

1.5.2 Solar Thermal Collector

Solar thermal collector converts solar irradiance in to heat as the consumable form of energy. In this project, the collector is selected from SPF online collector catalog [13] which is based on the European standards. We selected “Consolar PLANO 27H”, flat plate solar thermal collector which can be simply installed in domestic environment. It gives a reasonable power output which is good enough to fulfil the domestic heat requirement. A detailed description about Consolar PLANO 27H collector is given in Chapter 2 (See Section 2.5). Power output of the collector can be estimated based on the incoming irradiance and other collector parameters provided by the collector data sheet (See Appendix D). It is intended to locate the collector with a tilted angle of 45° to the horizontal. Theoretical background on collector modelling will be further discussed on Chapter 2.

1.5.3 Solution

To achieve the desired outcomes of this research, it is essential to work on a statistical analysis of the measured irradiance data over seven years. Initially, irradiance and atmospheric data is sorted out in to a simple formats; hourly, daily, and monthly values. Proposed method for forecasting is a probabilistic approach, i.e. one-day-ahead forecasting of global irradiance based on analysis of historic hourly and daily values. The available solar data set consists of Global Horizontal Irradiance and Global Tilted Irradiance for a tilted angle of 20°. However as per the project requirement, solar thermal collectors are typically with a tilted angle of 45°. Hence, global tilted irradiance for a tilted plane of 45° has to be calculated from the information on the horizontal irradiance.

When prediction approach for cloud behavior is concerned, it is mandatory to work on clearness index which provides information on cloud formations. Based on measured values of Global Horizontal Irradiance and Global Extraterrestrial Irradiance, daily clearness index and hourly clearness index are calculated. As the initial step towards a probabilistic approach of forecasting, daily sum of tilted irradiance and daily sum of clearness index are obtained.

It is a known fact that, variability and characteristics of solar radiation is influenced by position of the sun, i.e. day-night cycle and seasonal cycle within a year. Hence month by month, irradiance intensity varies. Nevertheless, for individual months change in sun position affects in uniform scale. For an instance, in every year, month of May, sun's trajectory is positioned within a fixed distance to the earth surface. Therefore, if prediction approach could be implemented based on the analysis of individual monthly data rather than data set altogether for the whole year, the impact of change in sun position could be substantially avoided. Subsequently, daily irradiance sum is sorted out for individual months. Thereafter, irradiance classes are defined for each month, depending on the minimum and maximum value of irradiance sum. Consequently, for a single month, the possibility of one-day-ahead daily irradiance sum is investigated based on the irradiance class of the previous day. Such investigation reveals that the expected daily irradiance sum could behave much closer to the irradiance class of the previous day, though certain divergence would be possible. In such a way, it is possible to obtain a most probable irradiance class based on the irradiance sum of previous day. Apart from the most probable behavior, it is also possible to obtain an average outcome for the expected daily irradiance sum as an alternative forecasting scheme. Finally, forecasted irradiance sum for each day of individual months as well as forecasted hourly irradiance profiles for each day of individual months are presented.

Having obtained forecasted information for irradiance, consequently research focuses on predicting daily energy gain of a selected solar thermal collector. The collector is chosen from European standard, SPF online collector catalog and daily energy gain is calculated based on the irradiance data, collector model and parameters [13]. As the overall output, energy gain of the solar thermal collector is forecasted based on the forecast irradiance values. Eventually, success of the research outcome has to be investigated thorough a comparison of real data with forecasted data. Hence, the quality of forecasting is presented by means of statistical parameters, monthly bias and monthly RMSE (Root Mean Square Error) for the forecasted daily irradiance sum as well as forecasted hourly irradiance profiles. Theoretical background for this work is revealed in Chapter 2 and the adopted method for the prediction, i.e. probabilistic approach of one-day-ahead forecasting is comprehensively explained in Chapter 3.

1.6 Contributions to the Scientific Society

The thesis work has brought forward and demonstrated an approach to forecast daily energy gain of a domestic solar thermal collector. The proposed method can provide one-day-ahead forecasted information on hourly energy gain of a specified collector, based on previous day values. Such information on available energy gain on tomorrow or future interval, can be applied to build up an efficient energy management system for optimum harvesting of energy out of renewable sources. Based on this type of information the correct design and dimensioning of solar energy systems can be done. For a real time adaption of the system control for optimal system performance forecast information of the irradiance is necessary [4]. Thus, a proper control scheme could be introduced to regulate the contribution of intermittent energy sources based on the demand. In domestic level, if we can predict the next hour energy gain of the collector on our rooftop, we can tight early preparation based on energy demand for next hours. Hence, such scheme provides distinct benefits in both domestic and commercial level.

1.7 Report Outline

The remaining part of the thesis is organized as follows. Chapter 2 introduces the theoretical background of the research with respect to solar irradiance measurement, clear sky calculations and modelling of solar thermal collectors with meteorological parameters. In a nutshell, chapter 2 deepens the background information which is directly influenced to develop the proposed approach of forecasting. Chapter 3 explains the method of irradiance forecasting, beginning at the point where irradiance data and other meteorological parameters are measured. Further, it reveals all necessary calculations to obtain energy gain of a specified collector. Chapter 4 presents the forecasting method of clearness index and Chapter 5 explains the final outcome of the research, forecasting energy gain of a solar thermal collector. Subsequently, Chapter 6 discusses and evaluates the results obtained in Chapters 3, 4 and 5. It compares the forecast quality by evaluating statistical parameters on real measured data and forecast data. Lastly, Chapter 6 concludes the thesis commenting on the overall success. Further it proposes possible improvements as future work.

2. Theoretical Background

This chapter includes the fundamental material which is necessary to implement forecasting approach of energy gain in solar thermal collectors. It is not meant as a general introduction to meteorological parameters although it covers modelling techniques which are essential for the final outcome. For examples, transferring irradiance from horizontal plane to tilted plane, use of satellite derived irradiance data to obtain cloud information, etc. will be presented.

2.1 Solar Irradiance

Solar irradiation is a form of electromagnetic energy produced by the sun. It is measured as the power received on a unit area of the earth's surface. This energy is the driving force of all creatures in the planet. Thus, it is paramount of importance to analyze the behavior of this natural form of energy in order to harvest in maximum scale. Energy is produced through the nuclear reactions in the sun's core and the energy output of the sun's surface is fairly constant. However, on the perceivable surface; earth, solar irradiance "varies significantly from one place to another and changes throughout the year"[14]. The solar irradiance incident on the earth's surface is mainly affected by the position of the sun with respect to the receiving surface. Thus, the key parameters with respect to sun's position, i.e. latitude, declination, solar time, azimuth and their relationships to an inclined plane will be explained in the following sections.

2.1.1 Irradiation Flux Received by the Earth's Surface

Radiation laws describe the radiant flux emitted by sun. It is assumed that sun as a black body emitter with an effective surface temperature of 5780K [4]. As per the laws in Physics, total radiant flux density emitted by a blackbody (M) at temperature T is given by,

$$M = \sigma T^4 \tag{2.1}$$

Where $\sigma = 5.67 \times 10^{-8} Wm^{-2} K^{-4}$ is the Stefan-Boltzmann constant with the value of T=5780K.

$$\begin{aligned} M_{Sun} &= 5.67 \times 10^{-8} \times 5780^4 Wm^{-2} \\ M_{Sun} &= 6.33 \times 10^7 Wm^{-2} \end{aligned} \tag{2.2}$$

Surface are of the sun, A_{Sun} is calculated as; $A_{Sun} = 4\pi r_{Sun}^{\ 2}$ **,** where $r_{Sun} = 6.96 \times 10^8 m$

Total sun radiation flux, $\phi_{Sun} = M_{Sun} \times A_{Sun} = 3.85 \times 10^{26} W$ (2.3)

2.1.2 Solar Constant

The solar constant is the solar radiant flux received on a surface of unit area perpendicular to the sun's direction at the average sun-earth distance outside the earth's atmosphere.

From energy conservation principles the total radiant flux through the surface of the sun (ϕ_{Sun}) equals the flux through any spherical surface concentric to the sun. Especially, for a sphere with a radius r_{ES}, the mean distance between sun and earth (See Figure 2.1),

$$4\pi r_{Sun}^2 M_{Sun} = 4\pi r_{ES}^2 E_{Sc} \tag{2.4}$$

From this, the solar constant, i.e. the solar radiant flux passing through a unit area at the mean distance of the earth from the sun can be found from equation 2.5.

$$E_{Sc} = \left(\frac{r_{Sun}}{r_{ES}} \right)^2 M_{Sun} = 1367 Wm^{-2} \pm 4 Wm^{-2} \tag{2.5}$$

Therefore, with the help E_{Sc}, solar flux received by the cross sectional area of the earth disk as seen by the sun can be calculated,

$$\phi_{Earth} = A_{Earth} E_{Sc} = \pi r^e E_{Sc} \tag{2.6}$$

Where r^e is the mean earth radius 6371 *Km.*

Finally, $\phi_{Earth} = 3.142 \times (6.371 \times 10^6 m)^2 \times 1367 Wm^{-2} = 1.75 \times 10^{17} W.$ (2.7)

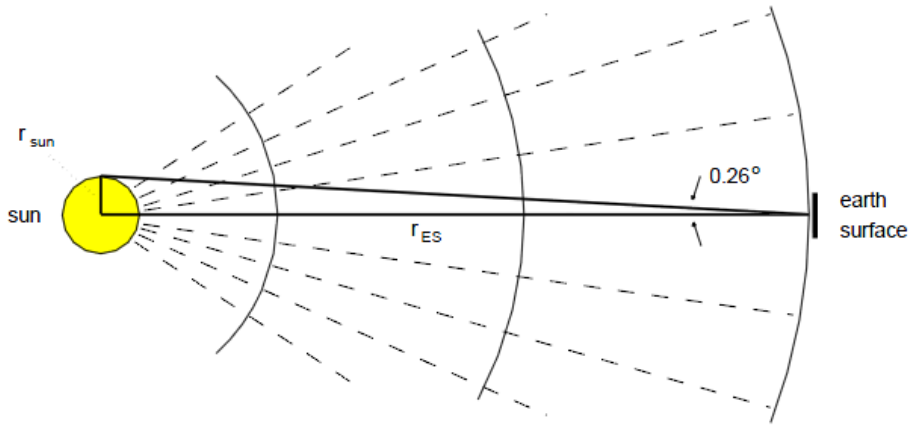

Figure 2.1. Sun-Earth Geometry [4]

2.1.3 Extraterrestrial Irradiation

The intensity of the sun at the top of the earth's atmosphere varies throughout year due to earth's elliptical orbit. Hence, sun-earth distance, r_{ES} varies and it induces certain eccentricity. This difference can be compensated by means of an eccentricity correction factor (ε_0), which had been empirically derived by Spencer, 1971.

$$\varepsilon_0 \approx 1.00011 + 0.034221\cos d + 0.00128\sin d + 0.000719\cos 2d + 0.000077\sin 2d \qquad (2.8)$$

Where $d = 2\pi(n-1)/365$ (2.9)

Simple approach of the equation 2.8 is commonly used,

$$\varepsilon_0 \approx 1 + 0.033\cos\left(\frac{360n}{365}\right) \qquad (2.10)$$

Therefore Extraterrestrial Irradiance can be calculated as;

$$G_{Ext} = \varepsilon_0 E_{Sc} \approx E_{Sc}\left[1 + 0.033\cos\left(\frac{360n}{365}\right)\right] \qquad (2.11)$$

2.2 Sun-Earth Astronomy

2.2.1 Solar Declination

Earth moves along the elliptical plane with a tilted axis of approximately 23.45° with respect to the earth's orbit around the sun (See Figure 2.2). During the summer (Eg. June 21) in northern hemisphere, the orientation of the earth's axis is pointed towards the sun. Also the earth's axis is pointed away from the sun during the winter (Eg. December 22) in northern hemisphere. The angle between the earth's equatorial plane and the plane of its revolution around the sun is called the solar declination δ .

Solar declination for a particular day n, can be expressed as;

$$\delta \approx 23.45 \cdot \sin\left(\frac{360(284+n)}{365}\right) \tag{2.12}$$

Where n varies from 1-365 for a year.

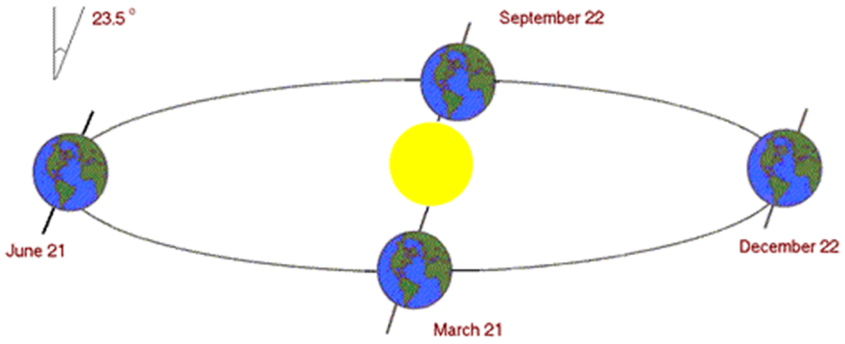

Figure 2.2. Earth's Axis View from Space [15]

2.2.2 Solar and Local Standard Time

Solar time is an important benchmark which is used to calculate the variation of solar irradiance for different locations. Thus, depending on the longitude on the earth surface solar time varies. The relationship between solar time and local standard time is the key to describe the position of the sun. A single day is defined as the time from highest solar altitude to lowest solar altitude. These instances give the noon in true solar time. The average length of this period is defined as 24 hours. Due to the fact that earth does not move on a circle but an ellipse and the fact that the earth axis is not perpendicular to the ecliptic plane, the actual length of day varies during the year. Local time runs each day with exact 24 hours. This difference between the solar time and the local mean time in minutes can be expressed via the equation of time, E in 2.13,

$$E \approx 9.87\sin 2B - 7.53\cos B - 1.5\sin B, \tag{2.13}$$

The standard time is determined by the time zone. Solar time differs from standard time with respect to variations of the length of the solar day and, difference between the local longitude and the standard longitude of the appropriate time zone (See Figure 2.3).

$$True\ \ Solar Time = Local\ Time + E \tag{2.14}$$

Local time depends on local longitude, L_l and the standard time corresponds to the standard longitude, L_s. True Solar Time *(TST)* can be calculated from the Local Time *(LST)*,

$$TST = LST - DST + 4(L_s - L_l) + E \tag{2.15}$$

Where *DST* = 1 hour during daylight saving time and = 0 otherwise.

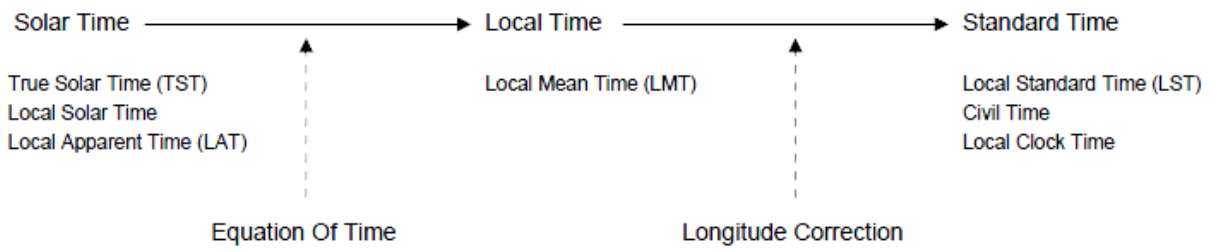

Figure 2.3. Terms of Time and Their Relationships [4]

2.2.3 Hourly Angle

Measurement unit of the *TST* is hours. Hour angle (ω) is defined to make it easy for calculations in equations of Sine and Cos formats. Hour angle equals the angular displacement of the sun from the local meridian due to the rotation of the earth. It is in units of radians. The relationship between hour angle and time is given by,

$$\omega = \pi * (12 - TST)/12 \tag{2.16}$$

The angle of the sun with respect to a line perpendicular to earth's surface is called zenith angle (θ). Also, sun's position relative to the north-south axis is called as the azimuthal angle (ψ).

2.2.4 Position of the Sun

To calculate the irradiance normal to a given tilted plane, it is required to know the position of the sun with respect to that particular plane. Sun's position with respect to sky hemisphere is described by solar altitude, α (elevation above horizon) and solar azimuth, ψ (See Figure 2.4). Sun's altitude is given by,

$$\sin\alpha = \sin\delta\sin\phi + \cos\delta\cos\phi\cos\omega \tag{2.17}$$

The solar azimuth is given by,

$$\cos\psi = \frac{\sin\alpha\sin\phi - \sin\delta}{\cos\alpha\cos\phi} \tag{2.18}$$

The angle of incident, θ stands as the angle between the incoming solar beam radiation and the normal to the receiving surface (See Figure 2.4). This angle depends on geographical location (latitude), solar declination (time of the year), hourly angle (time of the day) and orientation of the tilted surface. Orientation of the plane is described with the slope angle; β between the collector plane and the horizontal surface and, the azimuth angle; γ as the deviation of the normal of the plane from the local meridian.

The angle of incident; θ is given by,

$$\cos\theta = \sin\delta(\sin\phi\cos\beta + \cos\phi\sin\beta\cos\gamma) + \cos\delta\cos\omega(\cos\phi\cos\beta - \sin\phi\sin\beta\cos\gamma) - \cos\delta\sin\beta\sin\gamma\sin\omega \quad (2.19)$$

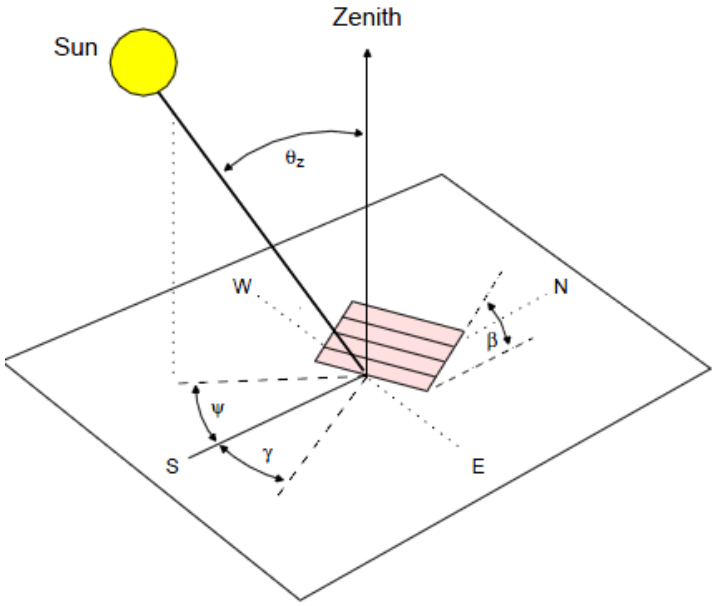

Figure 2.4. Angles to Define the Position of the Sun and the Orientation of a Tilted Plane [4]

2.3 Clearness Index

As solar radiation passes through the earth's atmosphere, some of it is absorbed or scattered by air molecules, water vapor, aerosols, and clouds. The solar radiation that passes through directly to the earth's surface is called direct solar radiation [4]. The radiation that has been scattered out of the direct beam is called diffuse solar radiation [4]. Thus, the global solar irradiance on a horizontal surface is the combination of both direct component of sunlight and the diffuse component of skylight falling together.

Because of atmospheric turbidity and clouds, the incoming radiation is reduced. Such reduction can be quantified by means of the parameter clearness index which normalizes the global irradiance to the extraterrestrial irradiance. Hence, clearness index is a dimensionless number giving the percentage of the reduction of extraterrestrial radiation due to absorption and scattering by air molecules, aerosols, water vapor and clouds. Hourly clearness index, k_t can be defined as,

$$k_t = \frac{Global\ Horizontal\ Irradiance\ (Wm^{-2})}{Extraterrestrial\ Irradiance\ (Wm^{-2})} \tag{2.20}$$

Also daily clearness index K_t can be defined as,

$$K_t = \frac{Global\ Horizontal\ Daily\ Irradiance\ Sum(Wm^{-2})}{Extraterrestrial\ Daily\ Irradiance\ Sum(Wm^{-2})} \tag{2.21}$$

2.4 Solar Irradiance on a Tilted Plane

At present, measurement of irradiance is vastly performed on the horizontal plane. However, for solar energy research and applications, it is required to obtain non horizontal irradiance data for tilted surfaces as it is of interest in solar energy conversion systems. Therefore, data recordings of horizontal irradiation has to be modelled to yield estimates of the irradiance on tilted surfaces. To achieve this, firstly it is necessary to build conversion models on inclined planes.

It is current practice for evaluating the irradiation on a tilted surface (G_t) to decompose the solar radiation into the components; Direct Beam Irradiance, (G_{bt}), Sky Diffuse Irradiance, (G_{dt}) and Ground Reflected Irradiation, (G_{rt}).

$$G_t = G_{bt} + G_{dt} + G_{rt} \tag{2.22}$$

Direct radiation component of the global tilted irradiance can be described as,

$$G_{bt} = G_b \frac{\cos\theta}{\cos\theta_Z} \tag{2.23}$$

Where G_b is the global horizontal radiation and θ, θ_Z are incident angle and zenith angle respectively (See section 2.2.4).

Ground reflected radiation component of the global tilted irradiance can be presented under the assumption that ground reflects irradiation isotropically;

$$G_{rt} = G_b \rho \frac{1-\cos\beta}{2} \tag{2.24}$$

Where $\rho = G_r / G_b$ is the albedo (reflectance) of the surface.

Diffuse radiation component of the global tilted irradiance is presented by the model discovered by Liu and Jordan, 1963. The diffuse sky radiance is assumed to be uniformly distributed (isotropic) over the sky dome. The diffuse radiation on a tilted surface, (G_{dt}) is hence given by the horizontal diffuse radiation and the view factor from the surface to the sky, $(1+\cos\beta)/2$;

$$G_{dt} = G_d \frac{1+\cos\beta}{2} \tag{2.25}$$

Where G_d, global diffuse horizontal irradiance and β, slope of the plane.

Finally, global irradiance on a tilted plane can be obtained through the equation 2.22;

$$G_t = G_b \frac{\cos\theta}{\cos\theta_Z} + G_d \frac{1+\cos\beta}{2} + G\ \rho \frac{1-\cos\beta}{2} \tag{2.27}$$

Global radiation can also be decomposed into their diffuse and global components through empirical models which relate the diffuse fraction to the clearness index. Authors in papers [17], [18], [19], [20], has introduced such methods, however the model discovered by authors, Collares-Pereira and Rabl in paper [18] is commonly used.

2.5 Solar Thermal Collectors

Solar thermal collectors are vastly used to give the hot water supply in domestic requirements, space heating systems, and process heating applications such as powering absorption chillers for solar air conditioning systems, etc.

2.5.1 Flat Plate Solar Thermal Collectors

Depending on the application, various types of collectors can be occupied to absorb solar energy; typically irradiation energy is used to heat up a fluid. For an instance, in solar power plants, parabolic trough collectors are used to generate electricity by heating water to drive turbines [21]. However, for the residential and commercial building applications, flat-plate and evacuated-tube solar collectors are commonly used to collect heat for space heating, domestic hot water or cooling with an absorption chiller.

In this study, a flat plate solar thermal collector is selected from SPF online collector catalog [13] which is based on the European standards. The selected collector; 'Consolar PLANO 27H' consists of fluid pipes with protecting cages and absorbing material built into roofs or building walls with temperatures in the range of [0; 100] *°C.* The collector gives neither a high energy output nor low energy output, but a medium energy output which can fulfill a typical in house energy requirement. The flat plate collector is installed under stationary conditions. Therefore the efficiency of the solar

thermal collector can be described by the stationary or steady-state collector model introduced by EN12975 standard (See Section 2.5.2). Figure 2.5 presents a physical model of the installed collector on a roof top and the sectional view.

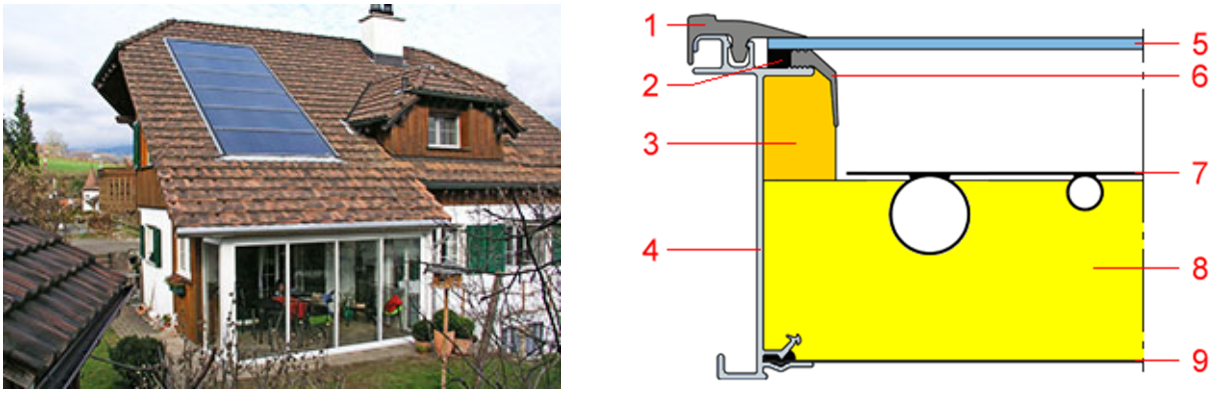

Figure 2.5. Solar Thermal Collector and Sectional View-Consolar PLANO 27H [13]

1	Glass fixing profile	6	Glass support rail
2	Sealing	7	Absorber
3	Lateral thermal insulation	8	Thermal insulation
4	Frame	9	Rear pannel
5	Glazing		

In hot water applications, water is usually circulated through tubing to transfer heat from the absorber to an insulated water tank [The collectors which are operating in colder climates, an anti-freeze liquid is added to the water]. This can be achieved directly or through a heat exchanger. A typical flat plate collector mainly consists a dark plate absorber (7), a back side insulation (8) and a transparent cover (5) that reduces the heat loss to ambient. Heat is usefully removed from the absorber by a heat transport fluid passing through pipes in contact with the absorber. Absorber consists of absorber sheet made of thermally stable materials with a black light absorbing surface. Table 2.1 presents the standard parameters of the collector and, detailed description about the performed testing can be found in the collector data sheet attached in Appendix D.

Table 2.1. Summary of Collector Parameters [12]

General information	
SPF-Nr.	C1194
Model	PLANO 27 H
Type	Flat-plate collector
Manufacturer	Consolar Solare Energiesysteme GmbH
PC, City	DE-60489 Frankfurt a. M.
Telephone	+49 (0)69 7409328 0
E-Mail	info@consolar.de
Internet	www.consolar.com
Dimensions	
Total length	1.178 m
Total width	2.218 m
Empty weight	43.0 kg
Aperture area	2.335 m²
Absorber area	2.258 m²
Efficiency coefficients	
Conversion factor η0	0.813
Loss coefficient a1	3.97 W/(m²K)
Loss coefficient a2	0.0108 W/(m²K²)
Angle factors	
K1, Longitudinal (50°)	0.94
K2, Transversal (50°)	0.94
Typical solar yields	
(With respect to the aperture area)	
Domestic hot water	496 kWh/m²
Water pre-heating	737 kWh/m²
Space heating	328 kWh/m²

2.5.2 Thermal Performance of Solar Thermal Collectors

Solar thermal collectors convert incoming radiation of the sun in to useful heat. Useful heat can be identified as the amount of water heated up to a desired temperature. The efficiency of a typical collector can be defined as,

$$Efficiency\ of\ the\ collector = \frac{Heat\ absorbed\ by\ water}{Incident\ solar\ irradiance\ on\ the\ collector} \tag{2.28}$$

In a solar thermal collector, power losses may exist variety of ways. Part of the irradiance incident on the aperture plate is reflected back to the sky. Also another component is absorbed by the glazing and the rest is transmitted through the glazing and reaches the absorber plate as short wave radiation. Apart from them, as the collector absorbs heat its temperature is getting higher than that of the surrounding and heat is lost to the atmosphere by convection and radiation. Such information about the thermal performance is essential to obtain overall power output of a typical solar thermal collector.

European efficiency standards can be used to obtain a conversion model for the thermal efficiency of a collector presented in equation 2.28. European standard EN 12975, 2000 provides the same test methods and thus comparable results for all collector tests performed in Europe. Also it helps validate the durability, reliability and safety requirements for solar thermal collectors. EN 12975 has introduced two alternative test methods; the steady state test method and the quasi-dynamic test method.

According to European standard EN12975, a model for the collector efficiency η;

$$\eta = \eta_0 - \frac{a_1(T_{collector} - T_{ambient})}{G_t} - \frac{a_2(T_{collector} - T_{ambient})^2}{G_t} \quad (2.29)$$

Where η_0 Zero-loss coefficient *[dimensionless]*

a_1, Heat loss coefficient *[$Wm^{-2}K^{-1}$]*

a_2 Heat loss coefficient *[$Wm^{-2}K^{-2}$]*

G_t Global tilted irradiance on the collector plane *[Wm^{-2}]*

$T_{ambient}$ Ambient temperature *[K]*

$T_{collector}$ Collector temperature *[K]*

Finally, the actual thermal power output of a collector, $\dot{Q}$ can be calculated as;

$$\dot{Q} = \eta * A * G_t \quad (2.30)$$

Where *A* is the aperture area, the area in which the solar radiation enters the collector. This model has been widely used both in testing (ISO 9806-1 and ASHRAE 93-77) and for simulation [23].

3. Irradiance Forecasting

This chapter explains the method which is used to obtain forecast information on solar irradiance. Statistical analysis of the historical data starts with the measured irradiance data as presented in the Section 3.1. The next section focuses on obtaining the solar irradiance in a plane of 45° tilt to the horizontal. For the calculations, solar irradiance parameters and equations as described in Chapter 2 are applied and some of the tools and methods are further annexed at the end in Appendices. The basis of the forecast generating scheme is described in the Section 3.3 and, Section 3.4, Section 3.5 and Section 3.6 describe its application for generating a day-ahead forecast for the daily irradiance sum and the expected irradiance profile for the month, May. At last, the quality of the forecast is investigated by considering the statistical parameters, relative monthly Bias and relative monthly Root Mean Square Error (RMSE) which are normalized to the mean of the measured irradiance. Further discussion is brought forward to the conclusion in Chapter 6.

3.1 Hourly and Daily Mean Values for Measured Irradiance Data

As given in the section 1.5.1, Geomodel Solar, Slovacia [12] provided satellite derived irradiance data covering seven years. They include Global Horizontal Irradiance (GHI), Diffuse Horizontal Irradiance (DIF), Global Tilted Irradiance (GTI) and collocated air Temperature. Table 3.1 shows a sample of data with time resolution of 15 minutes. Based on this set, a scheme to obtain one-day ahead forecast information of the daily irradiance sum and subsequently the daily irradiance profiles on hourly basis should be set up. For this as the first step of analysis, it is necessary to convert the minutely time resolved original set into hourly and daily mean values. Original spreadsheet which the sample data set (Table 1.1) is extracted, poses 219786 amount of data for 54938 hours of 07 years, starting from 01/01/2007 to 07/04/2013.

Table 3.1. Sample Data: Calculated Hourly Mean Values

Day	**Hour**	**Hourly mean GHI(Wm^{-2})**	**Hourly mean DIF (Wm^{-2})**	**Mean Temperature (°C)**
1/1/2007	0	0	0	8.325
1/1/2007	1	0	0	7.95
1/1/2007	2	0	0	7.65
----------	----	---------	--------	--------
1/2/2007	0	0	0	5.85
1/2/2007	1	0	0	5.75
1/2/2007	2	0	0	5.65
1/2/2007	3	0	0	5.55
1/2/2007	8	7.75	7	5.5
1/2/2007	9	60.75	36.25	5.575
1/2/2007	10	59.5	52	5.725
…….	…..	……..	……	…….
4/7/2013	21	0	0	-1.175
4/7/2013	22	0	0	-0.475
4/7/2013	23	0	0	0.275

3.2 Obtaining the Irradiance on a Tilted Plane of 45°

Although the set supplied by Geomodel contains data an inclined plane of 20° to the horizontal, a procedure to estimate global tilted irradiance on 45° inclined is set up, as it has been recognized that the tilt of 45° degree gives better collector output with a higher energy gain.

The equations which are necessary to obtain the irradiance on a tilted plane was presented in Chapter 2. It should be noted that, the calculations have to be performed on every hour for 54935 days over 7 years.

The measurements have been taken on local time intervals. But calculations are performed on True Solar Time (TST). Therefore, firstly local time has to be converted in to TST. This can be achieved by using equation 2.13 and 2.15. Having known the True Solar Time, the next attempt was to calculate hourly angle (ω) which is presented in equation 2.16. When, earth moves along the elliptical plane, the angle between earth's equatorial plane and the plane of its revolution around the sun, i.e. solar declination, δ changes day by day. Therefore, for each day, solar declination is calculated using equation 2.12. It should be noted that our location, Kristiansand city is given with north-east latitude, 58.153° and longitude, -8.002°. As the next step sun's altitude, α can be calculated for a given hour angle, solar latitude and solar declination by using equation 2.17.

The angle of incident; θ for a given tilted plane of 45° is a key parameter which is needed to be determined for the estimation of the direct irradiance on the tilted plane. Equation 2.19 can be directly applied to obtain the angle of incident provided that solar azimuth angle; ψ is known. Solar azimuth angle can be obtained using equation 2.18 and the surface azimuth angle, γ is counted clockwise from North where its value is zero on both hemispheres.

As explained in Chapter 2, for estimating the tilted irradiance all three components; direct, diffuse and ground reflected irradiance have to be converted separately. As global horizontal irradiance is available in the measured data, equation 2.23 can be applied to obtain the direct beam irradiance component. For the diffuse radiation component, the Liu and Jordan model as given by equation 2.25 is applied. For the ground reflected irradiance, equation 2.24 can be used. The global tilted irradiance is gained by taking the summation of above three components (Equation 2.22 and Equation 2.27). To illustrate the calculated values, Figure 3.1 compares the measured horizontal irradiance and calculated tilted irradiance for two days, January 2007. Further, Figure 3.2 presents the relationship between recorded maximum hourly tilted irradiance and the sum of daily tilted irradiance for seven years. It is quite clear that, for low values of irradiance sum and high values of irradiance sum, the characteristic behaves in nonlinear scale.

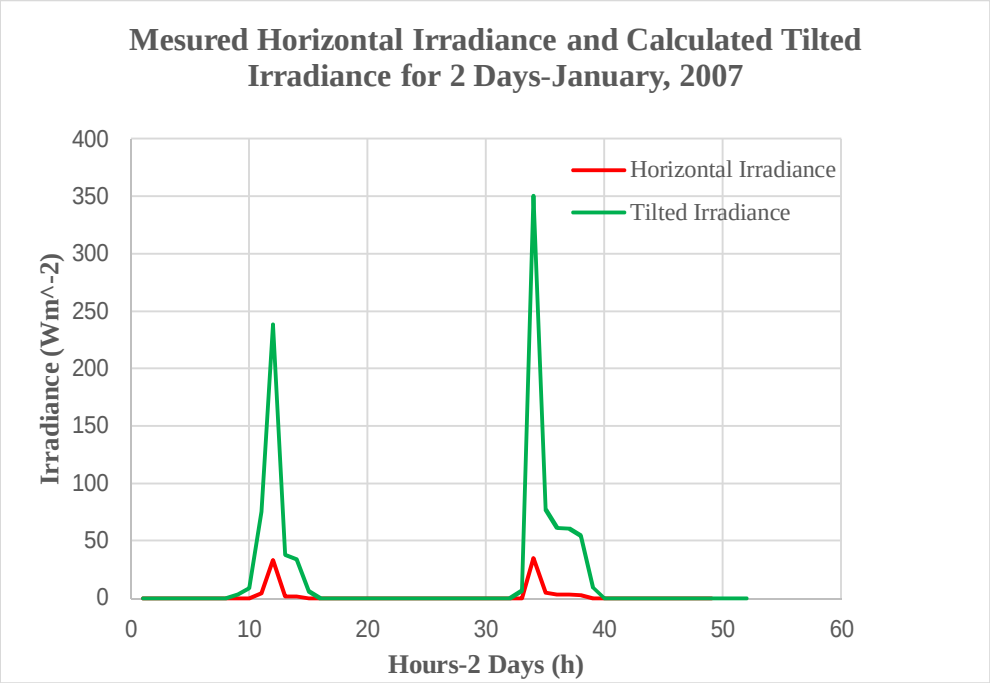

Figure 3.1. Horizontal and Tilted Irradiance for Two Conseqetive Days-January, 2007

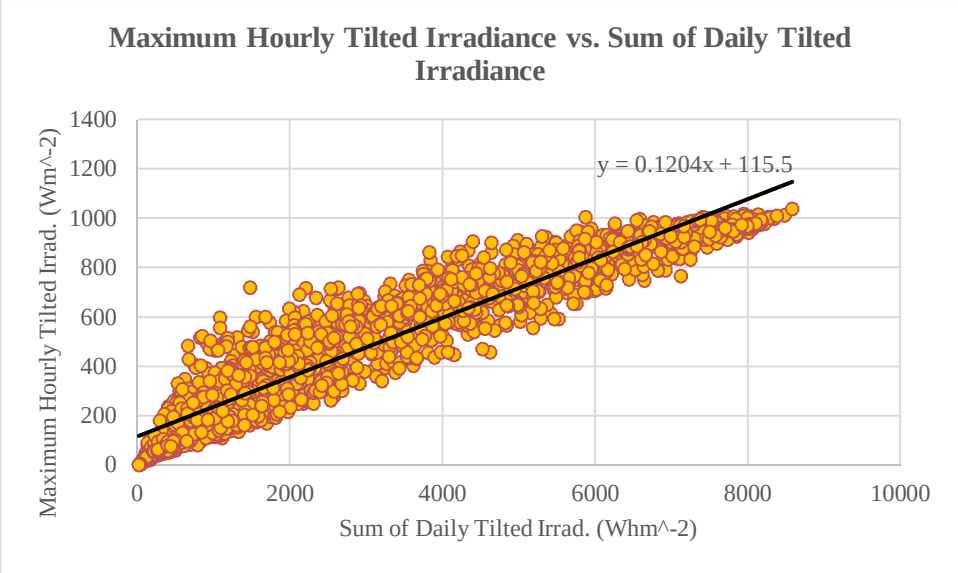

Figure 3.2. Maximum Hourly Tilted Irradiance vs. Sum of Daily Tilted Irradiance

3.3 Analysis of the Statistical Characteristic of the Historical Irradiance Data

In this section, a forecast scheme should be set up based on statistical analysis of the available historical data over seven years. For this it is assumed that the irradiance sum of today shows a dependence on the irradiance sum of yesterday (Markov Assumption [24]). However, this dependency may not be considered as a strict dependence, but in the statistical sense as will be shown in the following. In this analysis, we are going to quantify this dependency. Further, this approach is explained through an example of irradiance data for the month of May. This assess the day to day dependency of the irradiances sums, the conditional probability distribution of the irradiance sum for a given status of weather when the day before is analysed.

Further as an illustration, for the month of May, lowest irradiance sum is recorded as 1085.82 Whm^{-2} and highest irradiance sum is recorded as 8265.397 Whm^{-2}. Thus, irradiance sum ranges from 0 Whm^{-2} to 9000 Whm^{-2} . The irradiance sums are classified into nine classes, equally spaced between the minimal and the maximal daily sum. Figure 3.3 gives an example for this conditional probability.

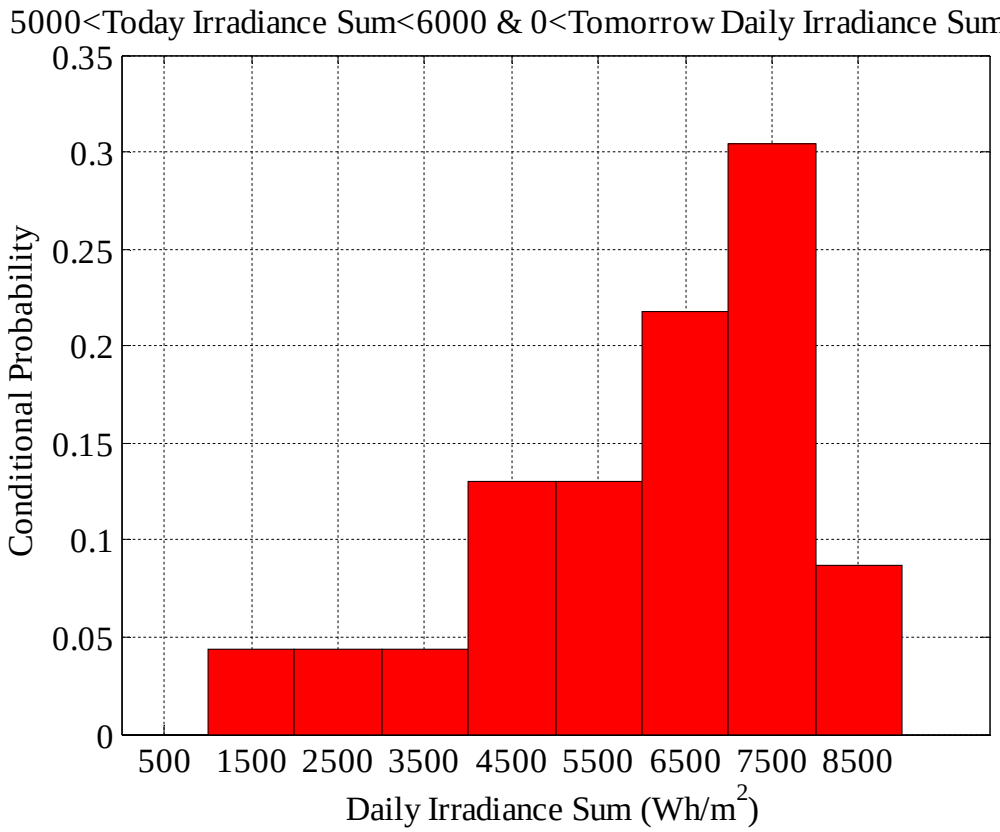

.

Figure 3.3. The Conditional Probability Distribution of the Today's Irradiance Sum, Given that the Previous Day was in the Class of Daily Irradiance $5000 Wh/m^2 < Sum < 6000 Wh/m^2$

Figure 3.3 shows a conditional probability distribution of tomorrow's irradiance sum for today's sum is within a class, $5000 Wh/m^2 < sum < 6000 Wh/m^2$ for the measured tilted irradiances of month-May, based on 186 (31x6) days. X-axis denotes the irradiance classes having a range of (0-9000) Whm^{-2} and y axis gives the probability of having irradiance in the different classes. The probabilities are calculated according to,

$$\Pr obability = \frac{Number\ of\ \ days\ which\ weather\ belongs\ to\ a\ \ particular\ class}{Total\ \ number\ of\ \ days\ in\ all\ the\ classes} \qquad (3.1)$$

Basically, equation 3.1 can be as well applied to irradiance, clearness index, power output of a collector, etc. As given in Figure 3.3, when today irradiance sum is belongs to a certain class of daily irradiance sum, tomorrow's irradiance can be presented by a conditional probability

distribution. The prime idea behind this probabilistic approach is, exploiting the possible dependency of today's irradiance information to forecast tomorrow's values. This approach is called as forecasting based on Markov model which has been widely used in many other irradiance modelling applications. Having knowledge about the conditional probability distributions, next sections focus on how to make use of it in our forecasting scheme.

3.4 Forecast Generating Scheme

Here we have to assume that the actual probability distributions are not different from those of the historical data analyzed. At this point we have obtained forecasted information about tomorrow's weather as a conditional probability distribution. However, it is required to obtain values for forecasting rather than a probability distribution. It is possible to obtain a single forecast value considering the center value of the most probable class. The forecast can also be achieved by calculating the average value expected from probability distribution. Now research focusses on generating forecasted values under above two options.

3.4.1 Generating Forecast based on Most Probable Behavior

The most probable class in the probability distribution can be picked up easily. It is the class with highest probability, i.e. the tallest one (See Figure. 3.4). If there are more than one most probable classes, i.e. few classes with the same height, we can decide the most probable class by considering the closest behavior for today's weather. Having picked up the most probable class, it is possible to sort out relevant days which give the most probable behavior. Having sorted out the days in most probable class, respective daily irradiance sum can be captured. If we know the irradiance sum for each individual day of the most probable class, it is possible to obtain the mean value for daily irradiance sum. For a typical irradiance class of today, tomorrow's irradiance forecast based on the most probable class can be expressed as, MPI which is the average of all daily sums in that class or

$$MPI = \frac{Irradiance\ sum\ of\ the\ days\ which\ give\ the\ most\ probable\ behavior}{Number\ of\ days\ in\ the\ most\ probable\ class} \qquad (3.2)$$

Bases on the daily sum, it can be tested whether an expected daily irradiance profile spanning over 24 hours can be defined. Having knowledge about the days in most probable class, respective daily irradiance pattern can be identified from the measured data. For an example, if there are five days in the most probable class, there will be 24x5 amount of irradiance data on hourly basis. Thus, each day, each hour (24 hours) occupies different irradiance data. To obtain the forecasted daily irradiance pattern, we can simply calculate the mean value for each hour by considering available data in 5 days. If there will be *n* number of days in the most probable class, corresponding mean irradiance for hour j,

$$G\_mean\,(j) = \frac{\sum_{i=1}^{n} Irradiance\ for\ hour\ j\ on\ n^{th}\ day}{n} \tag{3.3}$$

This defines the 24 hourly values for the expected irradiance profile under the condition of yesterday's irradiance class.

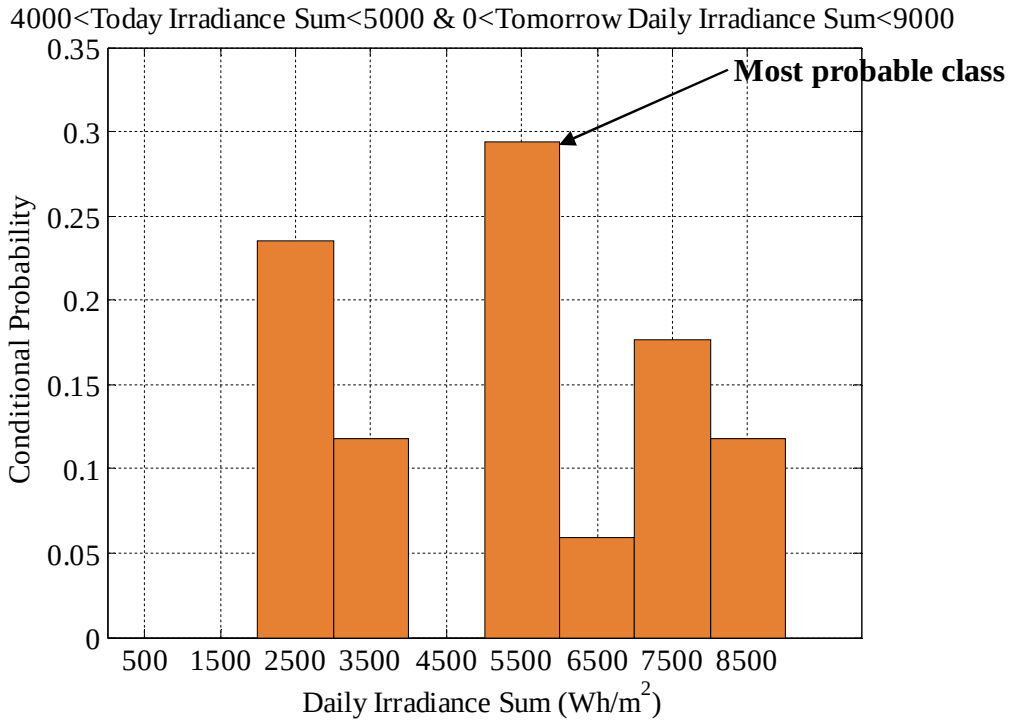

Figure 3.4. Conditional Probability Distribution for Tomorrow's Irradiance Sum for Today's Irradiance Sum is in between 4000 Whm^{-2} and 5000 Whm^{-2} for the month-May

Moreover, Figure 3.5 depicts the daily irradiance patterns for different days in the most probable irradiance class and the average irradiance pattern which can be generated by calculating the mean values. Alternatively, mean irradiance pattern has been graphically demonstrated in the Figure 3.5.

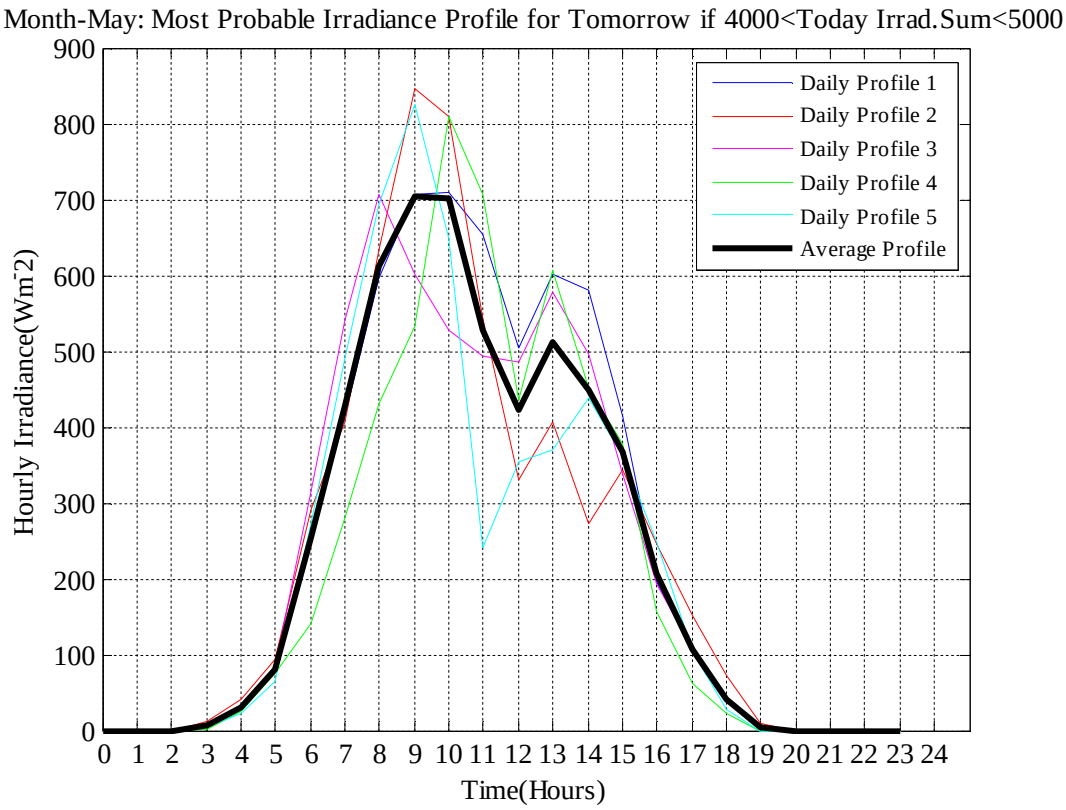

Figure 3.5. Daily Irradiance Patterns in the Most Probable Class and Resulted Average Daily Irradiance Pattern for Tomorrow's Irradiance Sum, if Today's Irradiance Sum is in between 4000 Whm^{-2} and 5000 Whm^{-2} for the month-May

3.4.2 Generating Forecast based on Average Values of the Irradiance Classes

Let's consider obtaining a point forecast based on average values of the available probabilities. On the basis of today's irradiance class, a single forecast value or point forecast may be given as the mean of the conditional probability distribution. Figure 3.4 illustrates a typical tomorrow's probability distribution provided that today's irradiance sum is in between 4000 Whm^{-2} and 5000 Whm^{-2}. The most probable irradiance class represents the irradiance sum in between 5000 Whm^{-2} and 6000 Whm^{-2}. The expected average irradiance; $\overline{H}$ from this conditional distribution is given by,

$$\overline{H} = \frac{Irradiance\ sum\ all\ the\ days\ within\ the\ previous\ day\ irradiance\ class}{Number\ of\ days\ within\ the\ previous\ day\ irradiance\ class} \tag{3.4}$$

A similar approach which was used in obtaining daily pattern can be applied to capture the respective daily pattern for average forecasting. Here, number of days are always higher than a typical most probable irradiance class. Finally, if there will be *n* number of days in the probability profile which gives tomorrow's weather based on a typical today's weather class, corresponding mean irradiance for the 01^{st} hour can be expressed using the same equation 3.2. Subsequently, daily irradiance pattern can be achieved with respect to the results in Table 3.1. Alternatively, obtaining average daily irradiance pattern can be graphically demonstrated as in the Figure 3.6.

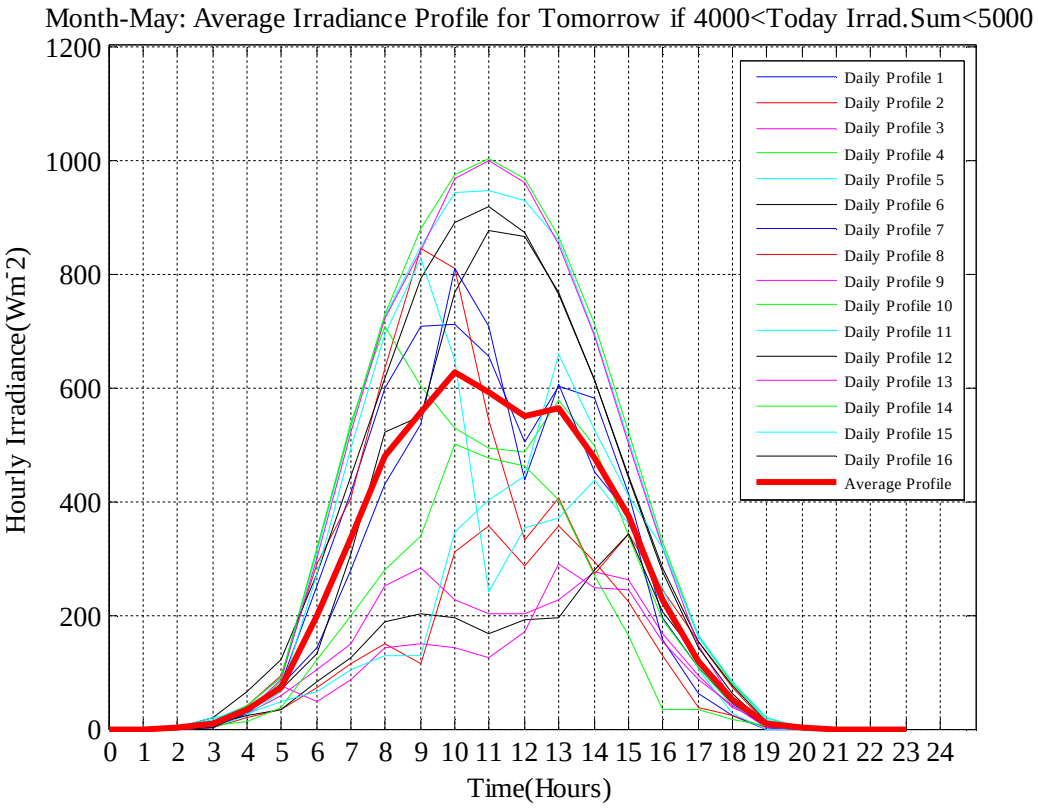

Figure 3.6. Daily Irradiance Patterns in All Probability Classes and Resulted Average Daily Irradiance Pattern, for Tomorrow's Irradiance Sum if Today's Irradiance Sum is in between 4000 Whm^{-2} and 5000 Whm^{-2} for the month-May

3.5 Illustration of Generating Schemes-Month, May

As the final step, it is required to obtain conditional probability distributions and apply forecasting generating scheme for each month individually. Successively, single value for forecast has to be achieved over twelve months. Since, the forecasting approach is similar for every individual month, methodology for all twelve months is not presented here. A month in summer period, i.e. May is considered to illustrate the procedure in detail. Moreover, results on monthly forecast for twelve months are given in Appendix A.

For this forecast, hourly irradiance values and daily irradiance sum for the month of May in each individual year has to be sorted out. In the measured data, hourly and daily values of May are available for six years. Hence altogether, historical data are available for of 186 (31x6) days. However, first day of the month is omitted when data sequence moves from one year to next year. For an instance, at the end of 31st May 2007, next day would be 02nd of May 2008 and likewise at the end of 31st of May 2008, next day would be 02nd of May 2009. Such elimination assures the higher accuracy of day-ahead forecasting. When the first day of the month is eliminated for each year, we can still analysis 181(31x 6-5) days. Also it should be noted that, 01st of May 2007 could be still considered as it is necessary to obtain the forecasted information of 2nd of May 2007.

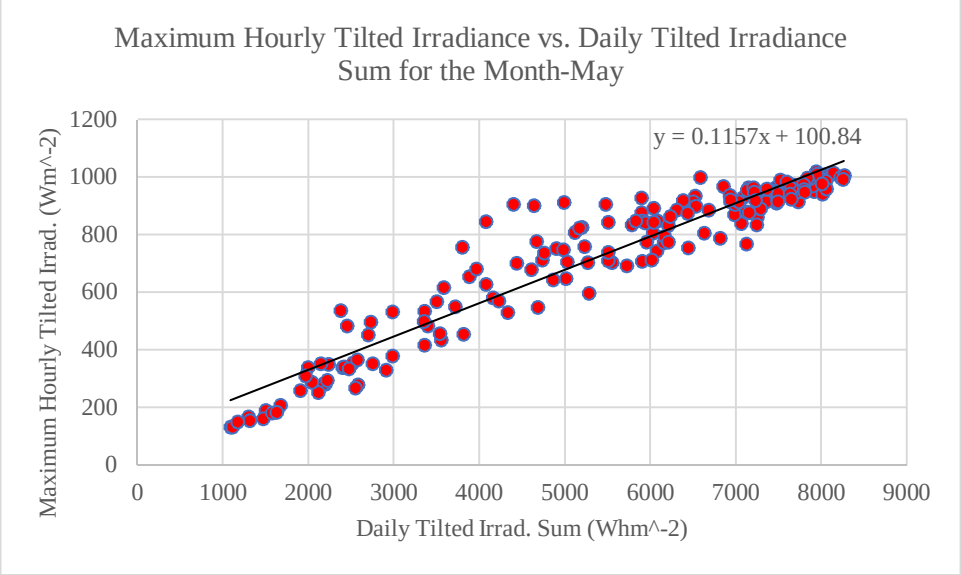

Figure 3.7. Maximum Hourly Tilted Irradiance vs. Daily Tilted Irradiance Sum for the Month-May

For the month of May, a maximum of 8265.397 Whm^{-2} and a minimum of 1085.82 Whm^{-2} for irradiance value is recorded (See Figure 3.7). As the next step, daily irradiance sum is divided in to 9 classes; i.e. $(0 \leq Daily\ Irrad. < 1000)\ Whm^{-2}$, $(1000 \leq Daily\ Irrad. < 2000)\ Whm^{-2}$, and so on, finally $(8000 \leq Daily\ Irrad. < 9000)\ Whm^{-2}$. Number of classes is decided by the range between minimum and maximum values of irradiance sum.

Such division easily allows to adopt a probabilistic approach in terms of conditional probability of the day ahead irradiance sum which depends on the irradiance sum of the previous day (See the explanation in Section 3.4). Finally based on the irradiance class of the previous day, conditional probabilities for the next day were obtained.

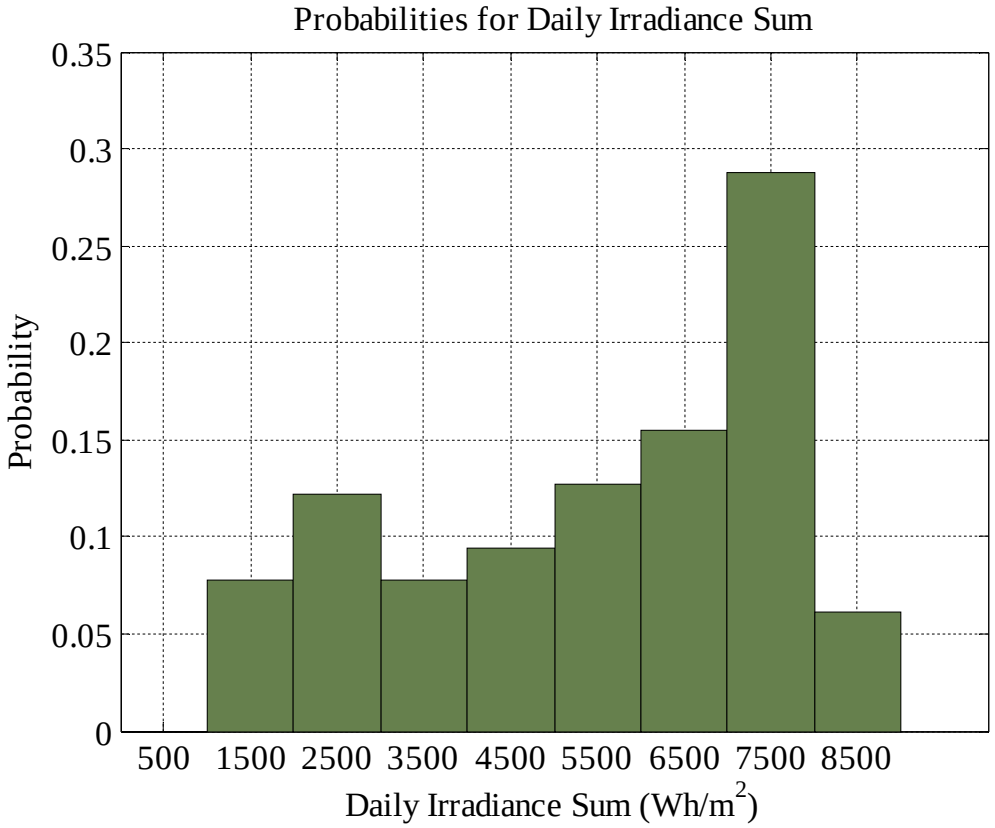

Figure 3.8. Probability Distribution for Available Irradiance Data on Month-May

Figure 3.8 presents the probability distribution for the daily irradiance on May based on historical data over seven years. There was no irradiance value recorded in the lowest class *(0≤ Daily Irrad.<1000) Whm*$^{-2}$. Also, as the most necessary step, the conditional probability distributions for the day ahead irradiance sum, were obtained based on the irradiance class of the previous day. Figure 3.9 to Figure 3.17 presents conditional probability distributions for nine irradiance classes. These figures provide key information about behavior of the irradiance on the following day. In each probability distribution, it is possible to identify a most probable irradiance class which stands with the highest conditional probability. Based on the most probable class of irradiance we can introduce the first prediction scheme as the most probable irradiance forecast of one day ahead.

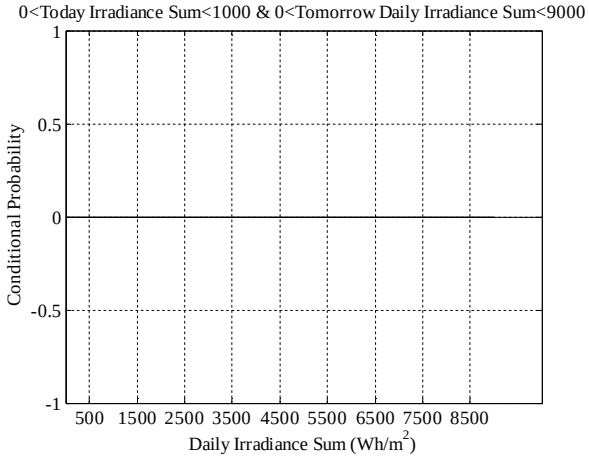

Figure 3.9. Conditional Probability Distribution for Tomorrow's Irradiance Sum for Today's Irradiance Sum is in between 0 *Whm*$^{-2}$ and 1000 *Whm*$^{-2}$ in May

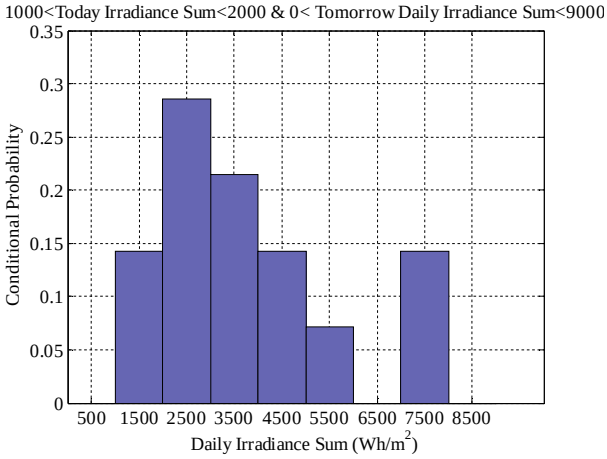

Figure 3.10. Conditional Probability Distribution for Tomorrow's Irradiance Sum for Today's Irradiance Sum is in between 1000 *Whm*$^{-2}$ and 2000 *Whm*$^{-2}$ in May

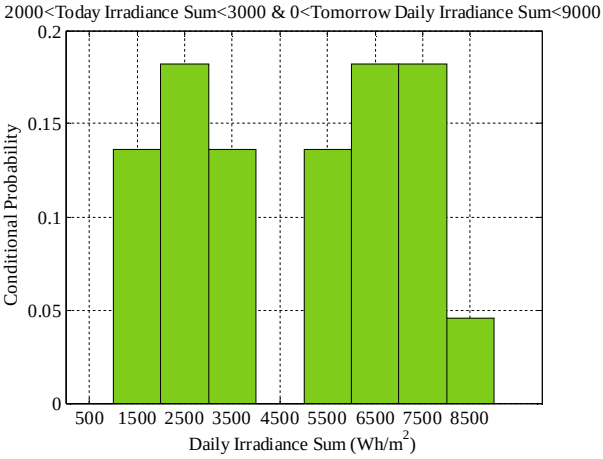

Figure 3.11. Conditional Probability Distribution for Tomorrow's Irradiance Sum for Today's Irradiance Sum is in between 2000 *Whm*$^{-2}$ and 3000 *Whm*$^{-2}$ in May

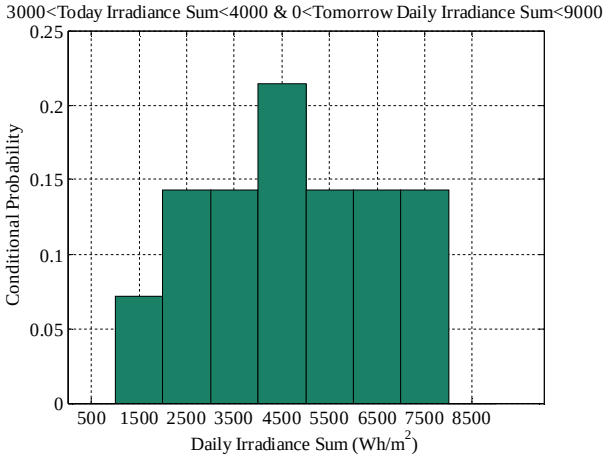

Figure 3.12. Conditional Probability Distribution for Tomorrow's Irradiance Sum for Today's Irradiance Sum is in between 3000 *Whm*$^{-2}$ and 4000 *Whm*$^{-2}$ in May

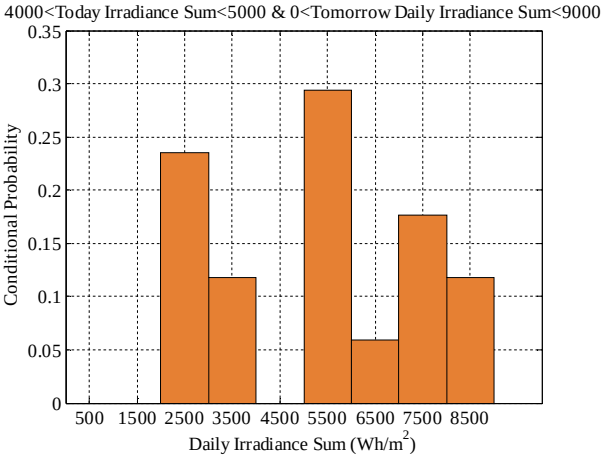

Figure 3.13. Conditional Probability Distribution for Tomorrow's Irradiance Sum for Today's Irradiance Sum is in between 4000 Whm^{-2} and 5000 Whm^{-2} in May

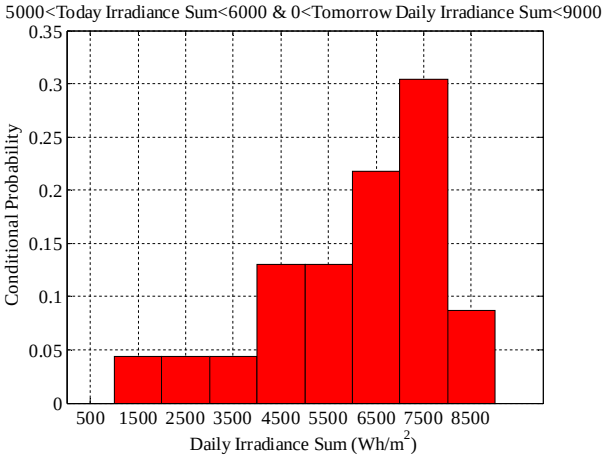

Figure 3.14. Conditional Probability Distribution for Tomorrow's Irradiance Sum for Today's Irradiance Sum is in between 5000 Whm^{-2} and 6000 Whm^{-2} in May

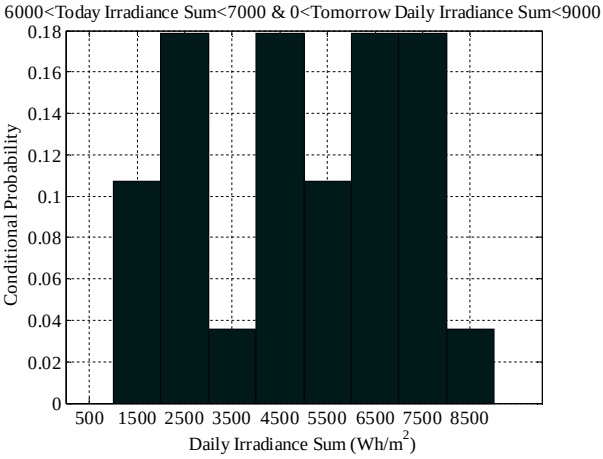

Figure 3.15. Conditional Probability Distribution for Tomorrow's Irradiance Sum for Today's Irradiance Sum is in between 6000 Whm^{-2} and 7000 Whm^{-2} in May

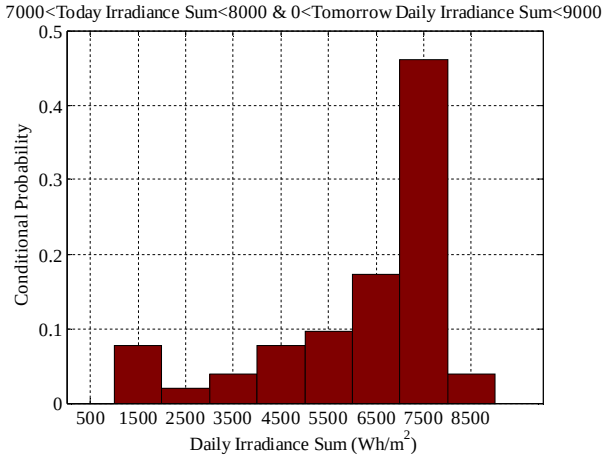

Figure 3.16. Conditional Probability Distribution for Tomorrow's Irradiance Sum for Today's Irradiance Sum is in between 7000 Whm^{-2} and 8000 Whm^{-2} in May

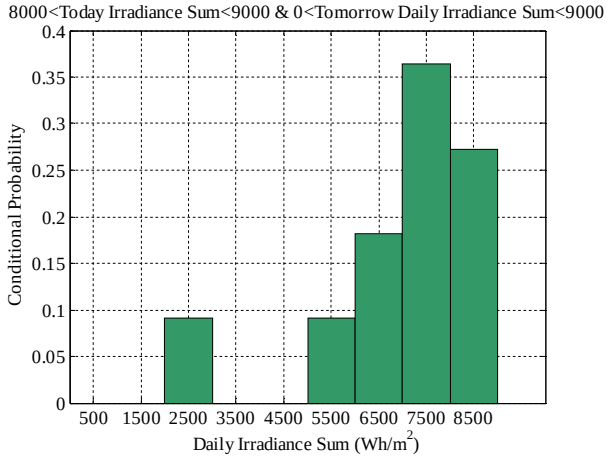

Figure 3.17. Conditional Probability Distribution for Tomorrow's Irradiance Sum for Today's Irradiance Sum is in between 8000 Whm^{-2} and 9000 Whm^{-2} in May

Having identified the most probable class of irradiance for the following day, it can be extended to obtain the most probable daily irradiance pattern on hourly basis.

Apart from the most probable behavior, it is also possible to obtain the average values for the forecasted probability distributions under different irradiance classes depicted in Figure 3.9 to Figure 3.17. It allows to introduce the second forecasting scheme, i.e. the prediction obtained through the average irradiance sum of the following day which is based on the irradiance class of the previous day. Figure 3.18 shows an example of forecasted hourly irradiance pattern obtained for the today's irradiance class in between 4000 Whm^{-2} and 5000 Whm^{-2} in May, 2012. It also compares the forecast with mesured daily pattern.

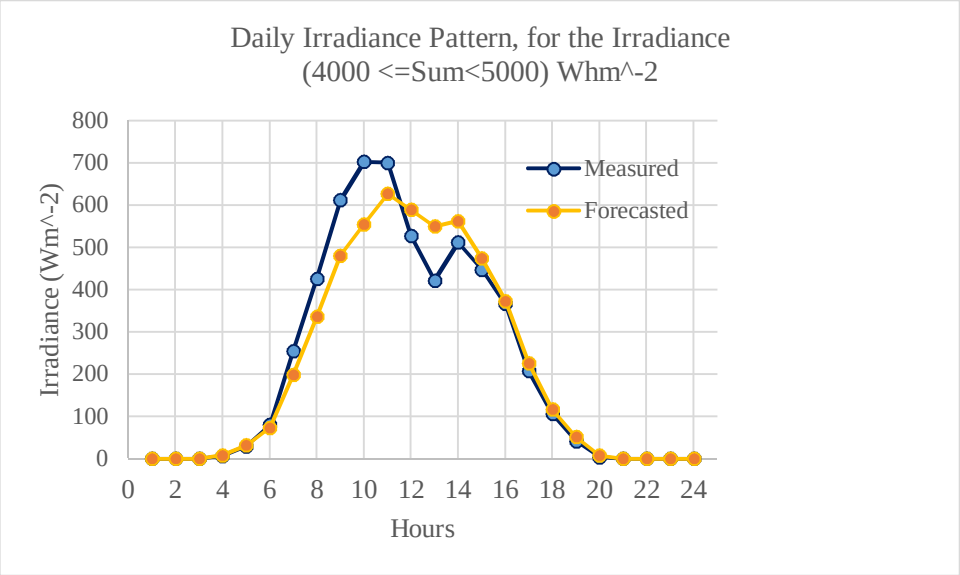

Figure 3.18. Comparison of Measured and Forecasted Daily Irradiance Pattern for the Month May, 2012 based on the Today's Irradiance (4000< Sum<5000) Whm^{-2}

3.6 Quality of Irradiance Forecasting

In this section the quality of the forecast scheme presented, is assessed. For this, the conditional probability distributions are derived for each month on the bases of 07 years, 2007-2013. The forecasting is performed over the twelve months of year 2012. So far we are successful of obtaining single point forecasted values for daily irradiance sum and, consequently forecasted daily irradiance pattern over 24 hours. The forecasting was achieved under two different forecasting approaches. The first one was based on the most probable behavior of the irradiance classes and the second scheme was based on calculated average value of the irradiance over the probability distribution.

Having forecasted values, next step is to investigate the accuracy of the forecast in terms of quality tests. For this, most recently measured values are compared with the forecasted values. The most recent monthly data for May 2012, we can present the irradiance time series in view of the daily values as well as hourly values. Figure 3.19 compares the measured irradiance with the forecasted irradiance for the most probable forecasting scheme and Figure 3.20 shows the same comparison for average forecasting scheme.

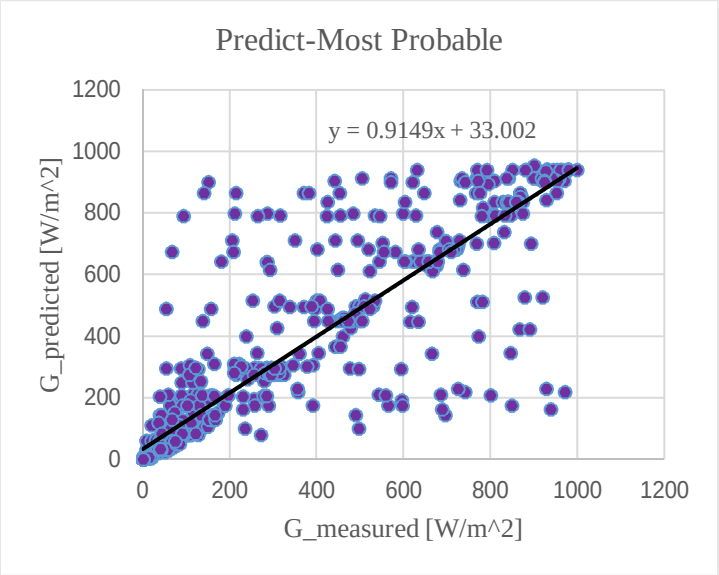

Figure 3.19. Forecasted Irradiance vs. Measured Irradiance for the Month-May, 2012 under Most Probable Forecasting Scheme

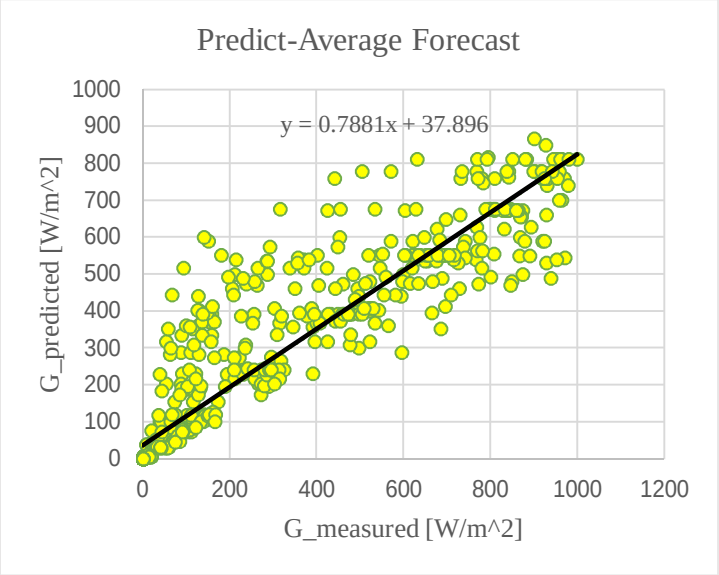

Figure 3.20. Forecasted Irradiance vs. Measured Irradiance for the Month-May, 2012 under Average Forecasting Scheme

When forecasted values are compared with measured values, it becomes quite clear that, Figure 3.19 shows more scatter leading to less accurate forecasting, whereas Figure 3.20 shows less scatter leading to high accurate forecasting. Thus it is proved that the average forecasting scheme which is represented by Figure 3.20 is the better choice for obtaining more accurate forecasted

values. The quality of the forecast can also be investigated by calculating the Monthly Bias and Root Mean Square Error (RMSE) which is normalized to the monthly mean.

Relative Monthly Bias for the daily irradiance can be defined as,

$$\text{Re}lative\ Monthly\ Bias = \frac{\sum_{i=1}^{N} \frac{1}{N} (Measured\ \ Irradiance(i) - Forecasted\ \ Irradiance(i))}{Monthly\ Mean\ of\ \ the\ Measured\ \ Irradiance} \tag{3.5}$$

Relative Monthly RMSE for the daily irradiance can be defined as,

$$\text{Re}lative\ Monthly\ RMSE = \frac{\sqrt{\frac{1}{N} \sum_{i=1}^{N} (Measured\ \ Irradiance(i) - Forecasted\ \ Irradiance(i))^2}}{Monthly\ Mean\ of\ \ the\ Measured\ \ Irradiance} \tag{3.6}$$

Above equations can be used to calculate monthly bias and RMSE for daily irradiance sum. Also the same can be applied to assess the quality of daily irradiance pattern as well. Irradiance in a single day spans over 24 hours, thus for a typical month, 724 (24x30) amount of measured and forecasted irradiance data has to be included to obtain monthly bias and monthly RMSE.

Equation 3.5 and 3.6 can be applied to assess the quality of adopted two forecasting schemes; most probable forecasting and average forecasting. Apart from that, we can apply them to differentiate our forecasting scheme with a very basis persistent forecasting scheme. In the persistent forecasting, it is assumed that tomorrow's behavior is exactly similar to today's behavior. Thus, we expect today's irradiance for tomorrow's forecasted irradiance. Table 3.2 depicts the comparison of all three forecasting schemes for the month of May.

Table 3.2. Quality Comparison for Different Forecasting Schemes

Forecasting Scheme	**Relative Monthly Bias for Daily Irradiance Pattern**	**Relative Monthly RMSE for Daily Irradiance Pattern**
Persistent forecasting	0.030	0.58
Most probable forecasting	-0.051	0.601
Average forecasting	0.055	0.481

As shown in the Table 3.2, least RMSE is recorded for average forecasting scheme. Also a high RMSE is recorded for the persistent scheme. Therefore it is proved that our probabilistic approach of forecasting stands taller as far as concerning the accuracy of the output. We can say, probabilistic approach really offers better information than the naïve forecast. Quality information about other eleven months are presented in the Chapter 6.

Figure 3.21 and Figure 3.22 compare the daily time series on predicted irradiance and measured irradiance with respect to different approaches of forecasting in May, 2012. The curves display the variations between measured and forecasting values. By observing the behavior of curves, it can be concluded that, average forecasting scheme offers better results with less divergences.

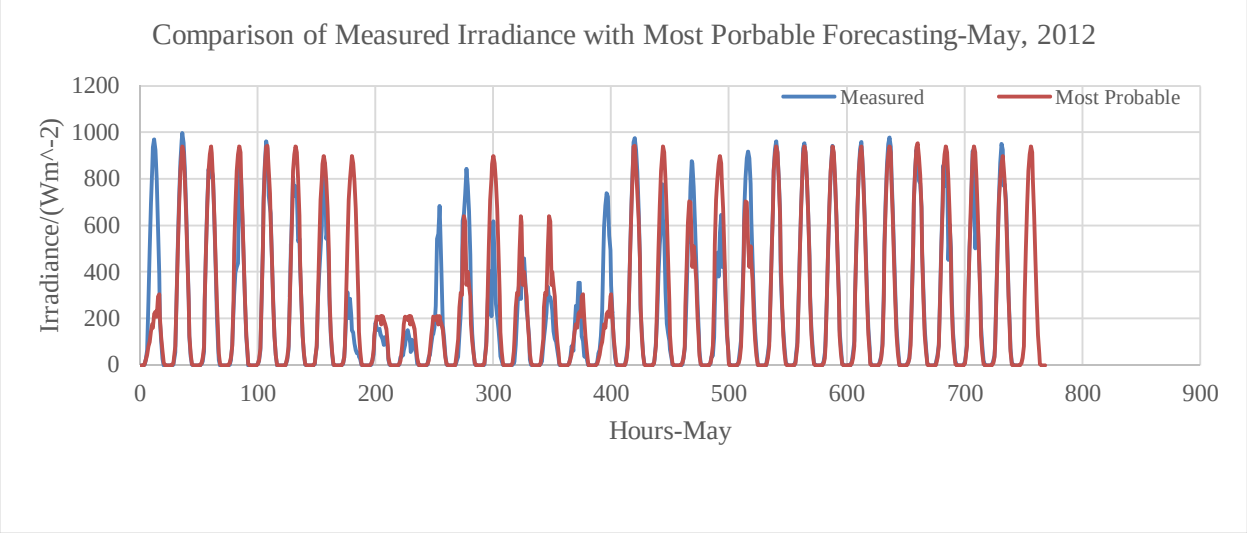

Figure 3.21. Daily Time Series for Measured and Forecasted Irradiance-May, 2012 under Most Probable Forecasting Scheme

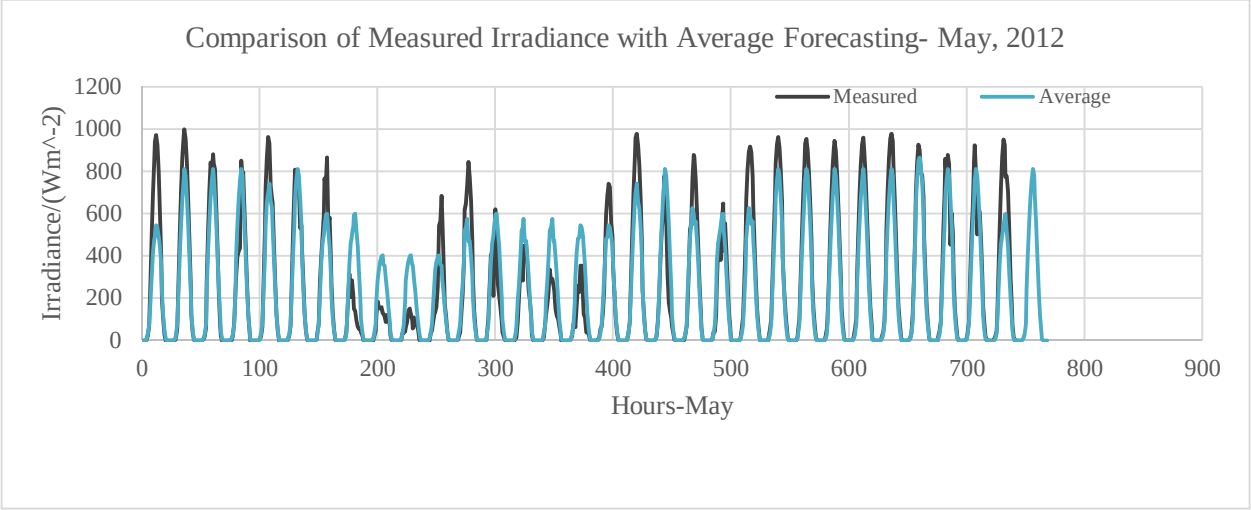

Figure 3.22. Daily Time Series for Measured and Forecasted Irradiance-May, 2012 under Average Forecasting Scheme

4. Clearness Index Forecasting

Overall, the chapter explains the procedure to obtain the forecasted values for the clearness index using the same probabilistic approach which was used in irradiance forecasting. Section 4.1 illustrates method of calculating the clearness index on hourly basis as well as daily basis. Forecasting approach is shortly explained and the quality of forecasting is investigated in the Section 4.2 and 4.3. Remarks on this forecasting is given in Chapter 6.

4.1 Calculation of Clearness Index

In this research, clearness index is calculated on hourly basis and daily basis. Equation 2.20 can be directly used to calculate the hourly clearness index (k_t) out of measured global horizontal irradiance and extraterrestrial irradiance. Clearness index varies hour to hour, thus daily clearness index (K_t) can be calculated by using daily horizontal global irradiance and daily extraterrestrial irradiance as depicted in the equation 2.21.

Table 4.1 shows a sample data set of calculated hourly clearness index and Table 4.2 shows the daily clearness index.

Table 4.1. Hourly Clearness Index

Date	Hour	k_t
5/1/2007	0	0
5/1/2007	1	0
5/1/2007	2	0
5/1/2007	3	0
5/1/2007	4	0.724
5/1/2007	5	0.694
……..	……	……..
4/30/2012	15	0.334
4/30/2012	16	0.263
4/30/2012	17	0.223
4/30/2012	18	0.123
4/30/2012	19	0
4/30/2012	20	0
4/30/2012	21	0
4/30/2012	22	0
4/30/2012	23	0

Table 4.2. Daily Clearness Index

Day	Daily Kt
1/1/2007	0.272
1/2/2007	0.313
1/3/2007	0.227
1/4/2007	0.312
1/5/2007	0.276
1/6/2007	0.397
…….	……..
11/1/2012	0.245
11/2/2012	0.511
11/3/2012	0.201
11/4/2012	0.290
……..	…….
4/3/2013	0.758
4/4/2013	0.758
4/5/2013	0.694
4/6/2013	0.602
4/7/2013	0.732

4.2 Clearness Index Forecasting Approach

Forecasting scheme for the clearness index is basically the same which was implemented in irradiance forecasting. Here, only the irradiance variable is changed as clearness index. Hence, instead of irradiance classes, now we have to define clearness index classes based on daily sum of the clearness index. As similar to irradiance forecasting, two approaches are used to generate forecasted values, i.e. the forecasting based on most probable behavior of the clearness index class and the calculating the average clearness index out of probability distribution. Figure 4.1 displays the forecasted conditional probability distributions for the clearness index on month-May. The minimum sum of the hourly values of clearness index in single day, iss found as 1.85 and the maximum is 11.96. Therefore, twelve classes are defined to obtain conditional probability distributions.

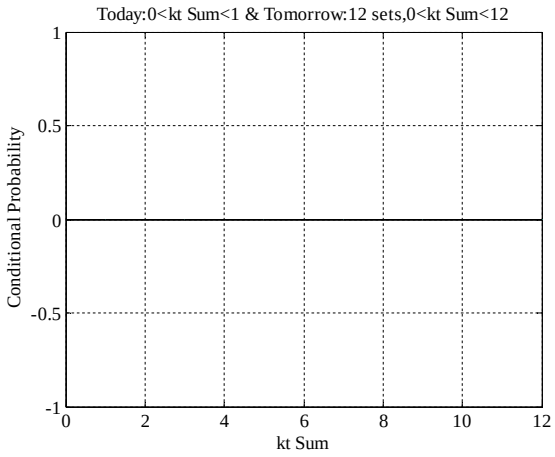

Figure 4.1. Conditional Probability Distribution for Tomorrow's Clearness Index Sum for Today's Clearness Index Sum is in between 0 and 1 for the Month- May

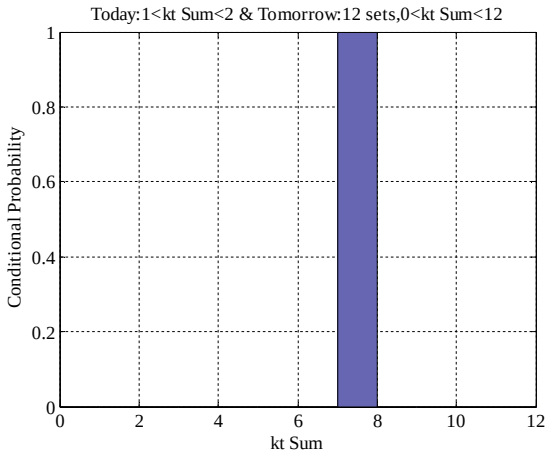

Figure 4.2. Conditional Probability Distribution for Tomorrow's Clearness Index Sum for Today's Clearness Index Sum is in between 1 and 2 for the Month- May

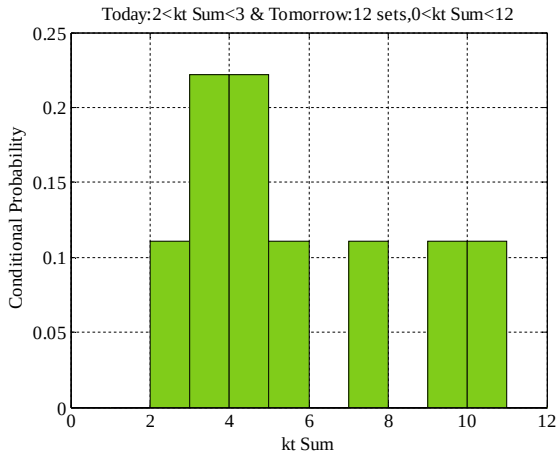

Figure 4.3. Conditional Probability Distribution for Tomorrow's Clearness Index Sum for Today's Clearness Index Sum is in between 2 and 3 for the Month- May

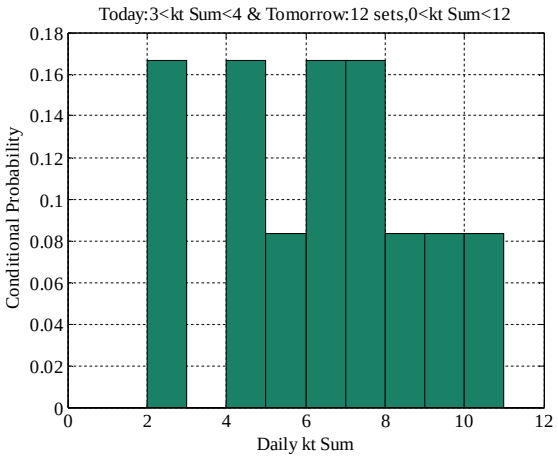

Figure 4.4. Conditional Probability Distribution for Tomorrow's Clearness Index Sum for Today's Clearness Index Sum is in between 3 and 4 for the Month- May

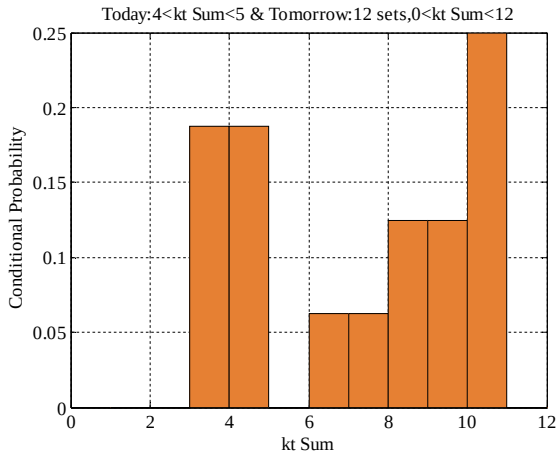

Figure 4.5. Conditional Probability Distribution for Tomorrow's Clearness Index Sum for Today's Clearness Index Sum is in between 4 and 5 for the Month- May

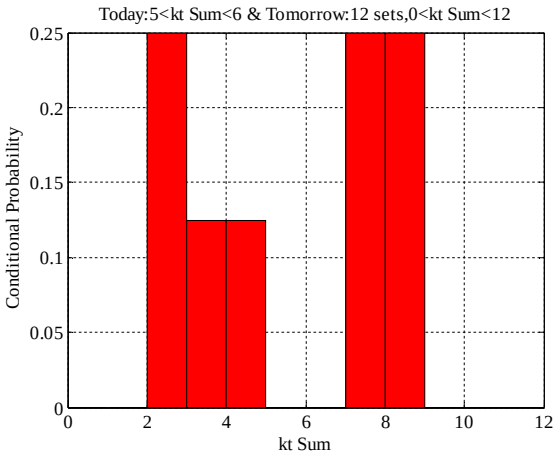

Figure 4.6. Conditional Probability Distribution for Tomorrow's Clearness Index Sum for Today's Clearness Index Sum is in between 5 and 6 for the Month- May

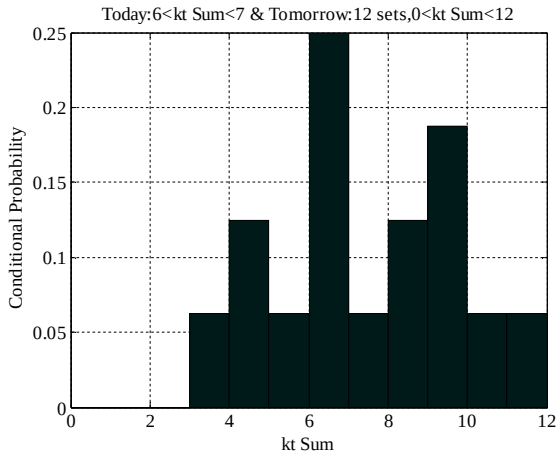

Figure 4.7. Conditional Probability Distribution for Tomorrow's Clearness Index Sum for Today's Clearness Index Sum is in between 6 and 7 for the Month- May

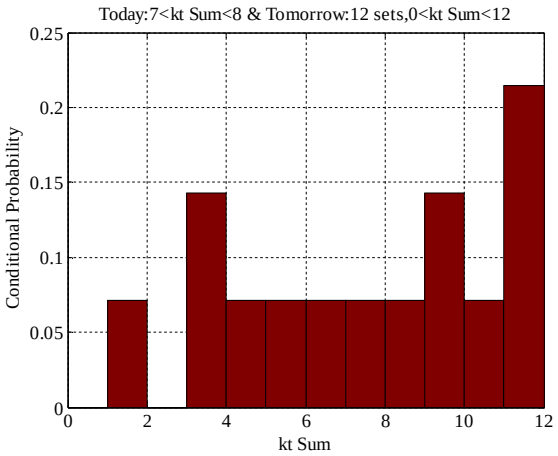

Figure 4.8. Conditional Probability Distribution for Tomorrow's Clearness Index Sum for Today's Clearness Index Sum is in between 7 and 8 for the Month- May

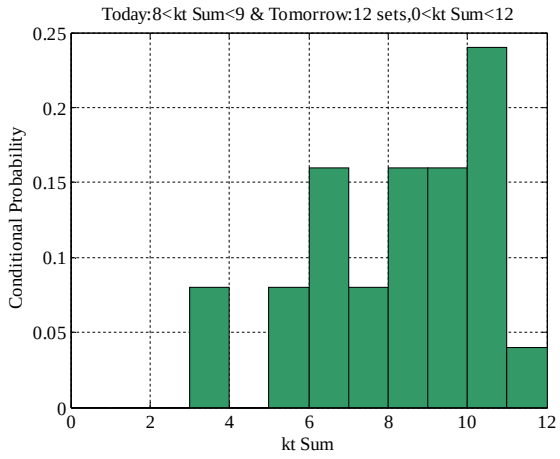

Figure 4.9. Conditional Probability Distribution for Tomorrow's Clearness Index Sum for Today's Clearness Index Sum is in between 8 and 9 for the Month- May

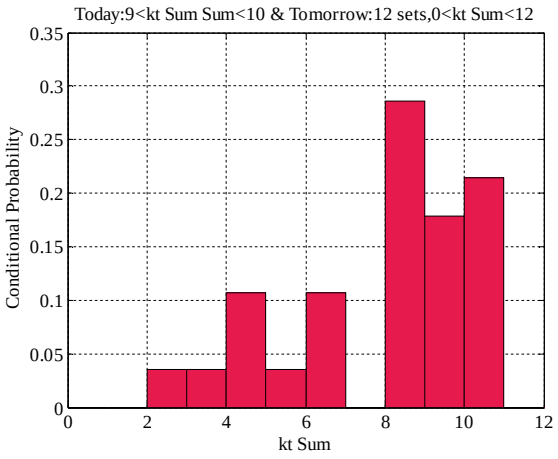

Figure 4.10. Conditional Probability Distribution for Tomorrow's Clearness Index Sum for Today's Clearness Index Sum is in between 9 and 10 for the Month- May

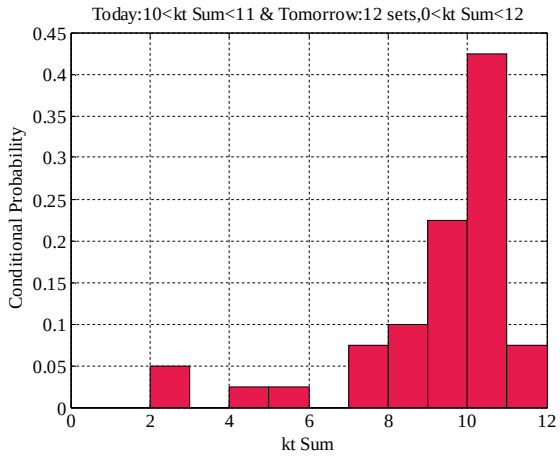

Figure 4.11. Conditional Probability Distribution for Tomorrow's Clearness Index Sum for Today's Clearness Index Sum is in between 10 and 11 for the Month- May

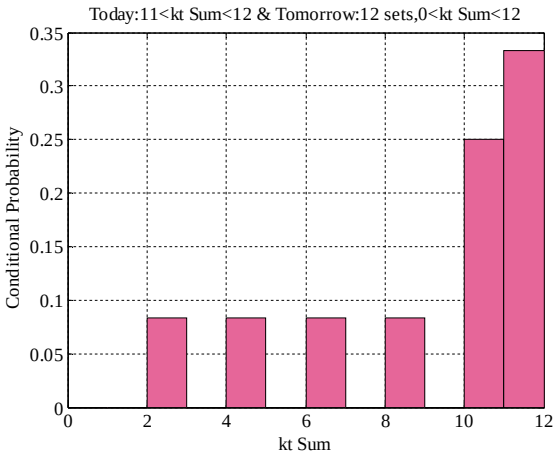

Figure 4.12. Conditional Probability Distribution for Tomorrow's Clearness Index Sum for Today's Clearness Index Sum is in between 11 and 12 for the Month- May

4.3 Quality of Clearness Index Forecasting

Quality tests are performed to investigate the accuracy of clearness index forecasting as similar to the procedure carried out in irradiance forecasting. The most recent period, May-2012, monthly clearness index values are compared with the forecasted values. Figure 4.13 compares the measured clearness index with the forecasted clearness index for the most probable forecasting scheme and Figure 4.14 shows the same comparison for average forecasting scheme.

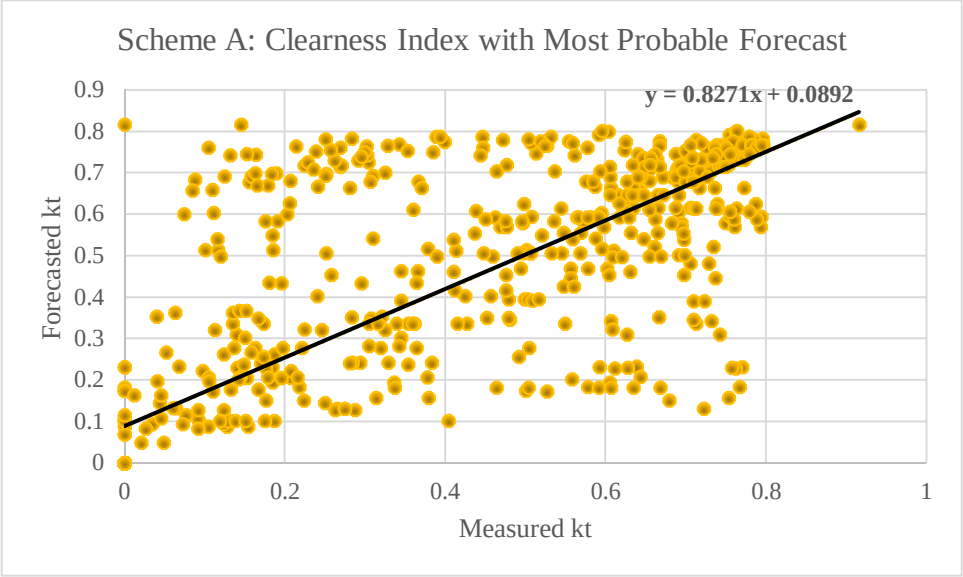

Figure 4.13. Forecasted Clearness Index vs. Measured Clearness Index for the Month-May, 2012 under Most Probable Forecasting Scheme

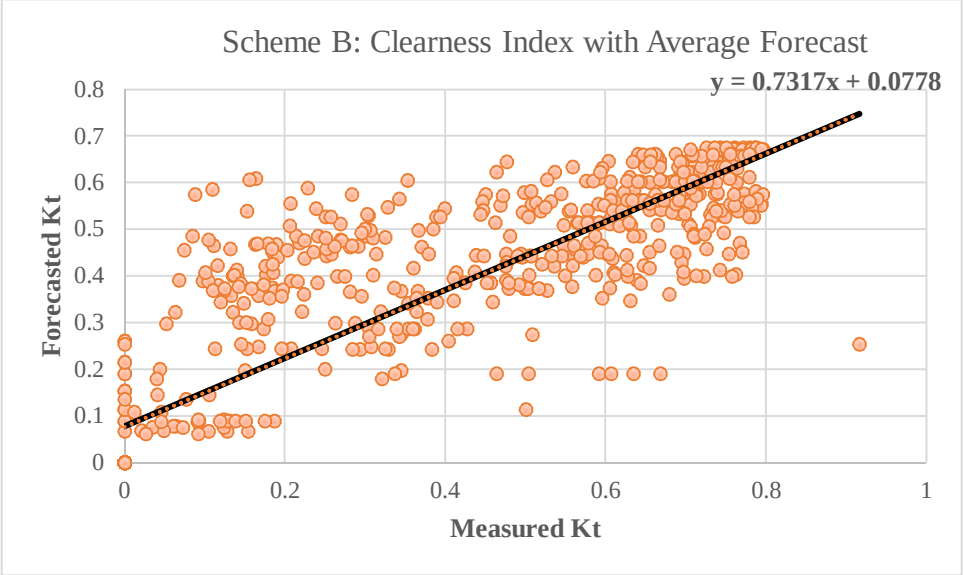

Figure 4.14. Forecasted Clearness Index vs. Measured Clearness Index for the Month-May, 2012 under Average Forecasting Scheme

Scatter distribution of the above figures proves that average forecasting scheme always offers higher accurate results than most probable forecasting scheme. Table 4.3 sums up the most probable, average and persistent forecasting schemes for the month of May, 2012.

Table 4.3. Quality Comparison for Different Forecasting Schemes on Clearness Index- May, 2012

Forecasting Scheme	**Relative Monthly Bias for Clearness Index**	**Relative Monthly RMSE for Clearness Index**
Persistent forecasting	0.029	0.473
Most probable forecasting	-0.091	0.551
Average forecasting	0.038	0.422

By observing the RMSE values in the table, it can be concluded that average forecasting scheme stands taller as far as more accurate forecasting is concerned. It gives the least RMSE and other two can be categorized under same quality. Therefore, we can continue working with average forecasting scheme in the probabilistic approach to obtain a better reliable forecast for the clearness index.

Figure 4.15 and Figure 4.16 compare the daily time series on predicted clearness index and measured clearness index with respect to different approaches of forecasting in May, 2012. The curve displays the variations between measured and forecasting values. By observing the behavior of curves, it can be concluded that, average forecasting scheme offers better results with less divergences.

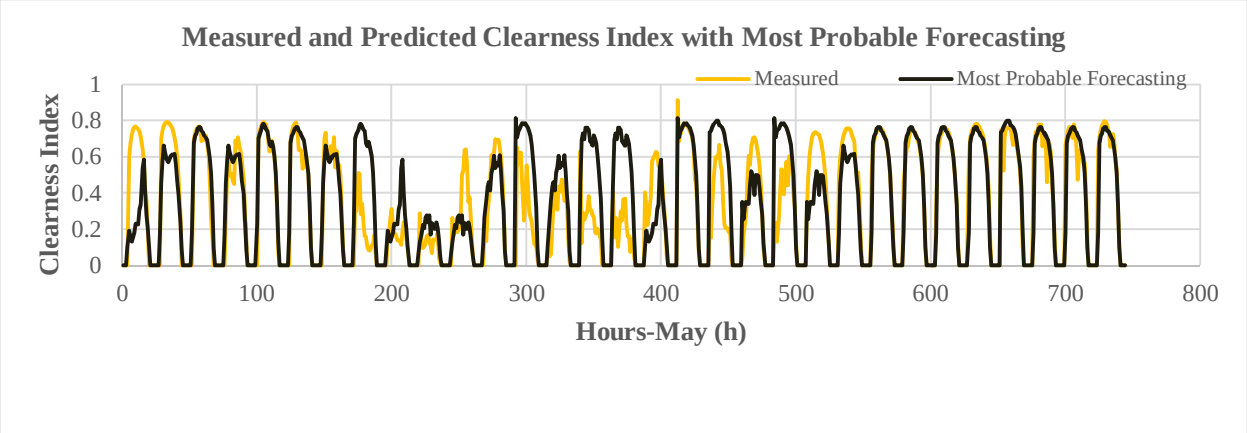

Figure 4.15. Daily Time Series for Measured and Most Probable Forecasted Clearness Index-May, 2012

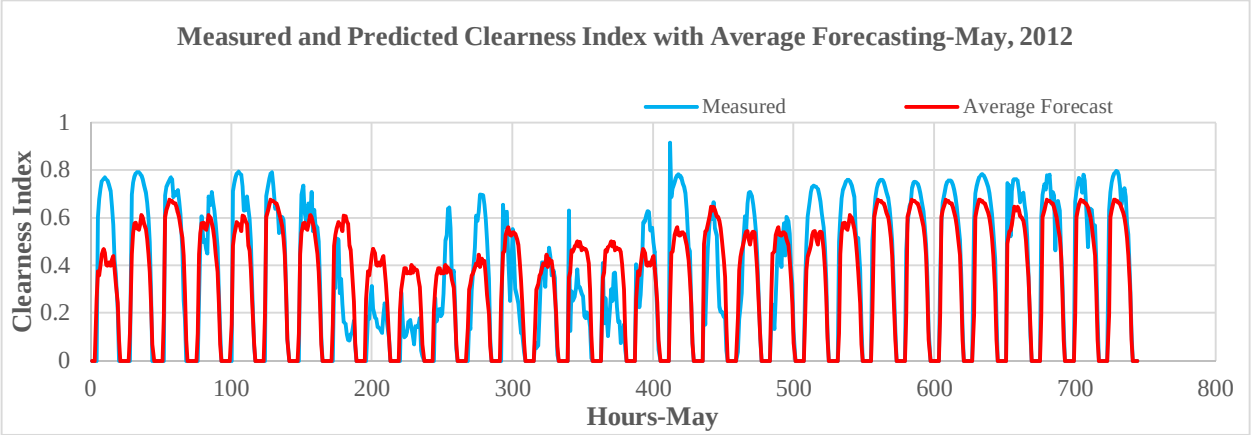

Figure 4.16. Daily Time Series for Measured and Average Forecasted Clearness Index-May, 2012

5. Energy Gain Forecasting

Chapter 5 presents final outcome of this project, i.e. forecasting energy gain of a solar thermal collector. Section 5.1 describes the thermal performance model of the solar collector standardized according to European standard EN12975. Parameter selection for the energy gain calculation is further discussed. Subsequently, measured and predicted irradiance values are applied for energy gain calculation and forecasting. Prediction scheme which has the least RMSE is considered to be the most qualified one to apply for energy gain calculations. It gives the better accurate forecasting results. Chapter concludes by discussing the quality of energy gain forecasting.

5.1 Energy Gain of Solar Thermal Collector.

In this section the performance of a flat plate solar thermal collector is modelled. Here it is assumed that the collector is installed with a 45° tilt to the horizontal, facing south. Power output of the collector is governed by its thermal performance. Hence, collector efficiency is the key parameter which is needed to be determined to calculate the power output. Equation 2.29 denotes the collector efficiency model introduced by European standard, EN12975. This can be applied to calculate the thermal efficiency based on the collector parameters, the irradiance in the collector plane and the operation temperatures. Parameters for the selected collector, 'Consolar PLANO 27H' are shown in Table 5.1. These parameters are extracted from collector data sheet annexed in the Appendix D. The selected collector gives a reasonable power output which is good enough to fulfil average domestic heat requirement.

Table 5.1. Consolar PLANO 27H, Collector Parameters

Parameter	**Value**
Aperture Area, A	2.335 m^2
Zero loss coefficient, η_0	0.813
Heat loss coefficient, a_1	3.97 $[Wm^{-2}K^{-1}]$
Heat loss coefficient, a_2	0.0183 $[Wm^{-2}K^{-2}]$

Further, equation 2.29 demands values for collector temperature and ambient temperature to calculate the thermal efficiency. Ambient temperature can be found on hourly basis in the measured data. However, we have to introduce a certain assumption to determine a value for the collector temperature as it is an unknown parameter. It is assumed that, the domestic hot water requirement in Southern Norway fulfills at 60 °*C*. For this, the collector has to deliver hot water at 60 °*C* in domestic level and it is further assumed that inlet temperature of the collector is 30 °*C*. Hence collector temperature, $T_{collector}$ can be determined by,

$$T_{collector} = \frac{T_{inlet} + T_{outlet}}{2} \qquad (5.1)$$

$$= \frac{(30+60)}{2}\,^0C$$

$$T_{collector} = 45\ ^0C$$

Also, tilted irradiance on the solar thermal collector is a known parameter as depicted in Section 3.1. Having known all the parameters in equation 2.29, we can obtain values for thermal efficiency at each hour. Finally, equation 2.30 can be applied to calculate the power output of the solar thermal collector. It should be noted that the thermal collector does not always give a positive power output due to the variation of irradiance in each hour, each day and each month. Therefore, finally the negative power output has to be eliminated and positive power output is filtered as the recorded power output.

Figure 5.1 presents a similar characteristic what was shown in the irradiance (See Figure 3.2). Here, the characteristic of maximum power output with respect to the calculated daily energy gain over 07 years, is illustrated.

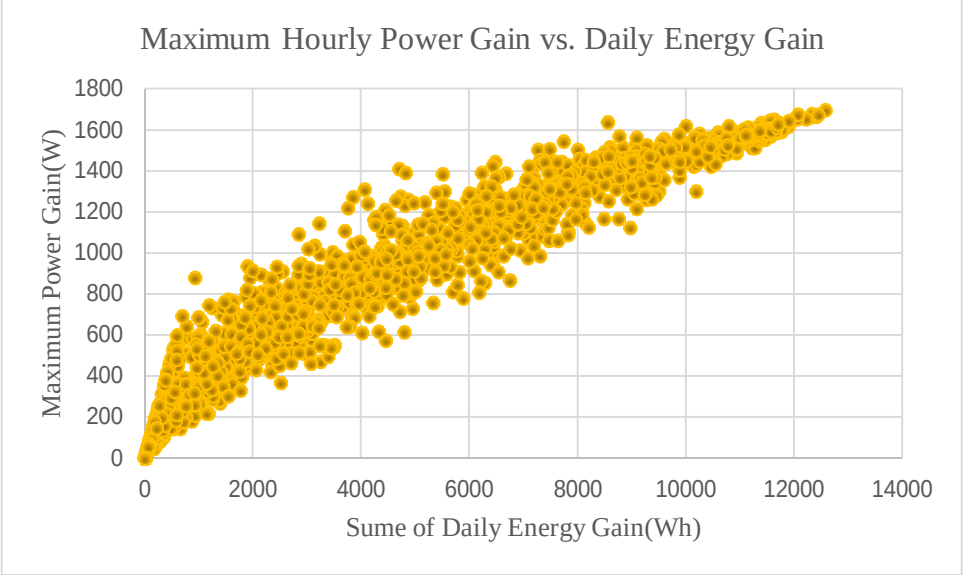

Figure 5.1. Maximum Power Output vs. Sum of Daily Energy Output of the Solar Thermal Collector

Figure 5.2 represents overall daily energy gain based on the sum of daily irradiance values. The graphs shows nonlinear behavior for low irradiance sums due to the fact that in the low irradiance, there is no power output from the collector at all. Therefore, more proportional losses can be observed at the first stage. Conversely, when more and more irradiance is received, collector starts to give power output, thus daily energy gain rises in linear scale.

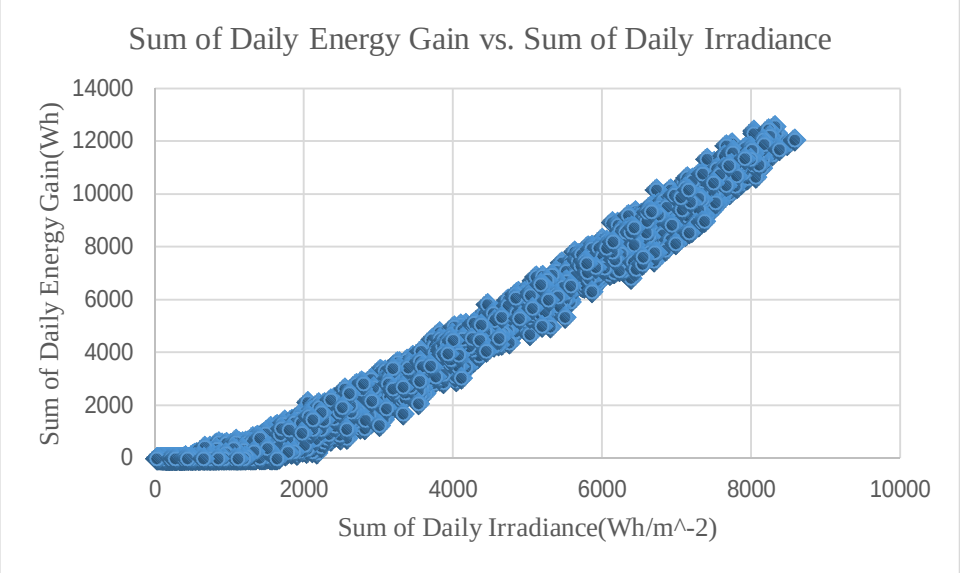

Figure 5.2. Sum of Daily Energy Gain vs. Sum of Daily Irradiance

5.2 Energy Gain Forecasting Approach-Month, May

Energy gain of the solar thermal collector is determined by the variables in equation 2.29 and equation 2.30. Aperture area (A), zero loss coefficient (η) and heat loss coefficients (a_1, a_2) are constant parameters for a specified collector. Also, it is assumed here that the collector operates at a constant temperature ($T_{collector}$) of 45° in order to fulfill the domestic hot water requirement of Southern Norway. By this we assume that, the flow through the collector is permanently controlled to stabilize the temperature.

There are two variables, which do not remain constant in energy gain calculations, i.e. ambient temperature (T_o) and global tilted irradiance (G_t). Ambient temperature is a physical parameter which can be easily measured. To forecast energy gain strictly, T has also to be forecasted. At last, we can calculate forecast values of energy gain by using forecasted tilted irradiance data and other known parameters. In a nutshell, we can obtain the forecasted values for energy gain, using forecasted irradiance data.

In Chapter 3, tilted irradiance was forecasted under two main schemes, most probable forecasting and average forecasting. It was proved that the irradiance forecasting based on average scheme gives better results with a least RMSE. Therefore, average irradiance forecasting scheme is brought forward for the calculation of energy gain.

A single month is considered here for demonstration. Forecasted irradiance values are applied to equation 2.29 and equation 2.30 to obtain forecast values of energy gain for the month, May 2012. Figure 5.3 shows the results on forecasting. Less amount of scatter witnesses the accuracy of energy gain forecasting.

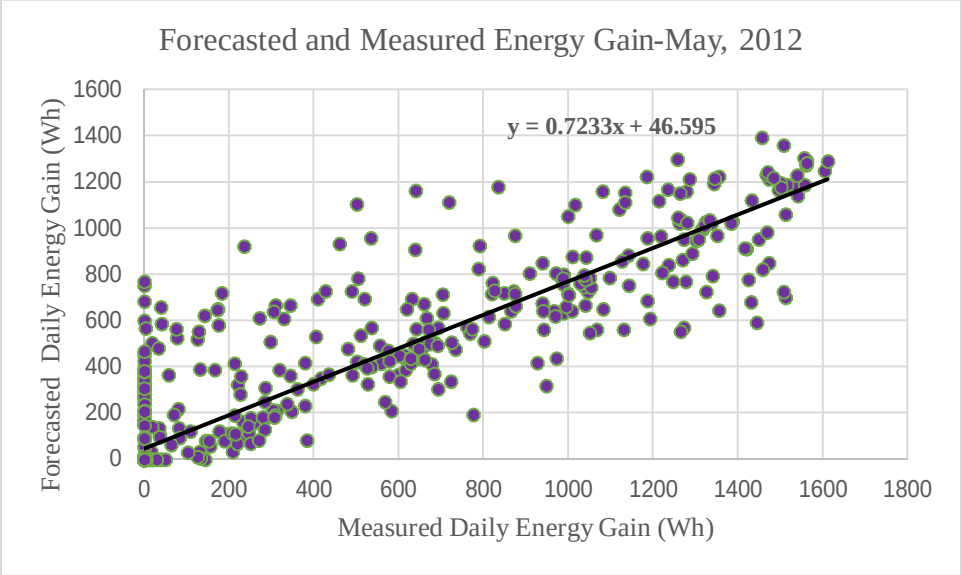

Figure 5.3. Predicted Daily Sum of Energy Gain vs. Measured Daily Sum of Energy Gain-May, 2012

Figure 5.4 compares the predicted and measured sum of daily energy gain in May, 2012. It is the daily energy gain time series for 744 hours (31 days) in the month May, 2012. The plot presents the quality of forecasting graphically. The Close behavior between measured and forecasted curves witnesses the accuracy of forecasting.

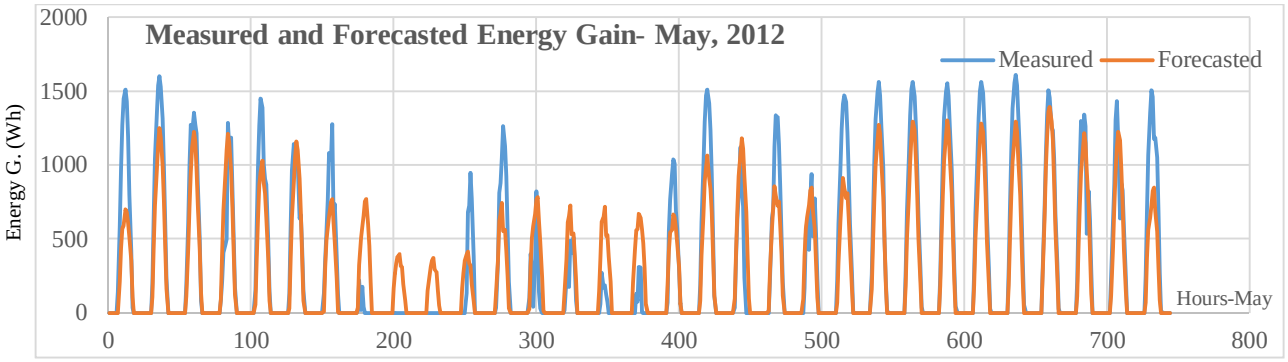

Figure 5.4. Daily Time Series for Measured and Forecasted Energy Gain-May, 2012

6. Discussion and Conclusion

This chapter continues discussion on the results in Chapters 4, 5 and 6. Section 6.1 outlines the overall achievement of this research, obtaining a forecast for the energy gain of a solar thermal collector. Also, it emphasizes the results on each individual month of the year. Finally, important findings and observations with respect to the quality of irradiance and energy gain forecasting for each month is presented. Section 6.2 gives a brief account with respect to the validation of forecasting scheme over months. It discusses the drawbacks of irradiance forecasting over the months in winter period. The possible reasons are in detail analyzed. Section 6.3 remarks on clearness index forecasting. Remarks on Conclusion in Section 6.4, claims on the goals of the forecasting and accuracy of outcome. The thesis suggests further improvements of the proposed scheme as the future work in Section 6.5.

6.1 Introduction to Conclusion

In the first stage, we have shown two forecasting schemes for solar irradiance forecasting named as most probable approach and average approach which are derived from the conditional probability distributions of the irradiance sum on next day. The quality tests were performed on both schemes to identify the best approach. This had shown that the average forecasting scheme gave better results with higher accuracy and we have applied it for energy gain forecasting. Results on forecasting irradiance, clearness index and energy gain were shown in detail by illustrating a single month, May in Chapters 3, 4 and 5 respectively. However, forecasting has to be performed for each month in the year. The forecasting results for individual months were obtained and they are shown in Appendix A. Finally, important findings and observations with respect to the quality of irradiance and energy gain forecasting in each month are summarized in Table 6.1 and Table 6.2 respectively.

Table 6.1. Quality Tests of Irradiance Forecasting for twelve Months

Month	**Irradiance Forecasting**					
	Persistent Forecasting		**Most Probable Forecasting**		**Average Forecasting**	
	Relative Bias	**Relative RMSE**	**Relative Bias**	**Relative RMSE**	**Relative Bias**	**Relative RMSE**
January	0.075	1.950	0.296	2.131	-0.007	1.851
February	0.027	1.221	0.407	1.655	0.515	1.567
March	0.021	0.865	-0.141	0.802	0.139	0.767
April	0.027	1.164	0.042	1.223	-0.041	0.967
May	0.030	0.580	-0.051	0.601	0.055	0.481
June	-0.026	0.957	-0.313	0.995	-0.248	0.885
July	0.001	0.967	-0.108	0.968	0.034	0.730
August	0.009	1.004	0.038	0.758	0.083	0.776
September	-0.060	1.125	-0.002	0.942	-0.142	0.973
October	-0.071	1.256	0.045	0.998	0.008	0.985
November	-0.091	1.358	0.023	0.968	0.003	1.134
December	0.012	0.988	0.003	0.979	-0.045	1.295

Table 6.1 witnesses that, there is more variability between in the months January, February which could be recognized as the peak months in winter.

Table 6.2. Quality Tests for Energy Gain Forecasting for 12 Months

Month	**Average Forecasting**	
	Relative Bias	**Relative RMSE**
January	0.640	4.657
February	0.812	2.606
March	0.341	1.334
April	-0.045	1.899
May	-0.051	0.695
June	-0.316	1.427
July	0.0265	1.385
August	0.060	1.300
September	-0.259	2.187
October	0.078	2.211
November	0.345	3.113
December	0.416	3.213

Table 6.3 compares the relative RMSE with respect to irradiance forecasting and energy gain forecasting. It is observed that there is small but clear difference between values due to the fact that, energy gain forecast shows a nonlinear relationship with the irradiance forecast. At the instances where collector power output is almost proportional to irradiance i.e. at higher irradiance levels, RMSE shows a close behavior.

Table 6.3. Comparison of Relative RMSE for Irradiance and Energy Forecasting in each Month

Month	**Relative RMSE-Irradiance Forecasting**	**Relative RMSE-Energy Gain Forecasting**
January	1.851	4.657
February	1.567	2.606
March	0.767	1.334
April	0.967	1.899
May	0.481	0.695
June	0.885	1.427
July	0.730	1.385
August	0.776	1.300
September	0.973	2.187
October	0.985	2.211
November	1.134	3.113
December	1.295	3.213

6.2 Validation and Outlook on Options to Increase Forecast Quality over Months

Table 6.1 reveals that the Relative RMSE stands with high value for the months December, January, and February during the winter season. Also, daily time series with respect to irradiance and energy gain forecasting shows higher variation when compared with measured values (See Appendix A)

These winter months are characterized by low irradiance, resulting low collector output. We can see, the recorded irradiance is more often less than *100* Wm^{-2} during the noon hours. It is witnessed in the conditional probability distributions, i.e. a high probability is shown in low irradiance classes. Therefore the forecasting scheme has to be improved for the months where low irradiance is recorded. A possible area to enhance the quality of forecasting is the choice of irradiance classes with respect to daily irradiance sum. Since, daily irradiance sum is more or less 500 Wm^{-2} during

the winter peak time, we can increase the number of irradiance classes by introducing a low width (range of the irradiance class) for the irradiance class. When there are more irradiance classes, the closeness of today's weather and tomorrow's weather is high as this approach works based on previous day weather characteristic. For an example, in the month January, minimum daily irradiance sum is calculated as 74.47 Whm^{-2} and maximum value as 3448.96 Whm^{-2}. Let's consider two approaches to define the irradiance classes. In the first approach, classes are defined with 500 Whm^{-2} class width, thus finally we analyze data in 07 classes between 0 Whm^{-2} and 3500 Whm^{-2} to obtain 07 conditional probability distributions (Illustrated in Appendix A). In the second approach, the class width is considered to be 100 Whm^{-2} and it results 35 conditional probability distributions in the data set between 0 Whm^{-2} and 3500 Whm^{-2}. Hence, probability distributions in the second approach builds up closer relationship between today's weather and tomorrow's weather, consequently a higher accurate forecast. Also, as far as months with high irradiance recordings are concerned the application is the same but it drives to the opposite direction. As an example, in August, the daily irradiance sum more often falls in to 7000 Whm^{-2} and 8000 Whm^{-2}. Here, the size of the class width is affected to enhance the precision of forecast in the high irradiance sum, but little variation between consecutive days. In a nutshell, it can be concluded that, the choice of class width makes a significant impacts to the precision of forecasting.

6.3 Remarks on Clearness Index Forecasting

It is noted that conditional probability distributions for the irradiance forecasting showed a significant difference when distributions move from one month to another month. However, in clearness index forecasting such large variation in the probability distributions is not visible due to the fact that the variation scale is quite smaller in the values. In a different explanation, forecasting of clearness index is more stable from month to month. Due to the different heights of the sun, irradiance values could vary a lot, but conditions for the clearness index remains much similar from one month to another. Thus, clearness index provides more stable information on conditional probabilities. In clearness index forecasting, the values of the clearness index can be considered together for the whole year and laid the statistical base for conditional clearness index.

6.4 Final Conclusion

The proposed method can provide one-day-ahead forecasted information on hourly energy gain of a specified collector, based on previous day values. The method was developed by analyzing the historical data in a local region. Such short time forecasting approach can be of its importance to apply for the control of local solar thermal applications. Control systems can be integrated with energy management systems to enhance the efficiency by way of harvesting optimum amount of energy out of available solar power. This single point forecast information can be used as an input variable to such control system. A solar thermal collector can be employed as a simple power management system in domestic level. When we have forecasted information, we can plan the use of available energy. As a results, such scheme will help cut down the energy bill.

Overall, we can conclude that the proposed forecasting scheme works with a reasonable accuracy for the summer period, yet it has to be improved for the winter months. Further analyzing of the generating scheme reveals that the forecasting is more accurate for the days which have similar weather sequence. When there is a substantial difference between today's weather and tomorrow's weather, the drawback emerges in both proposed forecasting schemes. Further to explain, if today shows a bad weather, as long as tomorrow also will show a bad weather with little variation, the forecast approach works quite well. Conversely, if today shows a bad weather and then tomorrow will show a sudden variation, possibly from bad weather to fine weather, the forecast will not accurately work due to the fact that, the probability of such huge variations are very low. Concisely, extreme changes in the weather, disturbs the stability of proposed predicting schemes. Therefore, further improvements are suggested as the future work.

6.5 Future Work

As explained in Section 6.1, the forecast approach does not give higher accurate results for winter months. Therefore, the precision of the forecast has to be improved for winter period by way of reducing the width of the weather class in the data analysis.

A key point was revealed that, the extreme variation in the parameter, disturbs the stability of proposed predicting schemes. It opens a new area for researching, i.e. we have to introduce a sophisticated method to cope up with these sudden changes by analyzing historical data. One option may be given by a link to routine weather forecasts that may feed warnings on sudden changes to the scheme.

As per the suggestion in remarks, all values of the clearness index can be considered together for whole year to obtain more stable conditional probabilities. Therefore, a future would be to implement a two-step forecasting approach, i.e. firstly, clearness index is forecasted and then forecasted clearness index values can be used to obtain the irradiance forecasting. The quality of this approach will have to be compared with the direct forecasting approach.

For the calculation of energy gain, ambient temperature was used as a parameter in equation 2.25 and equation 2.26. The energy gain was forecasted by applying predicted irradiance and measured ambient temperature. However, for strict energy gain forecasting, ambient temperature has also to be forecasted. Therefore, the quality of forecasting approach can be further enhanced if someone will use forecast temperature values rather than measured temperature values.

Bibliography

[1] M. Lange, “A mature market? The history of short-term prediction services,” presented at the POW’WOW Best-Practises Workshop, Delft, The Netherlands, 2006 [Online]. Available:http://www.powwow.risoe.dk/publ/emsresearch_to_business_powwow_Delft_2006.pdf

[2] Elke Lorenz, Johannes Hurka, Detlev Heinemann, Hans Georg Beyer, "Irradiance Forecasting for the Power Prediction of Grid-Connected Photovoltaic Systems," *IEEE JOURNAL OF SELECTED TOPICS IN APPLIED EARTH OBSERVATIONS AND REMOTE SENSING* , vol. 2, no. 1, March 2009.

[3] B. Lie, "Initial Report: HI RENERGY," Telemark University College, Porsgrunn, 2012.

[4] D. Heinemann, "Energy Meteorology, Postgraduate program in Renewable Energy," University of Oldenburg, Germany, 2002.

[5] Mellit, A., M. Benghanem, and S.A. Kalogirou, "An adaptive wavelet-network model for forecasting daily total solar radiation," Journal of Applied Energy, vol. 83, no. 7, pp. 705-722, 2006.

[6] Cao, J. and L. Xingchun, "Study of hourly and daily solar irradiation forecast using diagonal recurrent wavelet neural networks," Energy & Conversion Management, 2008. 49: p. 1396-1406., vol. 49, pp. 1396-1406, 2008.

[7] Cao, S. and Cao J., "Forecast of solar irradiance using recurrent neural networks combined with wavelet analysis," Applied Thermal Engineering, vol. 25, pp. 161-172, 2004.

[8] Girodo, M., ed. Solar radiation prediction based on numerical weather models, Ph.D. thesis. ed. E.a.S.R.L. Faculty of Mathematics and Natural Sciences. 2006, Carl von Ossietzky University: Oldenburg, Germany. 159 p.

[9] Hamill, T.M., Whitaker, J.S., Mullen S.L., Reforecasts, an important data set for improving weather predictions. Bulletin of the American Meteorological Society, 2005: p. 43.

[10] Guarnieri, R.A., Use of Artificial Neural Networks and Multiple Linear Regression on Refinement of Solar Radiation Forecasts Eta Model, Dissertation. CPTEC-INPE. 2006, São José dos Campos (SP).

[11] D. Heinemann, E. Lorenz, and M. Girodo, "Forecasting of solar radiation in Solar Energy Resource Management for Electricity Generation From Local Level to Global Scale," E. D. Dunlop, L.Wald, and M.Súri, Eds., Hauppauge, NY: Nova, 2005.

[12] "Methods and Inputs, How is SolarGIS data calculated?" GeoModel Solar, 2010. [Online]. Available: http://solargis.info/doc/methods. [Accessed 08 04 2013].

[13] Consolar, "SPF Online Collector Catalogue, Collector Factsheet" 2010. [Online]. Available: http://www.solarenergy.ch/index.php?id=111&L=6&no_cache=1. [Accessed 25 08 2013]

[14] Michael Boxwell, Solar Electricity Handbook: A Simple, Practical Guide to Solar Energy (2012), p. 41-42.

[15] F. Vignola, "Solar Radiation Monitoring Laboratory," University of Oregon, 2010. [Online].Available:http://solardat.uoregon.edu/SolarRadiationBasics.html#Fig1. [Accessed 21 05 2014].

[16] M. Collares-Pereira and A. Rabl (1979). The average distribution of solar radiation correlations between diffuse and hemispherical and betwen daily and hourly insolation values. Solar Energy, 22, 155-164.

[17] J.F. Orgill and K.G. Hollands (1977). Correlation equation for hourly diffuse radiation on a horizontal surface. Solar Energy, 19, 357-359.

[18] M. Collares-Pereira and A. Rabl (1979). The average distribution of solar radiation correlations between diffuse and hemispherical and between daily and hourly insolation values. Solar Energy, 22, 155-164.

[19] D.G. Erbs, S.A. Klein and J.A. Duffie (1982). Estimation of the diffuse radiation fraction for hourly, daily and monthly-average global radiation. Solar Energy, 28, 293-304.

[20] D.T. Reindl, W.A. Beckman and J.A. Duffie (1990). Diffuse fraction correlations. Solar Energy, 45 1-7.

[21] Norton, Brian (2013). Harnessing Solar Energy. Springer. ISBN 978-94-007-7275-5.

[22] Greensolarvacuum, "Solar panels for water heating on top of a hotel in Perissa, Santorini, Greece,"Wikipedia,[Online].Available:http://en.wikipedia.org/wiki/Solar_thermal_collector. [Accessed 21 05 2014].

[23] S Fischer, H Muller-Steinhagen, B Perers, "Collector test methods under quasi dynamic conditions according to the European standard EN 12975-2," University of Stuttgart, Stuttgart.

[24] B.O. Ngoko, H. Sugihara, T. Funaki, "Synthetic generation of high temporal resolution solar radiation data using Markov models," Solar Energy, vol. 103, pp. 160-170, May-2014.

Appendices

Appendix A. Forecasted Information on Irradiance

A.1. January

A.1.1. Conditional Probability Distributions for Forecasted Irradiance Sum on Next Day

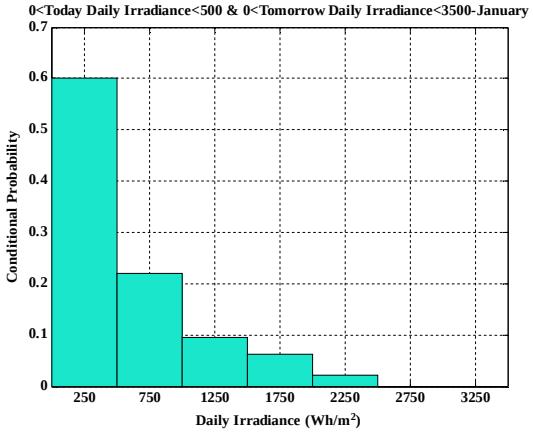

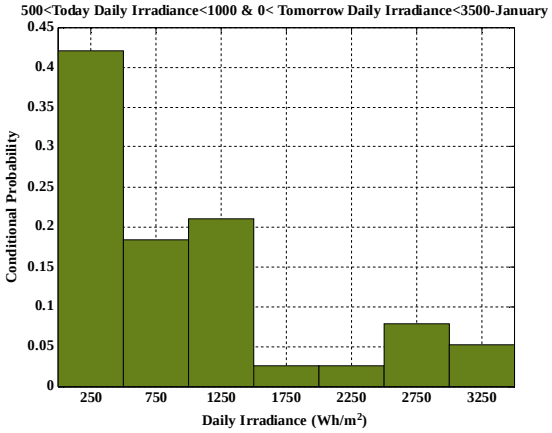

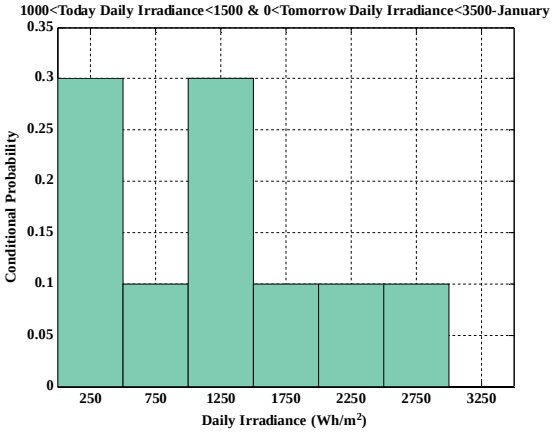

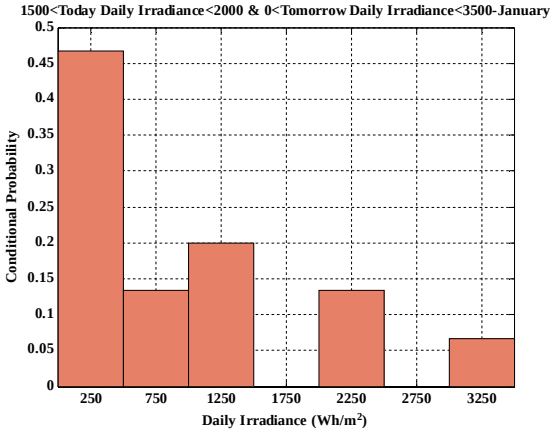

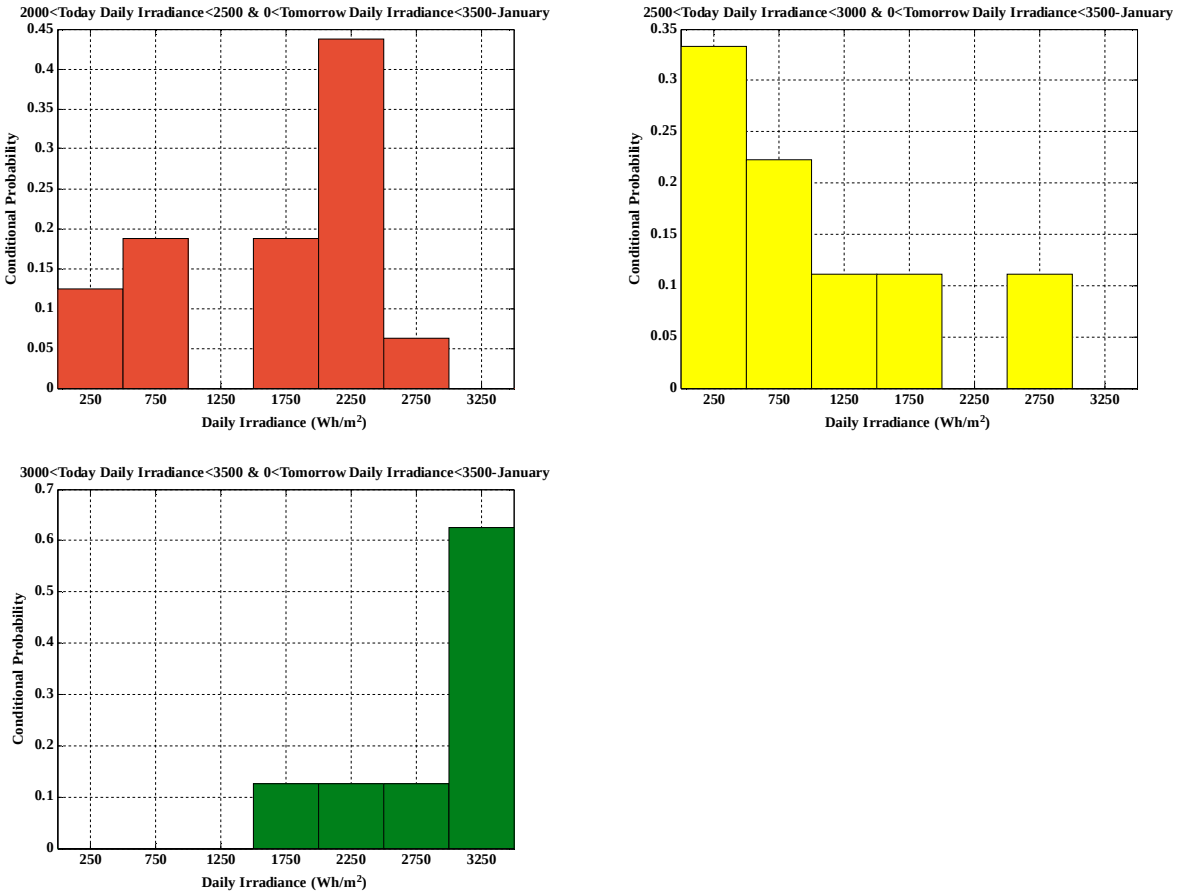

Figure A.1. Conditional Probability Distributions for Seven Irradiance Classes on Next Day's Irradiance Sum in Month-January

A.1.2. Daily Time Series for Forecasted and Measured Irradiance-January, 2013

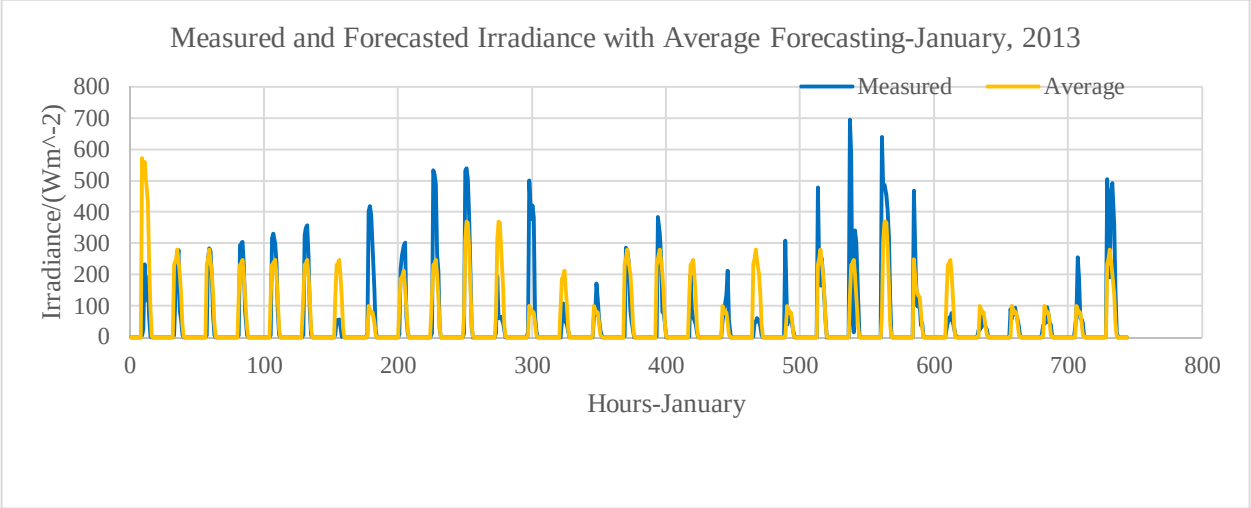

Figure A.2. Daily Time Series for Measured and Forecasted Irradiance-January, 2013

A.2. February

A.2.1. Conditional Probability Distributions for Forecasted Irradiance Sum on Next Day

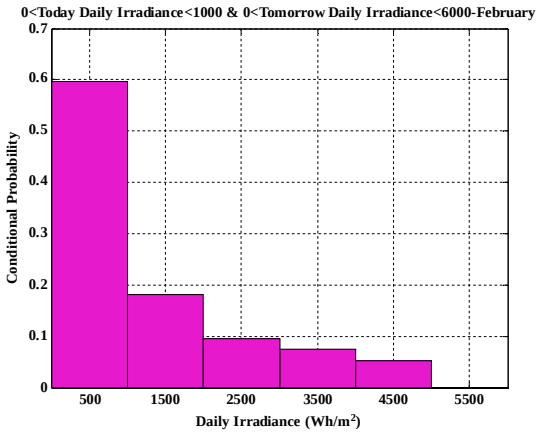

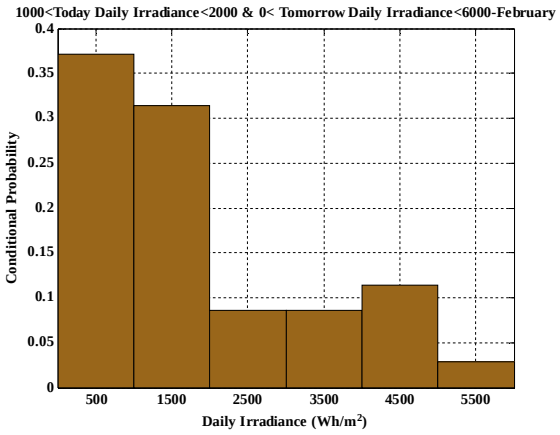

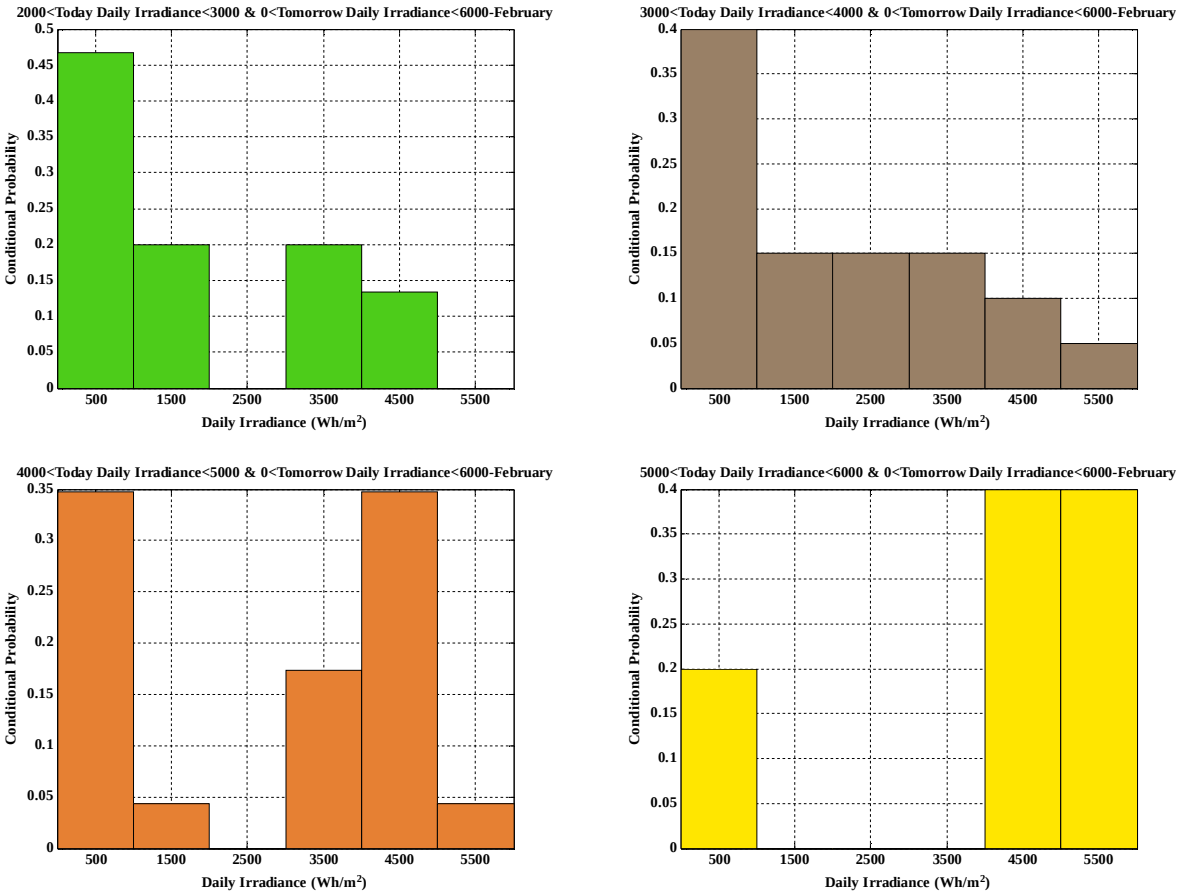

Figure A.3. Conditional Probability Distributions for Seven Irradiance Classes on Next Day's Irradiance Sum-Month, February

A.2.2. Daily Time Series for Forecasted and Measured Irradiance-February, 2013

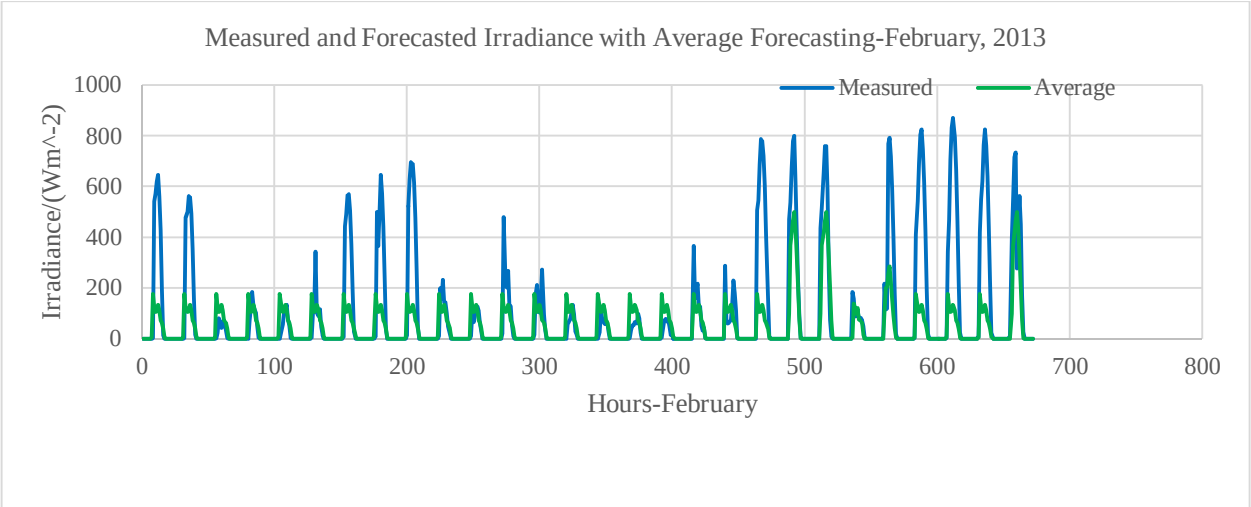

Figure A.4. Daily Time Series for Measured and Forecasted Irradiance-February, 2013

A.3. March

A.3.1. Conditional Probability Distributions for Forecasted Irradiance Sum on Next Day

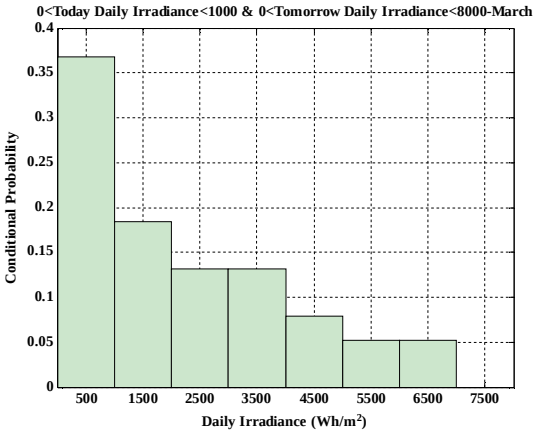

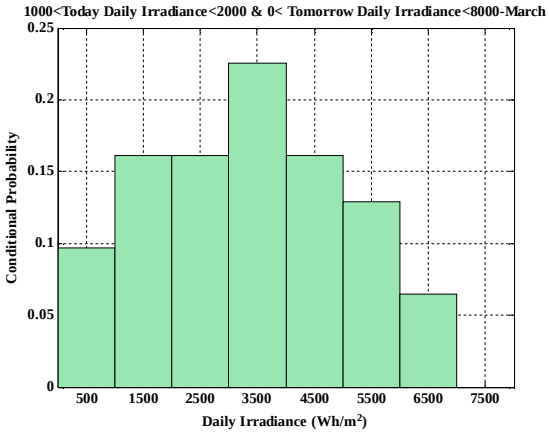

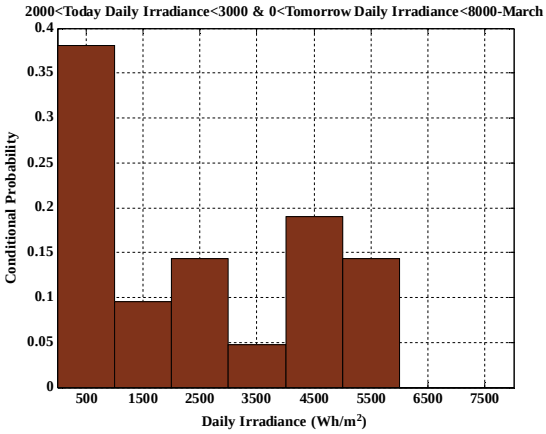

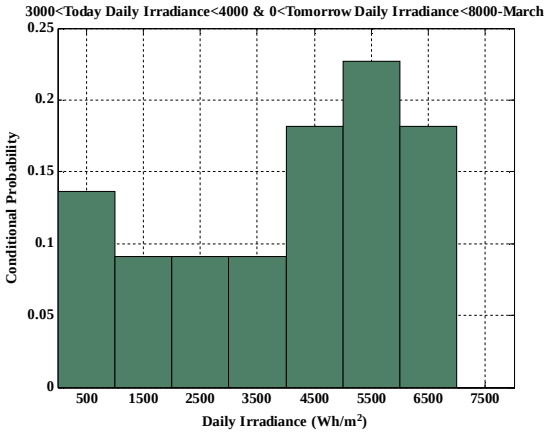

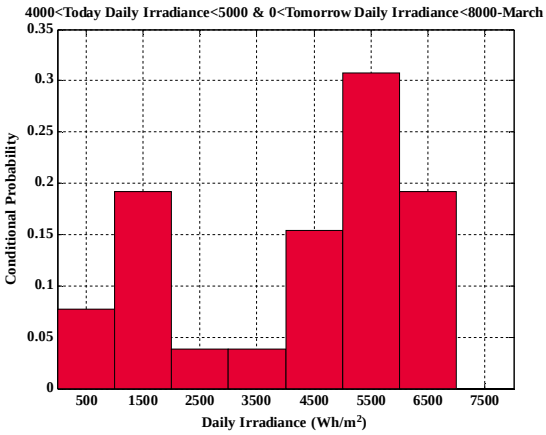

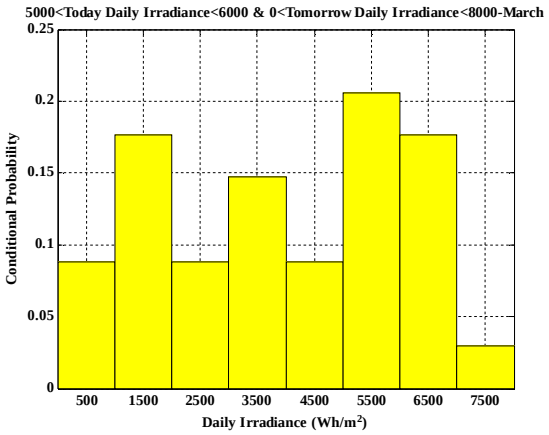

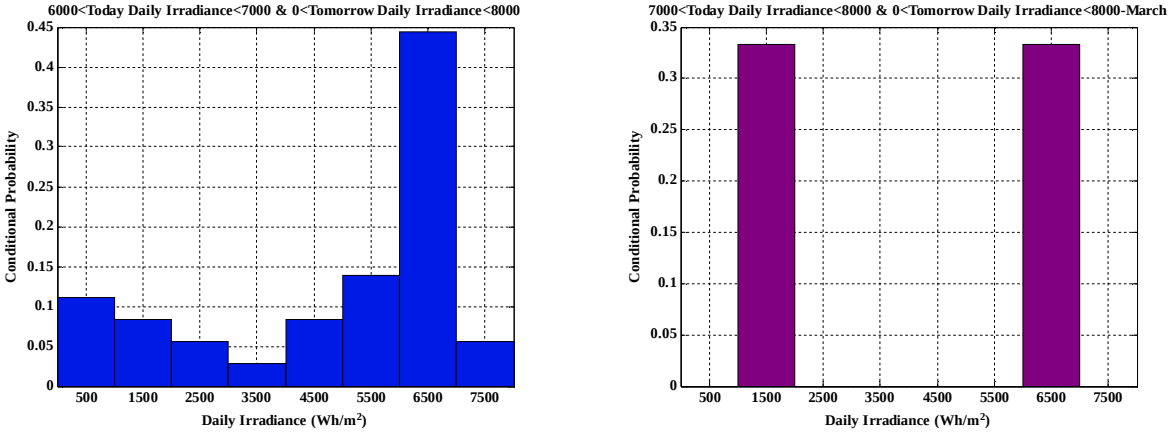

Figure A.5. Conditional Probability Distributions for 07 Irradiance Classes in Month-March

A.3.2. Daily Time Series for Forecasted and Measured Irradiance-March, 2013

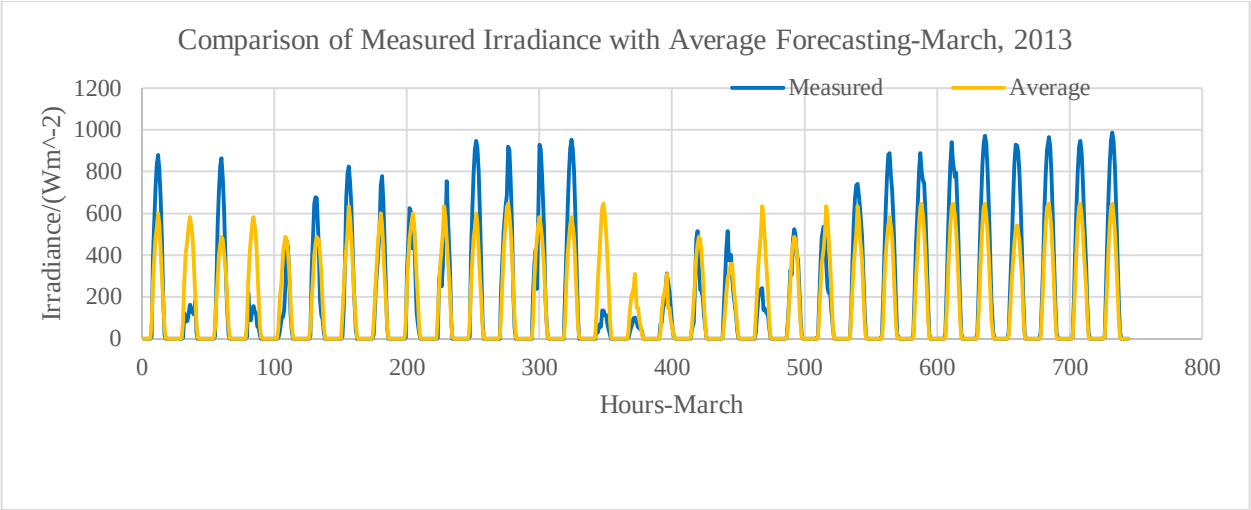

Figure. A.6. Daily Time Series for Measured and Forecasted Irradiance-March, 2013

A.4. April

A.4.1. Conditional Probability Distributions for Forecasted Irradiance Sum on Next Day

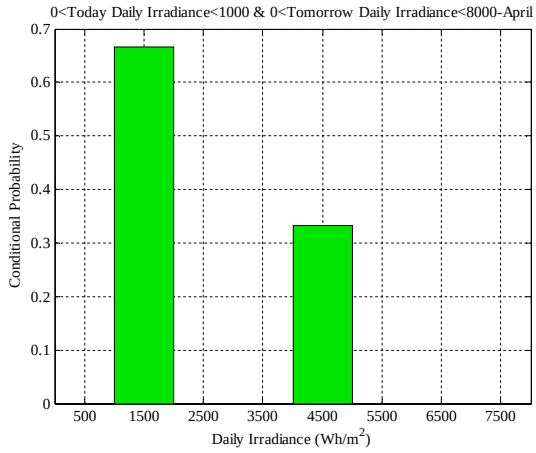

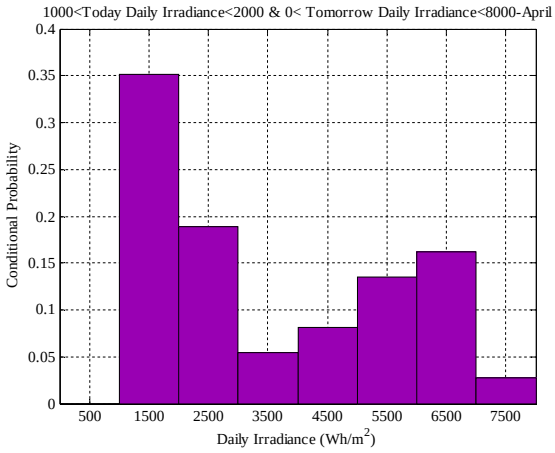

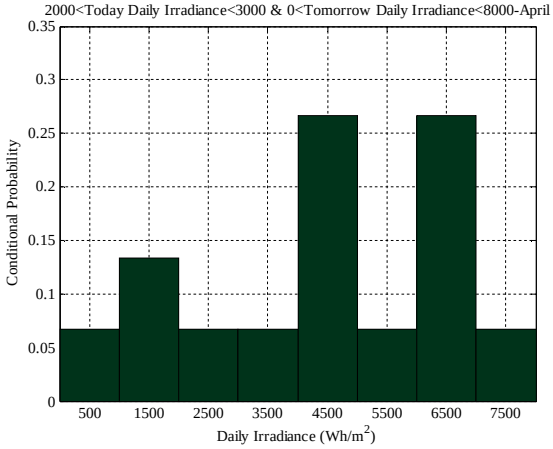

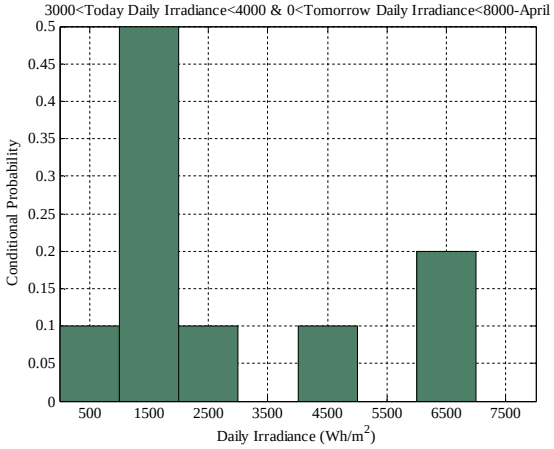

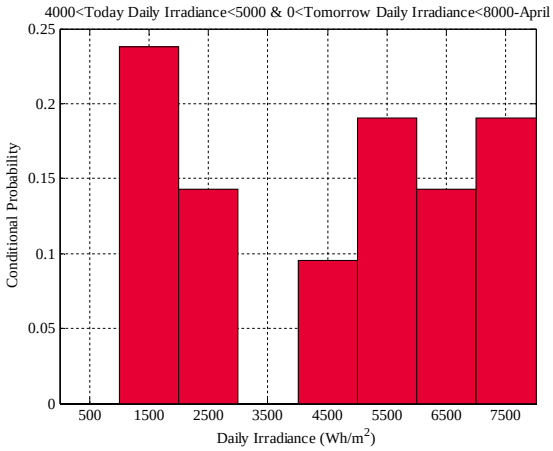

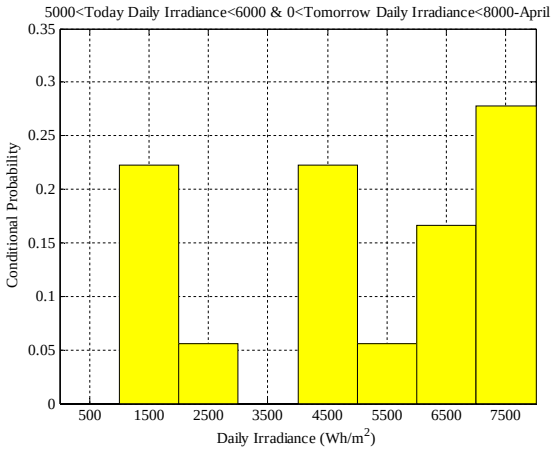

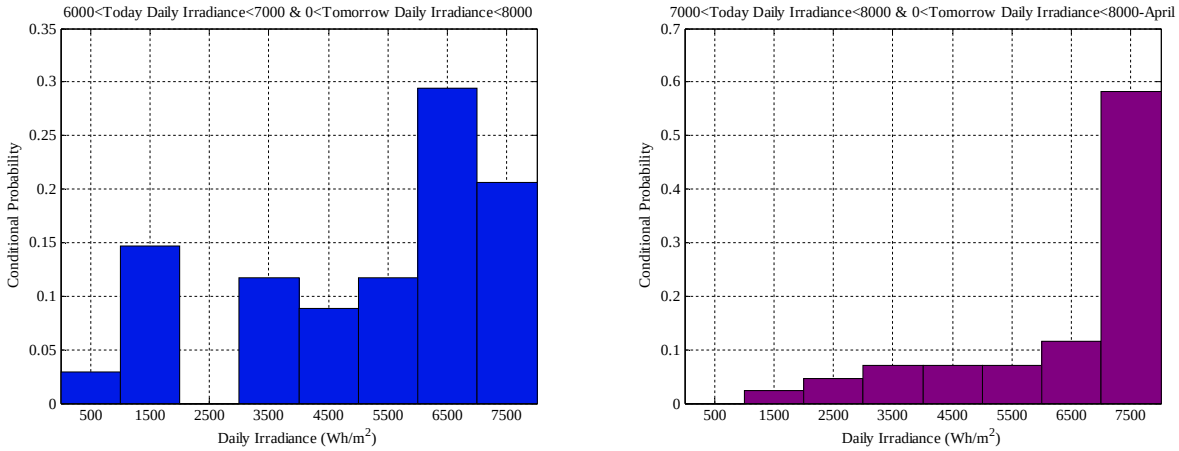

Figure A.7. Conditional Probability Distributions for 08 Irradiance Classes in Month-April

A.4.2. Daily Time Series for Forecasted and Measured Irradiance-April, 2013

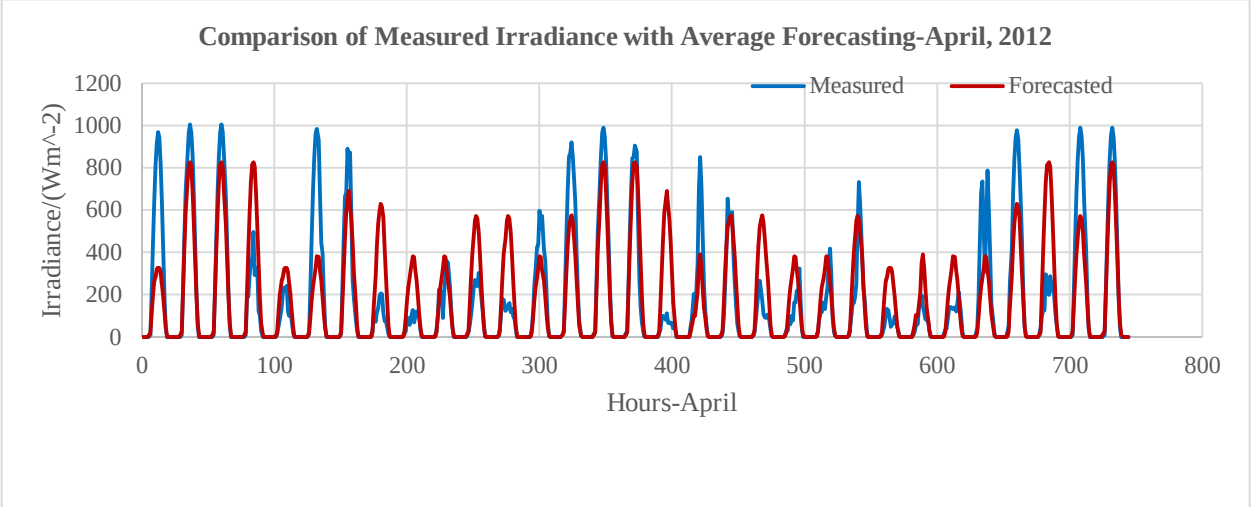

Figure. A.8. Daily Time Series for Measured and Forecasted Irradiance-April, 2013

A.5. May

Forecasted information on May is illustrated in the Chapters 3, 4 and 5.

A.6. June

A.6.1. Conditional Probability Distributions for Forecasted Irradiance Sum on Next Day

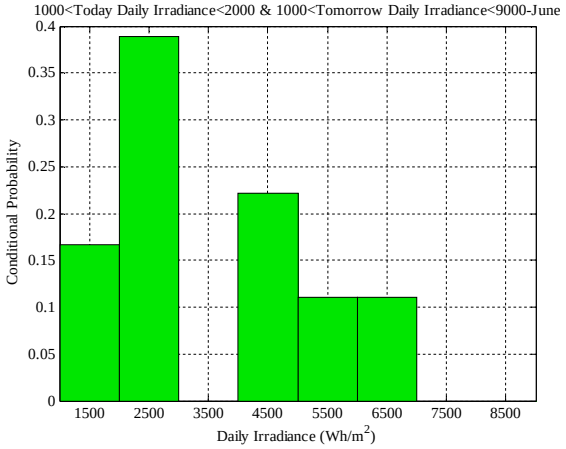

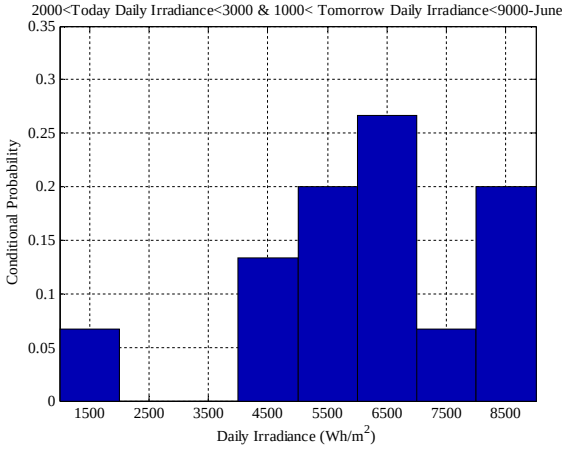

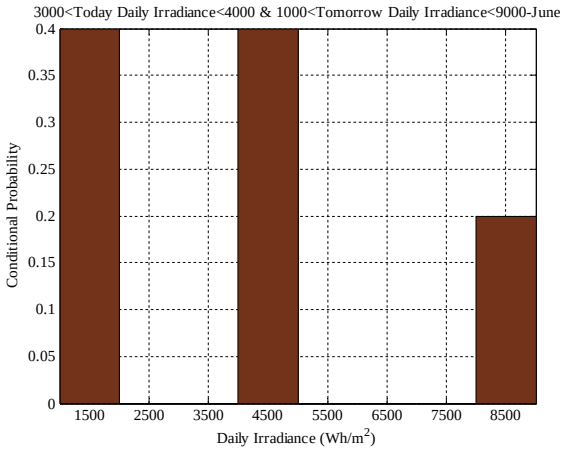

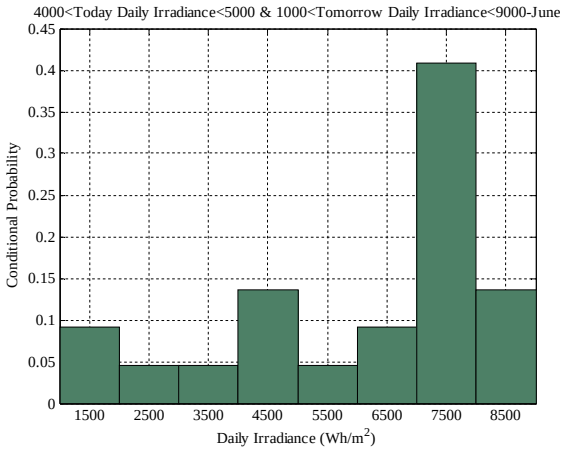

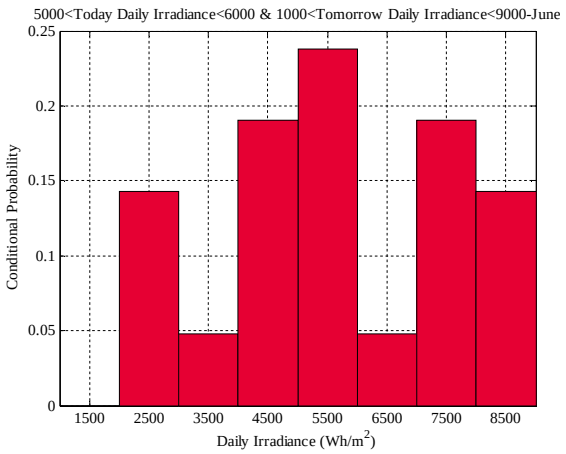

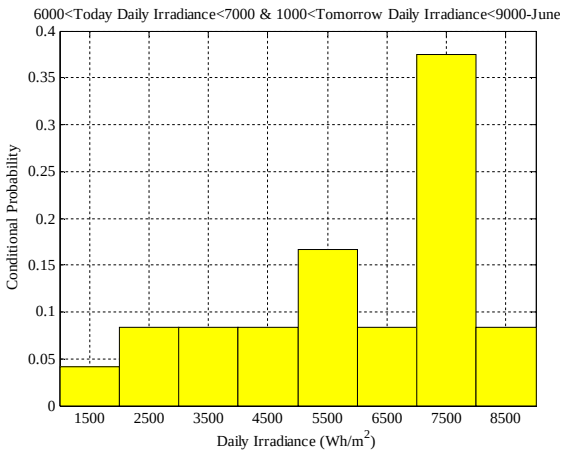

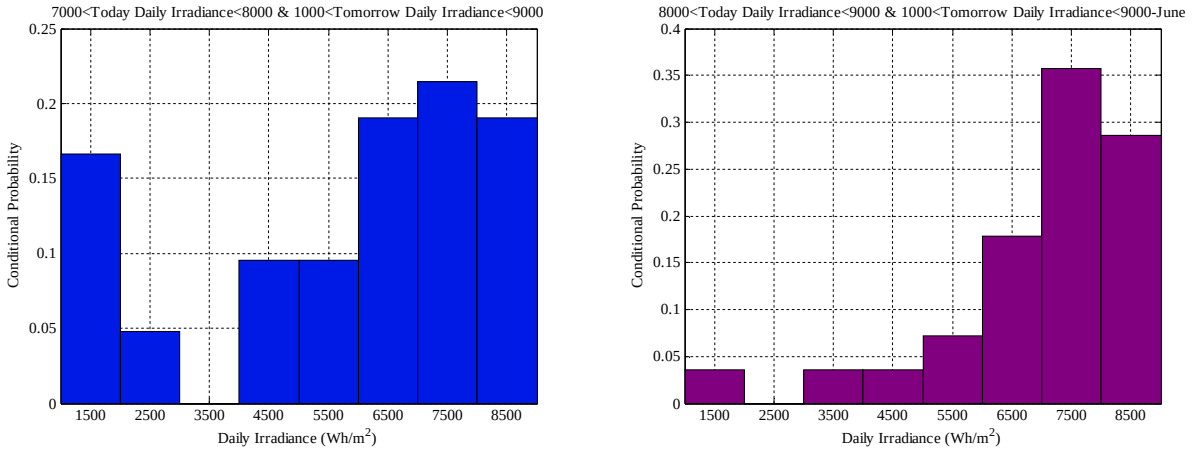

Figure A.9. Conditional Probability Distributions for 08 Irradiance Classes in Month-June

A.6.2. Daily Time Series for Forecasted and Measured Irradiance-June, 2012

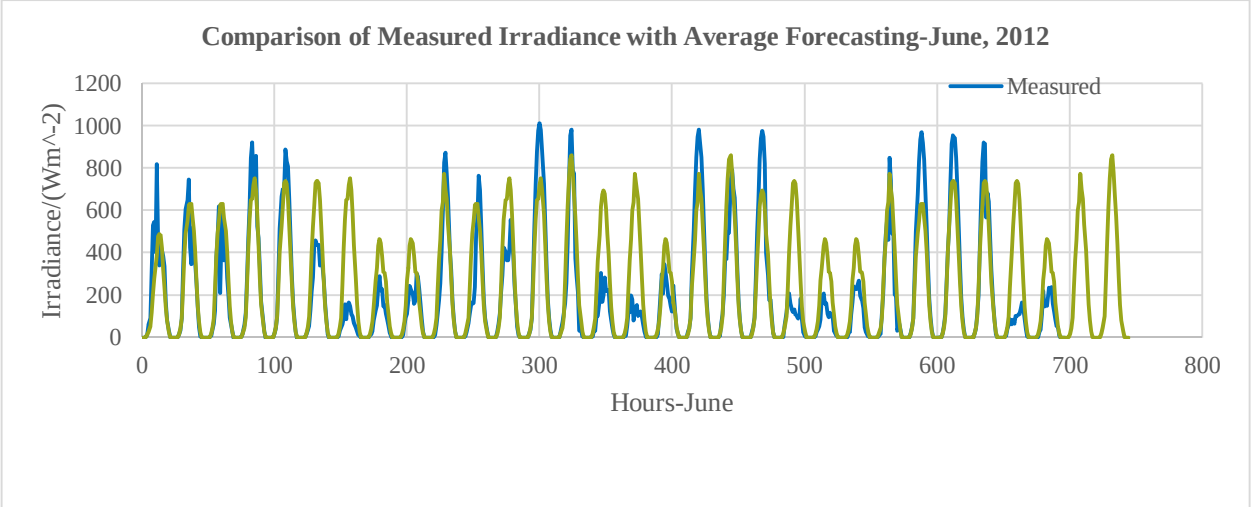

Figure. A.10. Daily Time Series for Measured and Forecasted Irradiance-June, 2012

A.7. July

A.7.1. Conditional Probability Distributions for Forecasted Irradiance Sum on Next Day

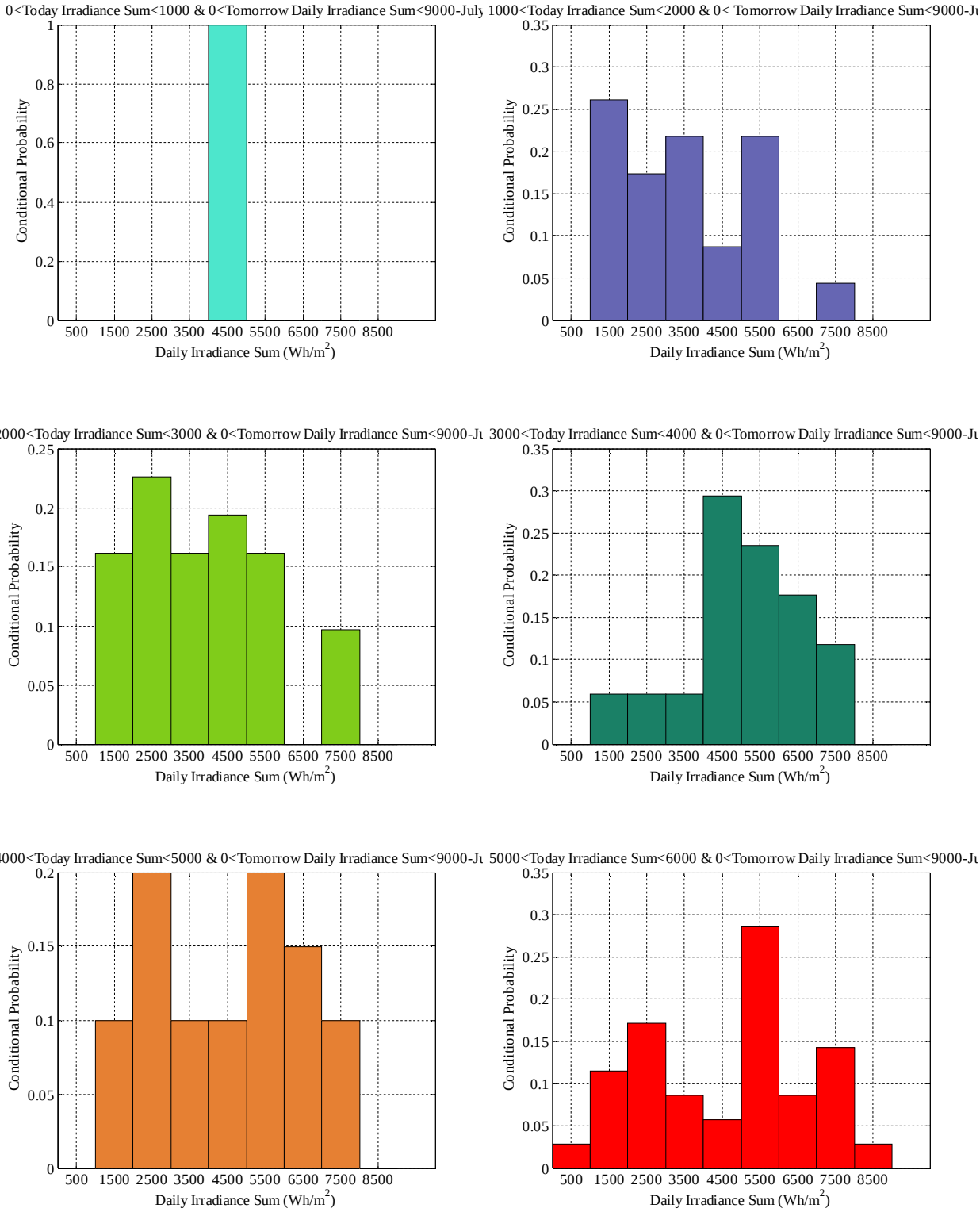

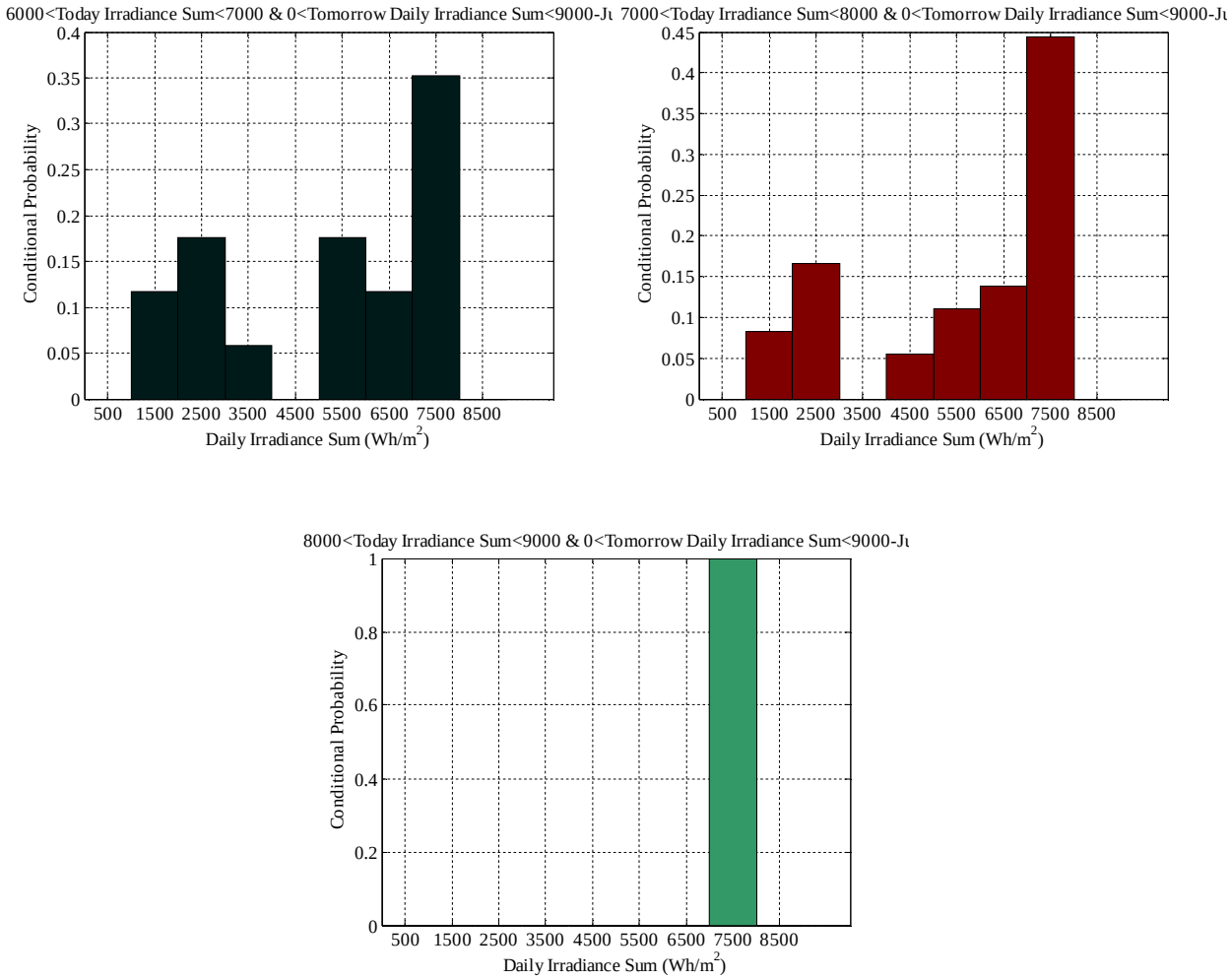

Figure A.11. Conditional Probability Distributions for 09 Irradiance Classes in Month-July

A.7.2. Daily Time Series for Forecasted and Measured Irradiance-July, 2012

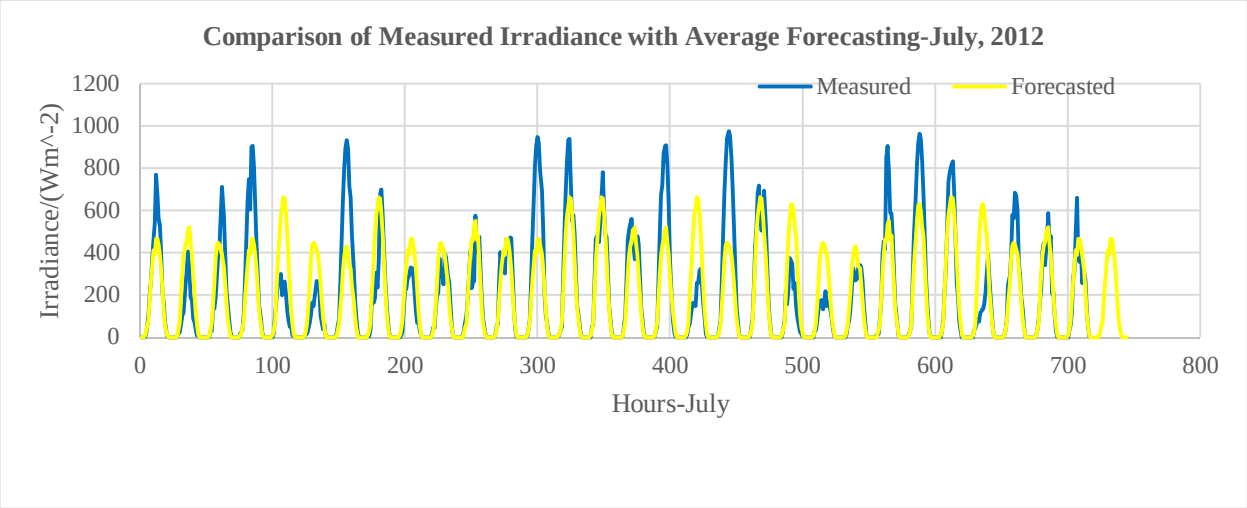

Figure. A.12. Daily Time Series for Measured and Forecasted Irradiance-July, 2012

A.8. August

A.8.1. Conditional Probability Distributions for Forecasted Irradiance Sum on Next Day

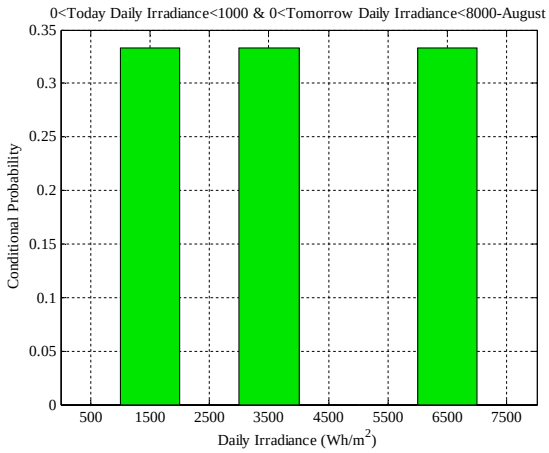

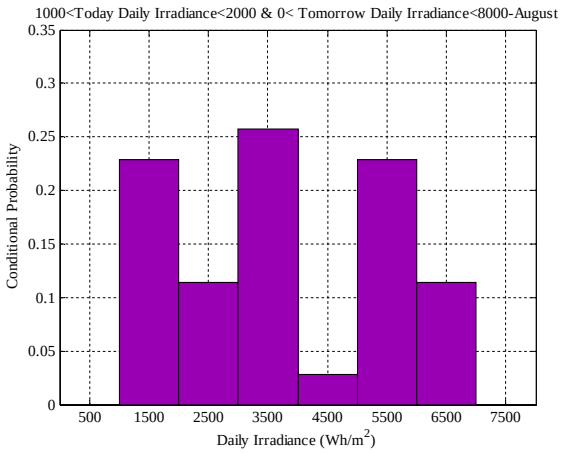

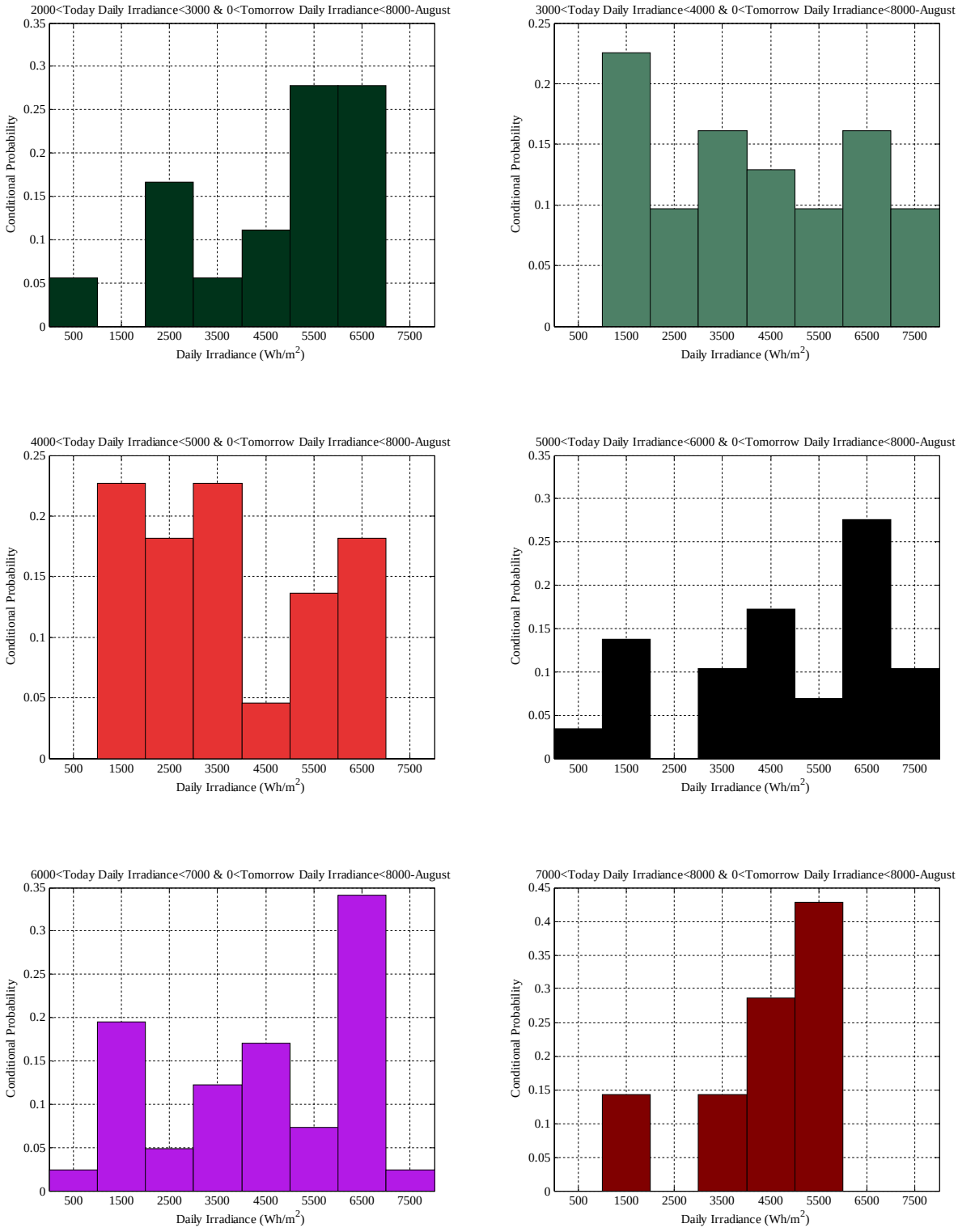

Figure A.13. Conditional Probability Distributions for 08 Irradiance Classes in Month-August

A.8.2. Daily Time Series for Forecasted and Measured Irradiance-August, 2012

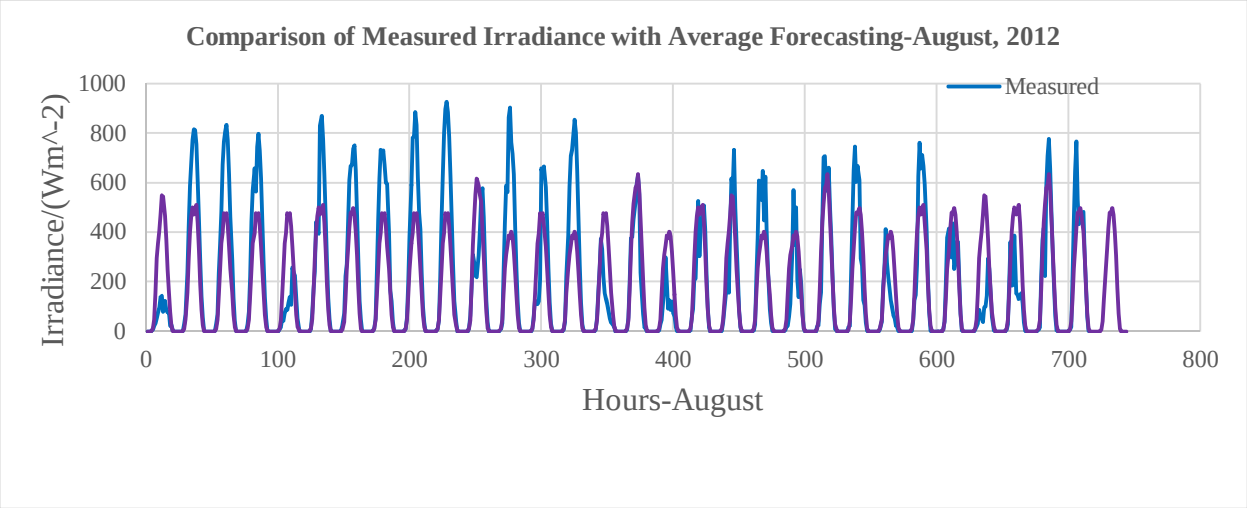

Figure. A.14. Daily Time Series for Measured and Forecasted Irradiance-August, 2012

A.9. September

A.9.1. Conditional Probability Distributions for Forecasted Irradiance Sum on Next Day

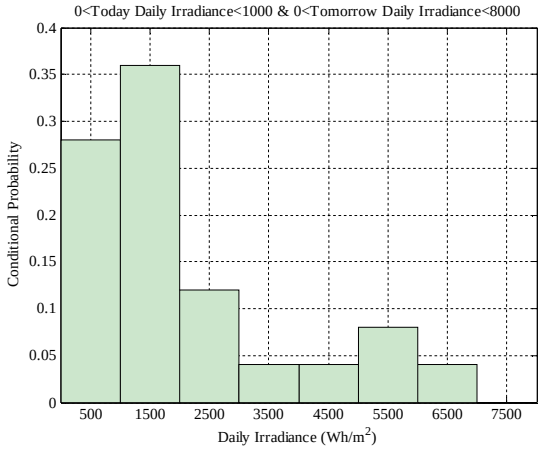

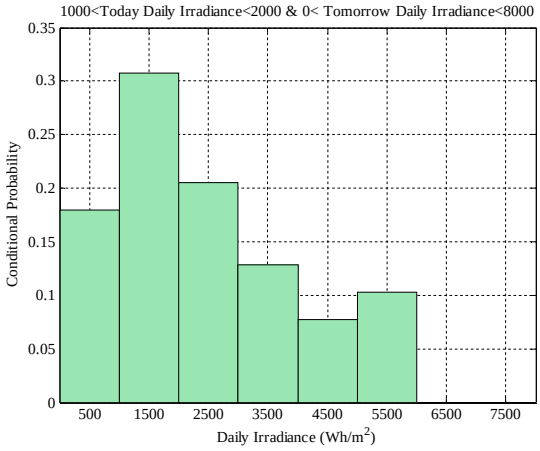

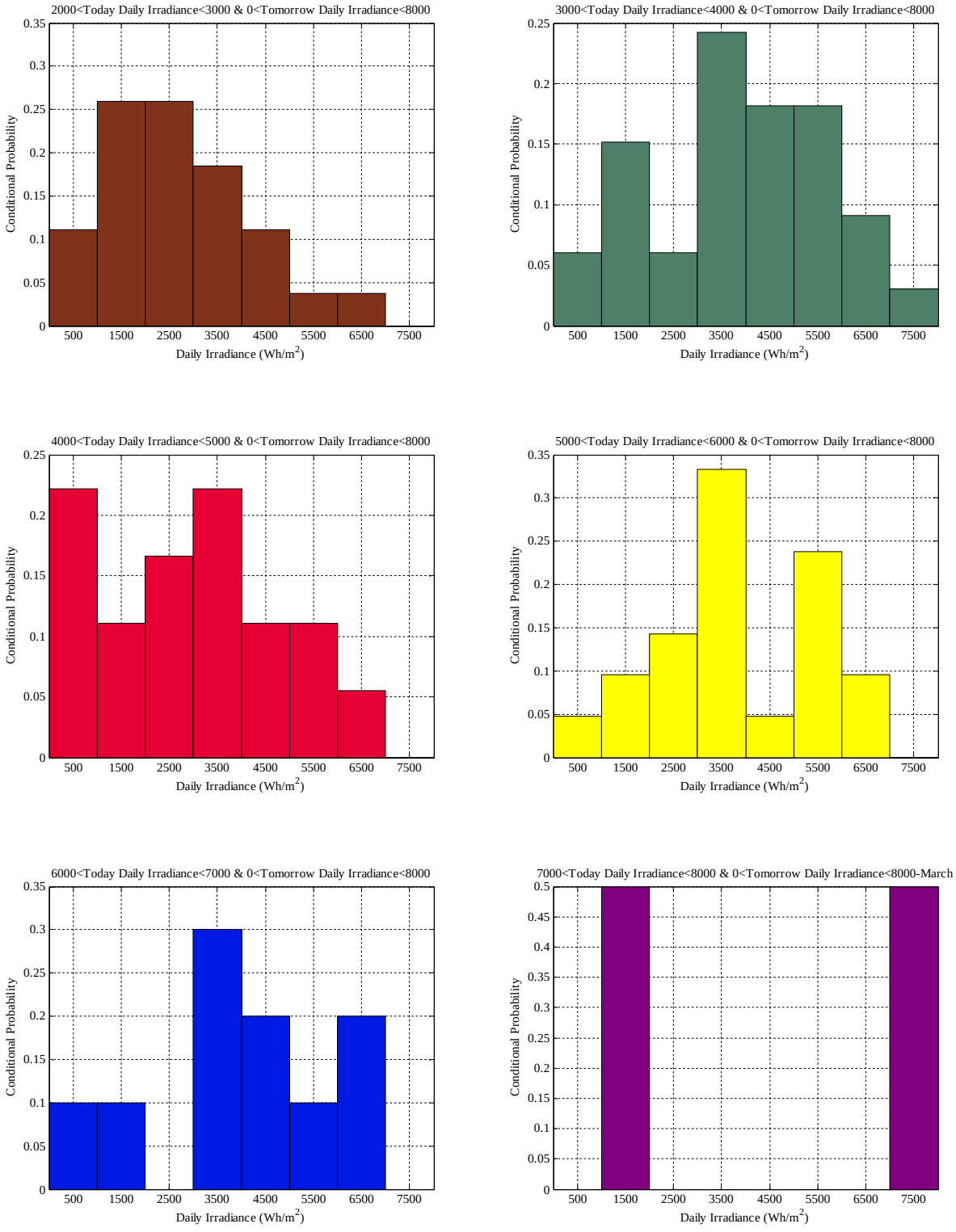

Figure A.15. Conditional Probability Distributions for 08 Irradiance Classes in Month-September

A.9.2. Daily Time Series for Forecasted and Measured Irradiance-September, 2012

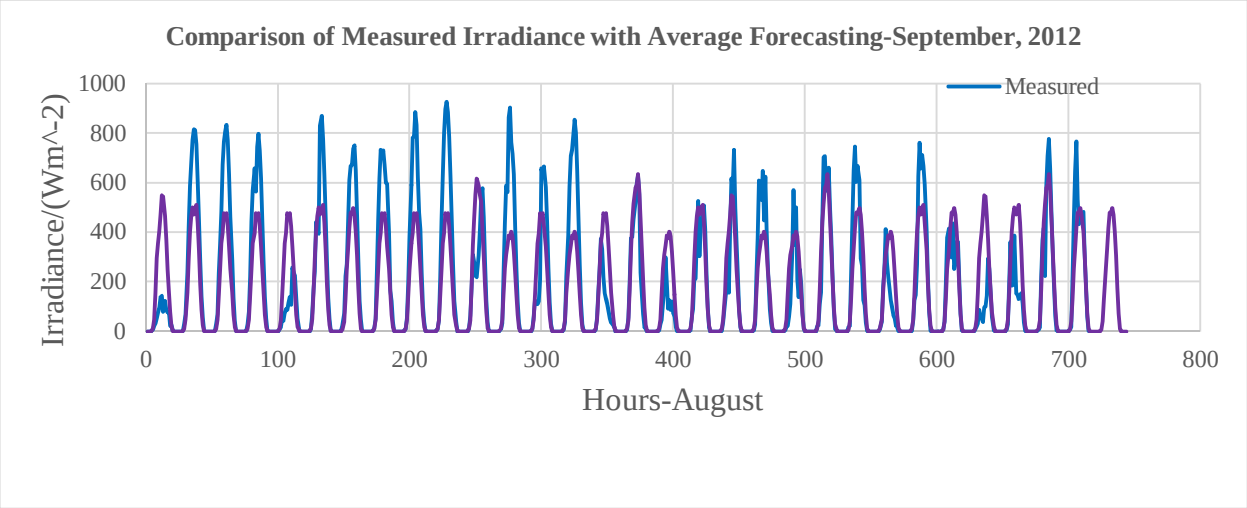

Figure. A.16. Daily Time Series for Measured and Forecasted Irradiance-September, 2012

Appendix B. Forecasted Information on Energy Gain

B.1. Illustration of Daily Time Series for Measured and Forecasted Irradiance, Month-May

Table B.1. Daily Time Series for Measured and Forecasted Irradiance, Month-May

Day	Measured Irradiance (Wm^{-2})	Forecasted Irradiance-Scheme A (Wm^{-2})	Forecasted Irradiance-Scheme B (Wm^{-2})
5/1/12	7336.466	2387.801	4735.168
5/2/12	7833.502	7529.636	6367.239
5/3/12	7115.407	7529.636	6367.239
5/4/12	5824.317	7529.636	6367.239
5/5/12	7356.709	7435.94	6025.745
5/6/12	6627.862	7529.636	6367.239
5/7/12	6227.789	7547.83	5015.783
5/8/12	1961.258	7547.83	5015.783
5/9/12	1621.069	2253.715	3608.468
5/10/12	1167.265	2253.715	3608.468
5/11/12	3959.713	2253.715	3608.468
5/12/12	6033.955	4523.273	4588.391
5/13/12	3578.414	7547.83	5015.783
5/14/12	3528.983	4523.273	4588.391
5/15/12	2472.942	4523.273	4588.391
5/16/12	2139.809	2387.801	4735.168
5/17/12	5498.421	2387.801	4735.168
5/18/12	7786.938	7435.94	6025.745
5/19/12	4665.272	7529.636	6367.239
5/20/12	6427.826	5446.273	5262.781
5/21/12	4857.531	7547.83	5015.783
5/22/12	7483.754	5446.273	5262.781
5/23/12	7641.958	7529.636	6367.239
5/24/12	7730.771	7529.636	6367.239
5/25/12	7629.826	7529.636	6367.239
5/26/12	7790.198	7529.636	6367.239
5/27/12	8004.819	7529.636	6367.239
5/28/12	7641.231	7720.606	7058.007
5/29/12	7145.836	7529.636	6367.239

5/30/12	6931.375	7529.636	6367.239
5/31/12	7801.772	7547.83	5015.783

Daily time series with respect to hourly data is obtained as per the Table B.2

Table B.2. Daily Time Series for Hourly Data-Month, May

Day	Hour	Measured Irradiance (Wm^{-2})	Forecasted Irradiance-Scheme A (Wm^{-2})	Forecasted Irradiance-Scheme B (Wm^{-2})
5/1/12	0	0	0	0
5/1/12	1	0	0	0
5/1/12	2	0	0	0.110355
5/1/12	3	1.544975	3.435213	6.580946
5/1/12	4	23.35474	23.21008	32.87331
5/1/12	5	65.66848	46.61162	70.38226
5/1/12	6	270.0222	79.73674	173.9974
5/1/12	7	495.5369	100.3133	299.8413
5/1/12	8	694.7605	144.5007	413.3526
5/1/12	9	848.3748	175.8384	479.5255
5/1/12	10	937.3053	162.682	488.0612
5/1/12	11	970.7661	218.8625	544.2075
5/1/12	12	926.8523	229.3882	531.3133
5/1/12	13	799.893	208.0479	492.9752
5/1/12	14	592.8686	293.8793	440.9474
5/1/12	15	390.4321	305.8619	356.7503
5/1/12	16	192.2669	203.8892	228.142
5/1/12	17	99.9568	119.4645	117.251
5/1/12	18	26.42128	62.29324	51.87542
5/1/12	19	0.441421	9.730496	6.960991
5/1/12	20	0	0.055178	0.020065
5/1/12	21	0	0	0
5/1/12	22	0	0	0
5/1/12	23	0	0	0
……	…..	……	……	……
5/31/12	0	0	0	0
5/31/12	1	0	0	0
5/31/12	2	1.103553	0.220711	0.055178
5/31/12	3	16.9378	7.961809	5.75491
5/31/12	4	39.44272	33.75725	31.4742
5/31/12	5	89.17715	85.0411	73.82349

5/31/12	6	313.3552	297.4845	217.6168
5/31/12	7	533.0123	516.5344	367.996
5/31/12	8	727.3516	712.2269	460.7849
5/31/12	9	872.6891	799.6866	499.071
5/31/12	10	950.6432	866.3406	538.809
5/31/12	11	923.2743	900.4471	588.8403
5/31/12	12	773.6675	866.4966	600.051
5/31/12	13	779.3712	790.0317	516.0628
5/31/12	14	708.3808	674.6723	444.0109
5/31/12	15	521.2298	490.4021	317.4524
5/31/12	16	301.0642	295.2474	202.6035
5/31/12	17	164.3749	143.7201	101.4759
5/31/12	18	73.61242	60.09752	44.56325
5/31/12	19	12.86319	7.424172	5.329579
5/31/12	20	0.220711	0.036785	0.007883
5/31/12	21	0	0	0
5/31/12	22	0	0	0
5/31/12	23	0	0	0

Note: Scheme A denotes the most probable forecasting scheme and Scheme B denotes the average forecasting scheme.

B.2 Monthly Time Series for Energy Gain Forecasting

B.2.1 January

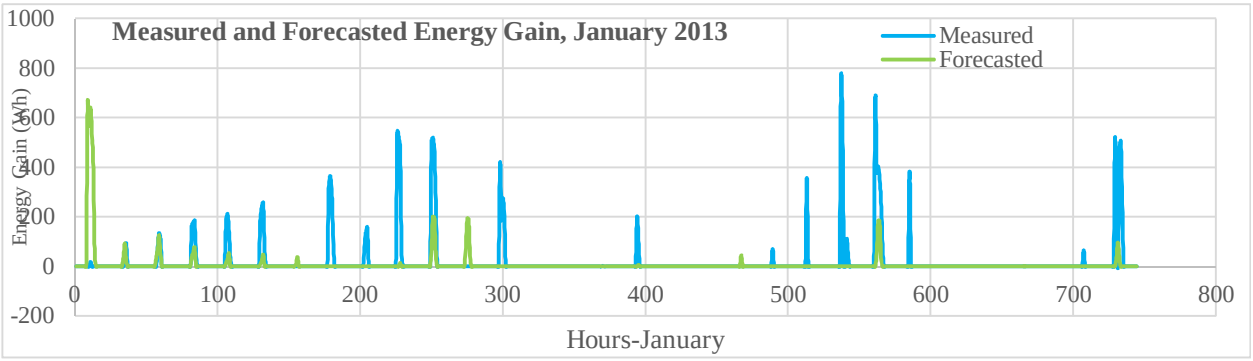

Figure B.1. Daily Time Series for Measured and Forecasted Energy Gain-January, 2013

B.2.2. February

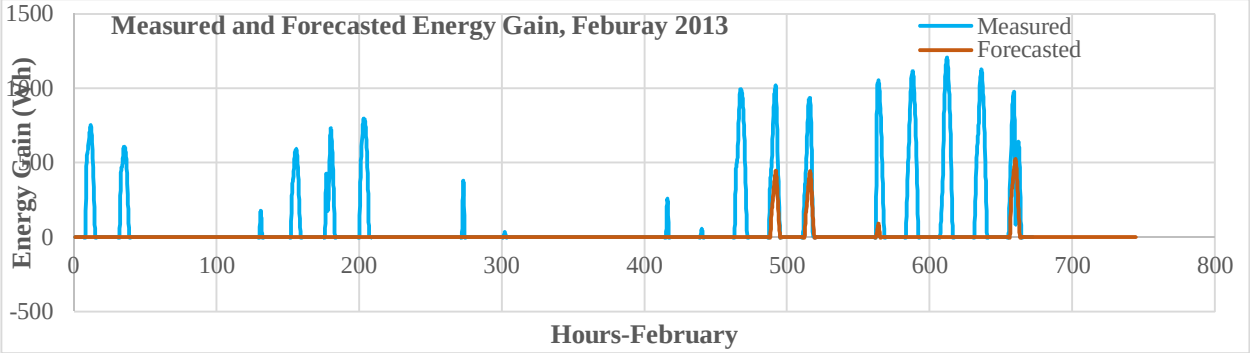

Figure B.2. Daily Time Series for Measured and Forecasted Energy Gain-February, 2013

B.2.3. March

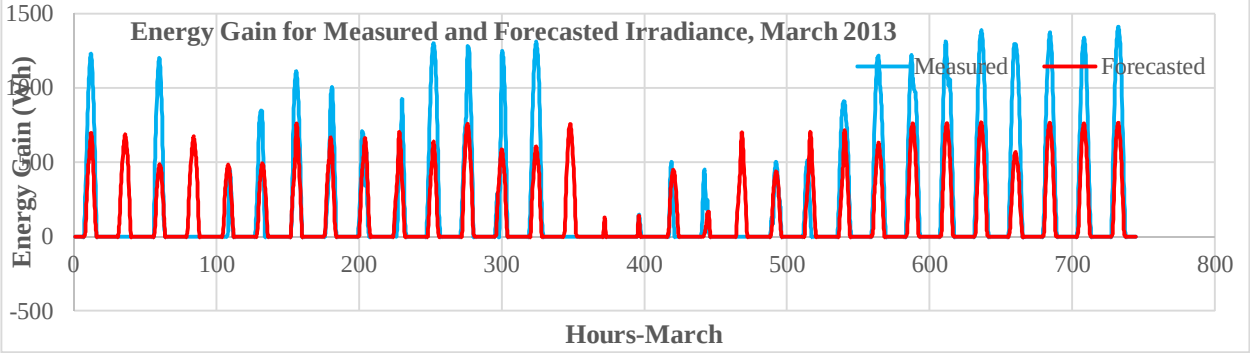

Figure B.3. Daily Time Series for Measured and Forecasted Energy Gain-March, 2013

B.2.4. April

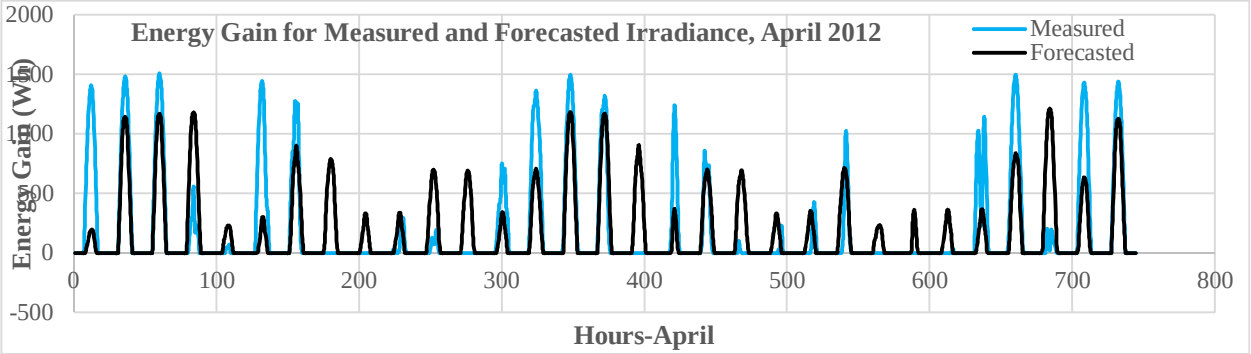

Figure B.4. Daily Time Series for Measured and Forecasted Energy Gain-April, 2012

B.2.5. May

Month-May was used to illustrate the forecasting schemes. The daily time series is given in Chapter 5.

B.2.6. June

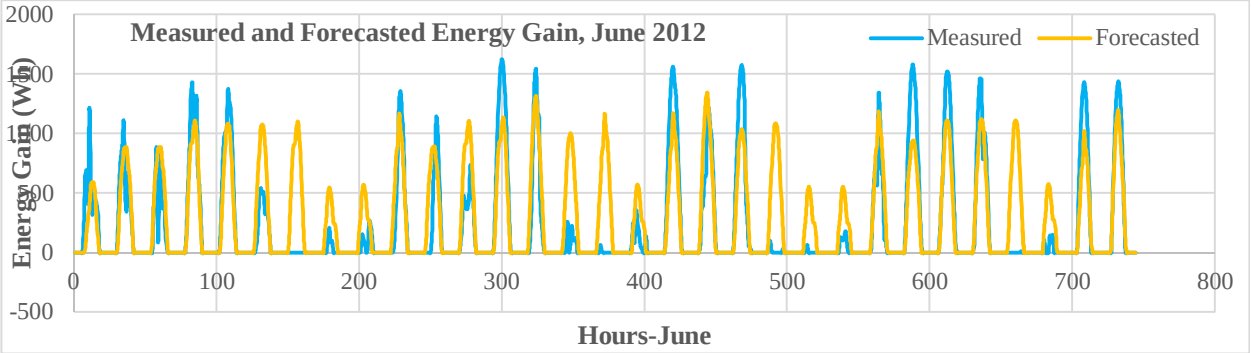

Figure B.5. Daily Time Series for Measured and Forecasted Energy Gain-June, 2012

B.2.7. July

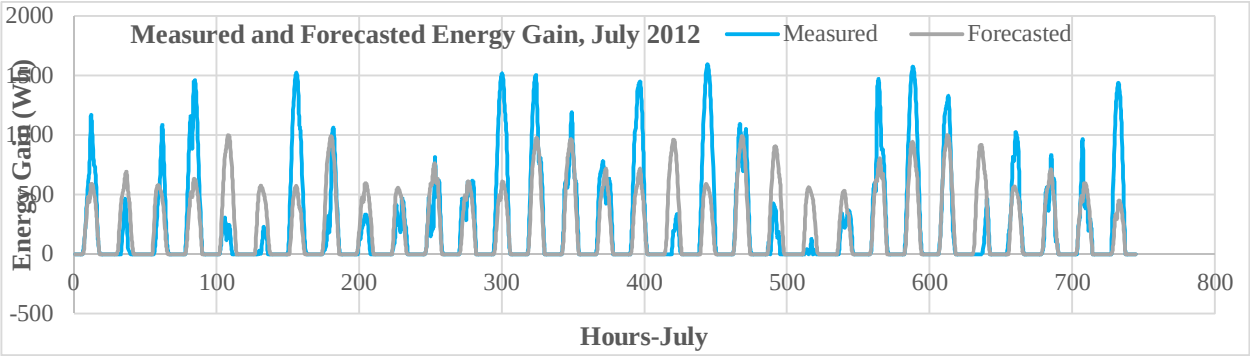

Figure B.6. Daily Time Series for Measured and Forecasted Energy Gain-July, 2012

B.2.8. August

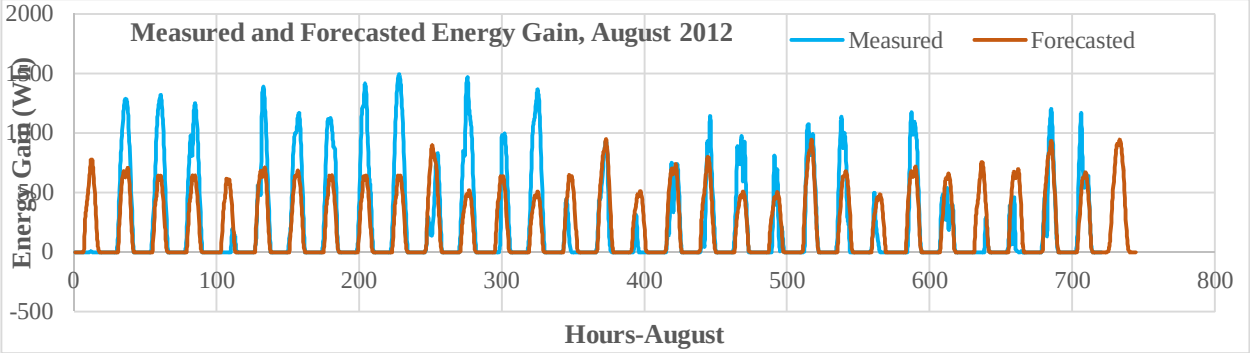

Figure B.7. Daily Time Series for Measured and Forecasted Energy Gain-August, 2012

B.2.9. September

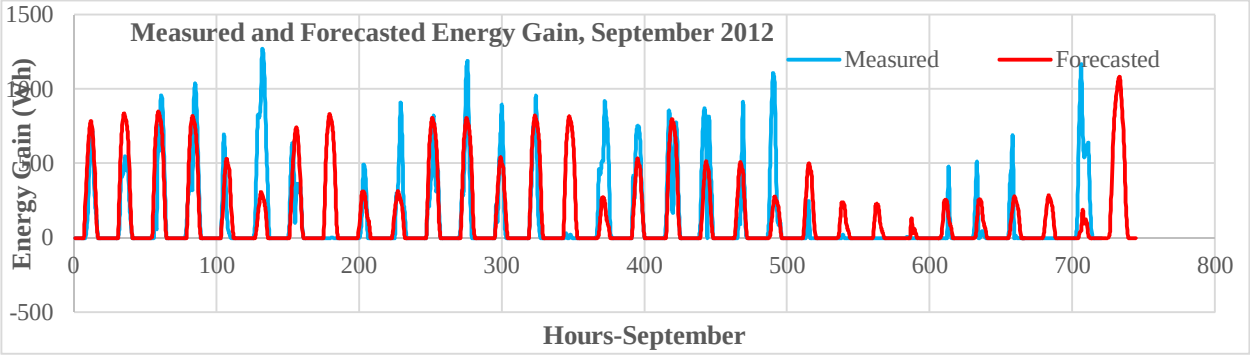

Figure B.8. Daily Time Series for Measured and Forecasted Energy Gain-September, 2012

Appendix C: Important Matlab Codes Used for Generating Forecasting Schemes

As the forecast approach is similar for every month, matlab codes are illustrated with respect to single month. Remaining necessary codes can be provided on request.

Generating Forecasted Probabilities for Irradiance: Month- May

```
clear all;
close all;
DEGS = xlsread('exceltomatlabirradiance_May.xlsx','Sheet1', 'Z3:Z183');
n = length(DEGS);
binCtrs = 500:1000:8500;
counts = hist(DEGS,binCtrs);
prob= counts/n;
set(0,'DefaultAxesFontName', 'Times New Roman')
H = bar(binCtrs,prob,'hist');
grid on;
set(gca,'fontsize',10,'fontWeight','bold')
set(H,'facecolor',[0.4 0.5 0.3]);
title('Probabilities for Daily Irradiance');
xlabel('Daily Irradiance (Wh/m^2)');ylabel('Probability');
for i=1:180;
    %Conditional Probabilities for DEGS>=0
    if (DEGS(i)>=0 && DEGS(i)<1000)&&(DEGS(i+1)>=0 && DEGS(i+1)<1000);
            D1_1(i)=DEGS(i+1);
    else
            D1_1(i)=0;
    end;
    if (DEGS(i)>=0 && DEGS(i)<1000)&&(DEGS(i+1)>=1000 && DEGS(i+1)<2000);
            D1_2(i)=DEGS(i+1);
    else
            D1_2(i)=0;
    end;
…….
if (DEGS(i)>=8000 && DEGS(i)<9000)&&(DEGS(i+1)>=8000 && DEGS(i+1)<9000);
            D9_9(i)=DEGS(i+1);
    else
            D9_9(i)=0;
    end;

end;
%Calculating counts as non zero values for each conditional bins
n1_1=nnz(D1_1);
……
n1_9=nnz(D1_9);
%Conditional probabilities as histogram charts
%for 0<TToday Daily IrradianceS<1000
cp1_1 =n1_1/counts(1);
……
```

```
cp1_9 =n1_9/counts(1);
figure;
H1_Y=[cp1_1 cp1_2 cp1_3 cp1_4 cp1_5 cp1_6 cp1_7 cp1_8 cp1_9 ];
H1=bar(binCtrs,H1_Y,1.0);
```

Sorting Average values for Irradiance Classes, May-2012

```
clear all;
close all;
DEGS = xlsread('exceltomatlabirradiance_May.xlsx','Sheet1', 'Z3:Z183');
for i=1:180;
    %Conditional Probabilities for DEGS>=0
    if (DEGS(i)>=0 && DEGS(i)<1000)&&(DEGS(i+1)>=0 && DEGS(i+1)<1000);
            D1_1(i)=DEGS(i+1);
    else
            D1_1(i)=0;
    end;
……..
    if (DEGS(i)>=8000 && DEGS(i)<9000);
            D1_9(i)=DEGS(i+1);
    else
            D1_9(i)=0;
    end;

end;

xlswrite('exceltomatlabirradiance_May_Version2.xlsx',D1_1','Sheet2',
'H4:H183' );
……..
xlswrite('exceltomatlabirradiance_May_Version2.xlsx',D1_9','Sheet2',
'P4:P183' );
```

Calculation of Energy Gain: Month- May

```
clear;
close all;
%parameters for Consolar PLANO 27H collector
A=2.335;
a1=3.97;
a2=0.0108;
eita0=0.813;
DT= xlsread('exceltomatlabEnergyGain_May.xlsx','Sheet1', 'C3:C54938');
G = xlsread('exceltomatlabEnergyGain_May.xlsx','Sheet1', 'E3:E54938');
%Energy gain of the collector through quardatric apporach
for i=1:54936
    if G(i)<=0
        Q_use(i)=0;
    else
        eita(i)=eita0-a1*DT(i)/G(i)-a2*DT(i)^2/G(i);
        Q_use(i)=G(i)*A*eita(i);
    end;
end;

xlswrite('exceltomatlab.xlsx',Q_use','Sheet1', 'B3:B54938' );
```

Appendix D: Data Sheet of the Solar Thermal Collector

SPF Solartechnik Prüfung Forschung

C1194

Solar Collector Factsheet
Consolar PLANO 27 H

Model	**PLANO 27 H**
Type	Flat plate collector
Manufacturer	Consolar Solare Energiesysteme GmbH
Address	Strubbergstrasse 70 DE-60489 Frankfurt a. M.
Telephone	+49 (0)69 7409328 0
Fax	+49 (0)69 7409328 50
Email	info@consolar.de
Internet	**www.consolar.com**
Test date	09.2010

☑ Performance test EN12975:2006
☑ Quality test EN12975:2006

Solar Keymark

Dimensions		Technical data	
Total length	1.178 m	**Minimum flowrate**	10 l/h
Total width	2.218 m	**Nominal flowrate**	15 l/h
Gross area	2.613 m^2	**Maximum flowrate**	200 l/h
Aperture area	2.335 m^2	**Fluid content**	3.3 l
Absorber area	2.258 m^2	**Maximum operating pressure**	6 bar
Weight empty	43 kg	**Stagnation temperature**	194 °C

Types of mounting

☑ Construction for sloping roof
☑ Integration into sloping roof
☑ On flat roof with stand
☑ Facade

Further information

☑ Units in different sizes available
☐ Glazing replaceable

Hydraulic connection

Special connection system of the manufacturer

Construction

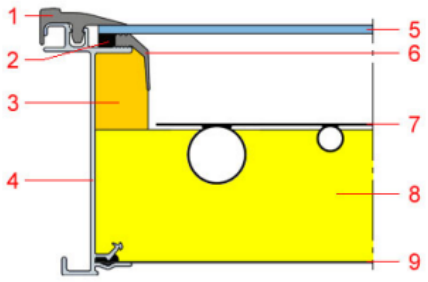

1 Glass fixing profile
2 Sealing
3 Lateral thermal insulation
4 Frame
5 Glazing
6 Glass support rail
7 Absorber
8 Thermal insulation
9 Rear panel

SPF Solartechnik Prüfung Forschung

C1194

Peak Power per collector unit W_{peak}

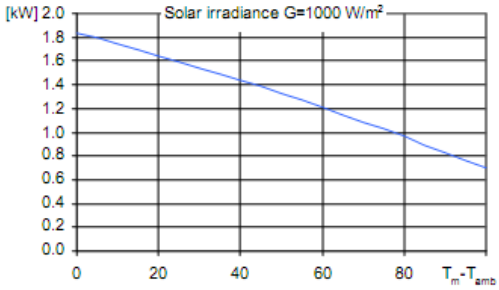

Relative efficiency η

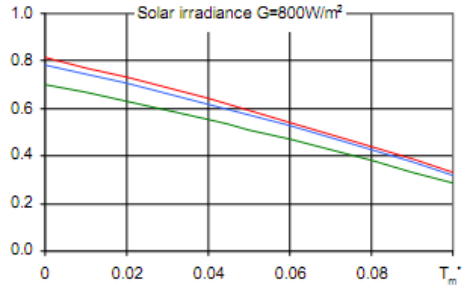

Peak Power W_{peak}	1836 W
Thermal capacity*	5.1 kJ/K
Flowrate during test	180 l/h
Fluid for test	Water-Glycol 33.3%

Reference	**Gross**	**Aperture**	**Absorber**
η_0	0.703	0.786	0.813
a_1 [$WK^{-1}m^{-2}$]	3.43	3.84	3.97
a_2 [$WK^{-2}m^{-2}$]	0.0093	0.0104	0.0108

*) Specific thermal capacity C of the collector without fluid, determined according to 6.1.6.2 of EN12975-2:2006

Incident angle modifier IAM

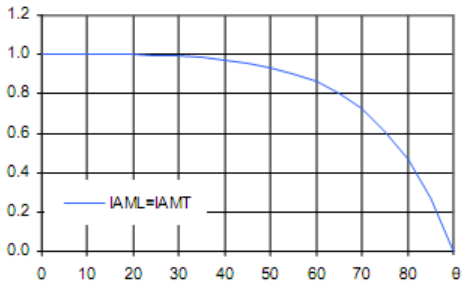

Pressure drop Δp

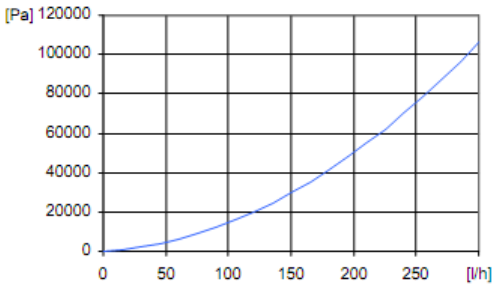

K1, transversal IAM at 50°	0.94
K2, longitudinal IAM at 50°	0.94

Pressure drop at nominal flowrate
Δp = 870 Pa (T=20°C)

SPF Simulation of systems using Polysun

Short description of the system	**Surface demand** Number of collectors**	**Solar yield****
Domestic hot water: Fss* = 60% Tank 450 l, collector inclination 45°, Daily energy demand 10 kWh (4-6 persons) Energy demand of the reference system 4200 kWh/year	5.13 m^2 2.2 collectors	496 kWh/m^2
Water pre-heating: Fss* = 25% 2 Tanks: 1500 l & 2500 l, collector inclination 30°, Domestic hot water consumption 10'000 l/day (200 persons) Daily heat losses (circulation and tanks) 60 kWh, Energy demand of the reference system 191'700 kWh/year	65.3 m^2 28.0 collectors	737 kWh/m^2
Space heating system: Fss* = 25% Combined storage1200 l, collector inclination 45°, Daily energy demand 10 kWh (4-6 persons), Building 200 m^2, moderately heavy construction, well insulated, Heating power demand 5.8 kW (ambient temperature -8°C), Energy demand space heating 12140 kWh/year, Energy demand of the reference system 16340 kWh/year	16.4 m^2 7.0 collectors	328 kWh/m^2

*) Fractional solar savings: Proportion of the final energy that, thanks to the solar system, can be saved compared to a reference system.
**) Surface demand and solar yield are given with respect to the aperture area.